Adultes avec déformation rachidienne : traitement chirurgical et évaluation musculaire

Bertrand Moal

2014-ENAM-0034

École doctorale n° 432 : Sciences des Métiers de l'Ingénieur

Doctorat ParisTech

T H È S E

pour obtenir le grade de docteur délivré par

l'École Nationale Supérieure d'Arts et Métiers

Spécialité " Biomécanique et Ingénierie pour la Sante "

présentée et soutenue publiquement par

Bertrand Moal

le 27 octobre 2014

Adultes avec déformation rachidienne : traitement chirurgical et évaluation musculaire

Directeurs de thèse: **Jean Marc Vital, Virginie Lafage et Wafa Skalli**

Jury

Mme Laurence CHEZE, Professeur, Université Claude Bernard Lyon 1, Lyon	Président
M. Pierre GUIGUI, Professeur, Hopital Beaujon (APHP), Paris	Rapporteur
M. Philippe GORCE, Professeur, Université du Sud Toulon-Var, La Garde	Rapporteur
M. Cédric BARREY, Professeur, Université Claude Bernard Lyon 1, Lyon	Examinateur
Mme Virginie LAFAGE, Docteur, NYU Hospital for Joint Diseases, New York	Examinateur
M. Jean-Marc VITAL, Professeur, Hôpital Pellegrin (CHU Bordeaux), Bordeaux	Examinateur
Mme Wafa SKALLI, Professeur, Arts et Métiers ParisTech, Paris	Examinateur
M. Philippe ROUCH, Professeur, Arts et Métiers ParisTech,	Invité
M. Jean DUBOUSSET Professeur, Arts et Métiers ParisTech.	Invité

T H È S E

Arts et Métiers - Centre de Paris
Laboratoire de Biomécanique

"Une chose qui est faite, n'est plus à faire."
Mon père

REMERCIEMENTS

Après trois années d'élaboration de cette thèse, les quelques lignes qui suivent ne suffiront pas à exprimer toute ma gratitude pour l'aide et le soutien qui m'ont été apportés, sans lesquels ce travail n'aurait jamais pu voir le jour.

Mes premiers remerciement vont à mes trois directeurs de thèse.

Tout d'abord au professeur Jean Marc Vital pour sa confiance et ses conseils dans mon travail. Je souhaite notamment lui exprimer ma très grande reconnaissance pour son aide au moment où je projetais d'entreprendre des études de médecine.

Cette aventure n'aurait pas été non plus possible sans le soutien inflexible du Professeur Wafa Skalli. Je la remercie encore pour m'avoir transmis son goût de la recherche et pour m'avoir toujours poussé à améliorer mon travail.

Enfin, au-delà des remerciements, je souhaite témoigner de tout le plaisir que j'ai eu à travailler avec le Docteur Virginie Lafage. Elle a été le professeur que tous les étudiants attendent.

Je souhaite aussi faire part de ma sincère gratitude aux docteurs Frank Schwab, Jean Pierre Farcy et Thomas Errico qui m'ont permis de mieux comprendre l'aspect clinique de mon travail et ont aussi largement contribué à mon éducation œnologique.

Sans le large temps consacré par le Professeur Jose G. Raya à mettre au point le protocole IRM et sans sa rigueur scientifique, ce travail n'aurait pas eu la même qualité et je lui en sais gré, de tout coeur.

Merci aussi au professeur Nicolas Bronsard et au docteur Benjamin Blondel pour tout ce qu'ils m'ont appris en me faisant partager leur expérience.

Remerciements aux financeurs du programme de chaires ParisTech BiomecAM en modélisation biomécanique personnalisée, porté par la Fondation ParisTech : la Société Générale, le Groupe COVEA, la Société PROTEOR et la Fondation Yves Cotrel pour la recherche en pathologie rachidienne, pour leur contribution à l'environnement scientifique qui m'a permis de conduire cette recherche dans les meilleures conditions. Je remercie tout particulièrement Madame Brigitte Roux.

Je tiens aussi à saluer l'équipe de la fondation Internationale Spine Study Group pour son soutien financier, pour les nombreux conseils des ses membres et pour l'aide précieuse de Madame Raymarla Pinteric.

Je suis également reconnaissant à toute l'équipe de la société Nemaris pour son aide technique et financière.

A l'occasion de l'élaboration de cette thèse, j'ai eu la possibilité de profiter de la structure et de la compétence des équipes du laboratoire de Biomécanique des Arts et Métiers et du laboratoire de recherche "Rachis" au NYU Hospital for Joint Diseases, et j'en suis très redevable.

Je tiens également à remercier spécialement, pour toute leur aide et leur sympathie, Thomas Joubert, Mohamed Marhoum, Aurélien Laville, Guillaume Dubois et Marine Souq, de même qu'Alex Lee, Jamie Terran, Mimi, Bassel Diebo et Renaud Lafage.

Enfin, je veux exprimer ma reconnaissance à mes amis et surtout à mes parents, mon grand père, ma tante, ma sœur et mon frère qui m'ont soutenu dans les moments difficiles, et ont partagé mes joies. Sans eux, cela n'aurait pas été possible.

Table of Contents

1. INTRODUCTION

Adult spinal deformity (ASD) refers to abnormal curvatures of the spine in patients who have completed their growth. Due to its prevalence, clinical impact, and the relatively high rate of surgical failures, they represent a therapeutic challenge.

The prevalence of ASD varies between 1.4% and 20% in the adult population [1–3] and can reach 60% in the population over 65 years of age [4]. This high prevalence can be put in perspective of the aging population in Western counties. For example, according to INED (National Institute of Demographic Studies), while in 2004 only 22% of the population in France was 60 or older, this proportion is likely to reach 35% in 2040. This example highlights the large population likely to be affected and its potential for growth.

Moreover, Bess et al[5] demonstrated that the mental and physical disability caused by spinal deformity was comparable to that caused by cancer or diabetes. It is obvious that this disability, multiplied by the number of patients entails a heavy cost to society, both in terms of care and shortfall. In the current climate of budget savings, the cost to society of these pathologies is a leading socioeconomic issue.

In addition to the preceding two factors, the proposed treatments, surgical or not, do not provide fully satisfactory clinical results. While various studies showed that the effectiveness of surgical treatment is better than non-surgical treatment[6–12], they also showed that between 33% and 54% of surgically treated patients did not experienced significant clinical improvement[9].

Using health-related quality of life (HRQOL) instruments and radiographic analysis, research has been able to demonstrate the relation between pain and disability experienced by patients and the deterioration in sagittal alignment[13,14]. Moreover, if the deformation, which can be local, regional or global, appears mainly in the spine[15], it can also have indirect impact on the hip[14,16], the lower limbs[17], and the soft tissues. Therefore, the preservation or the restoration of the global sagittal alignment[12,16,18] are key objectives of treatment and surgical treatment.

Surgical reconstructions for ASD and utilization of osteotomies to restore the sagittal alignment are now widely spread[19,20]. Many dedicated software and formulas were developed to assist surgeons in the surgical planning for such challenging procedures[21–24]. Nevertheless, reaching an optimal spino-pelvic alignment, as indicated by these tools, is still challenging. One of the limitations is the ability to anticipate the pre to post-operative behaviors of the musculoskeletal components involved in the compensation for the spinal deformity as previously mentioned[14,16,17].

Soft tissue, such as muscle, tendon, ligament, fascia and connective tissues, is significant a player of the postural system and has significant involvement in the body ability to maintain an erect posture. Therefore, assessment of the soft tissue is crucial to investigate the ability of musculoskeletal system to adapt and maintain an accomplished alignment following a surgical treatment for ASD.

The objective of this thesis is to analyze the treatment of ASD patients, with particular interest in restoration of sagittal alignment and to develop tools to assess the spino-pelvic musculature of ASD patients.

This thesis is a partnership between three sites, whose leaders are the co-directors of this thesis:

- Research Laboratory of Surgery of the Spine Hospital NYU Joint Disease in New York led by Virginie Lafage.
- The Department of Orthopaedic and Trauma Surgery B Pellegrin Hospital in Bordeaux led by Professor Jean Marc Vital.
- Biomechanics laboratory of Arts and Metiers in ParisTech headed by Professor Wafa Skalli.

The project has been funded by

- The International Spine Study Group (ISSG), a non for profit foundation including surgeons and engineers with the objective of providing better treatments for spinal disorders.
- The ParisTech BiomecAM chair program on subject-specific musculoskeletal modeling, with the support of Proteor, Covea, Société Général, ParisTech and Yves Cotrel Foundation.
- Nemaris Inc, a private corporation founded by Virginie Lafage and Frank Schwab

2. BIBLIOGRAPHIC SYNTHESIS

The first section of this bibliographic synthesis intends to briefly describe the anatomy of the main bones and muscles involved in the postural alignment and to provide an overview of the main radiographic spino-pelvic parameters and their evaluation.

The second section is dedicated to Adult Spinal Deformity (ASD). After describing the possible etiology, this thesis will focus on the clinical evaluation of patients suffering from ASD with a special emphasis on the relationship between patients reported outcomes and sagittal spino-pelvic parameters. The possible treatments, and their effectiveness will then be mentioned and a particular attention to surgical treatment for restoration of sagittal alignment.

Finally, the methods of muscular evaluation, a fundamental element to maintain an erected posture, will be explored in the context of ASD population.

2.1 OSTEO-ARTICULAR SYSTEM

2.1.1 THE SPINE

The spine is composed of seven cervical vertebrae (C1 to C7), twelve thoracic vertebrae (T1 to T12), 5 lumbar vertebrae (L1 to L5), and ends with the sacrum (Figure 2-1). The spine sits on the pelvis and supports the weight of the head.

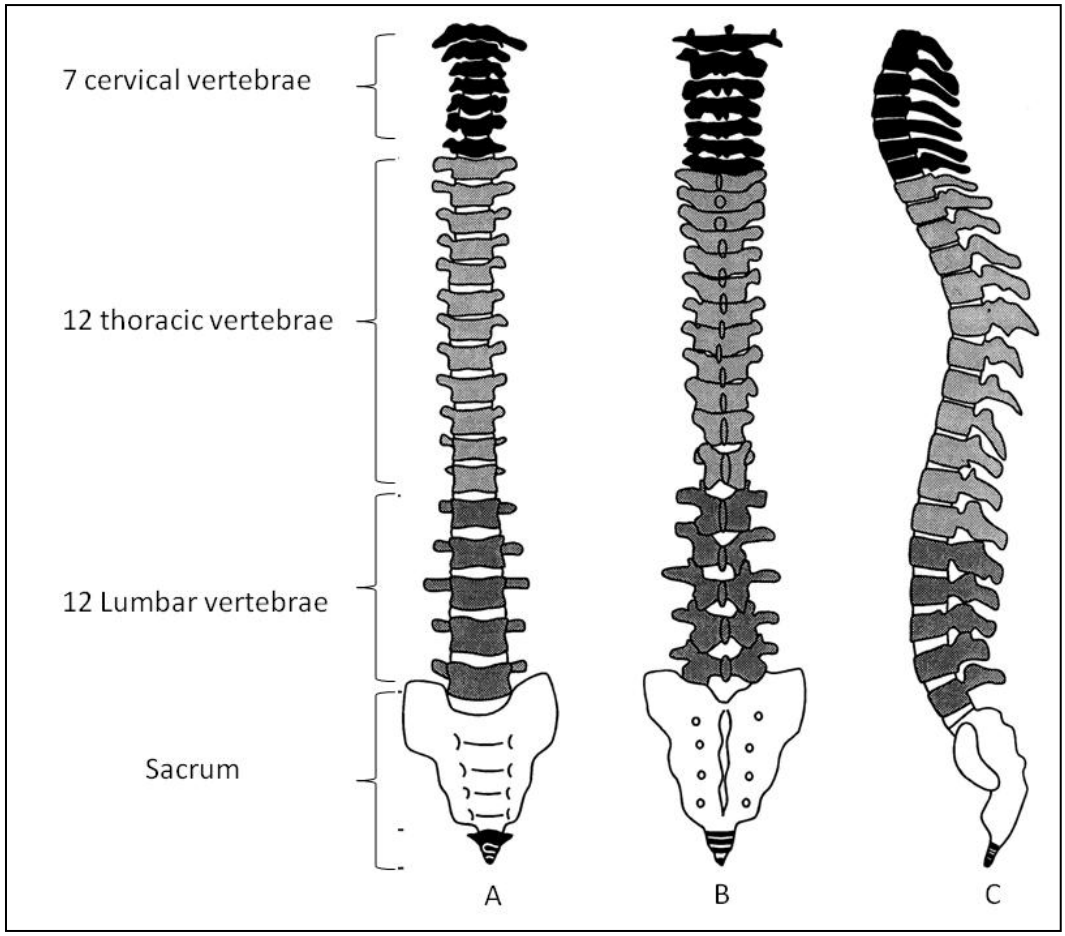

Figure 2-1: Anterior(A), posterior(B) and lateral(C) view of the spine and the sacrum (Picture from " Anatomie descriptive et fonctionnelle de l'appareil locomoteur",Jean Marc Vital[25]).

2.1.2 THE VERTEBRAE

Each vertebra presents a similar architecture (Figure 2-2): the vertebral body anteriorly, and the vertebral arch posteriorly. The vertebral arch consists of two pedicles, two laminae, two transverses processes, one spinous process, and four articular processes. The vertebrae are articulated with each other via the intervertebral discs anteriorly, and the superior and inferior articular processes posteriorly. The stability of the spine articulation is also ensured by a complex of ligaments and articular capsules (Figure 2-3).

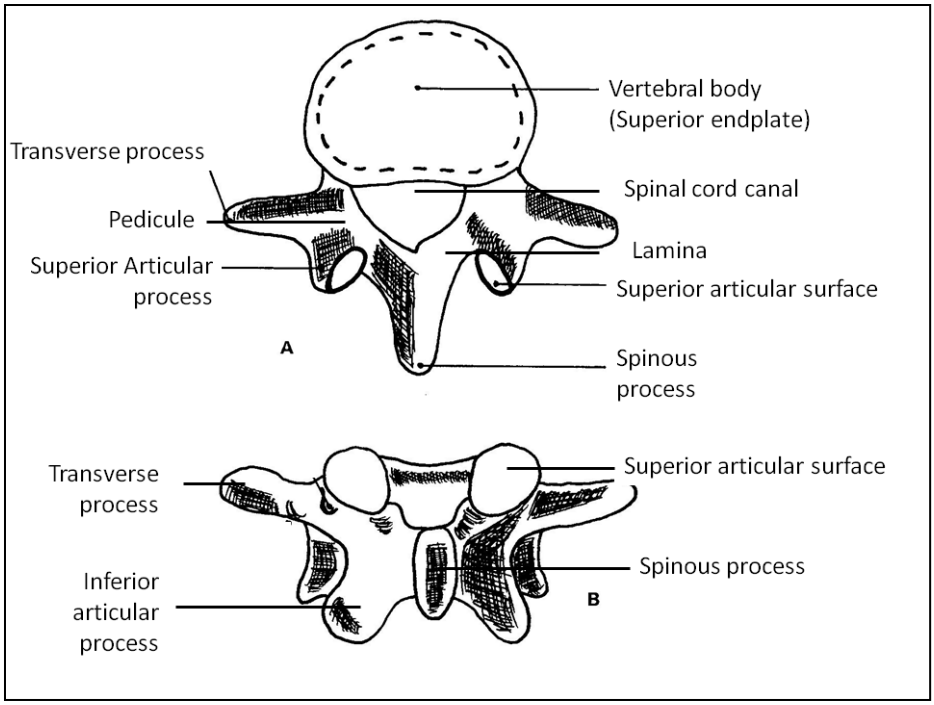

Figure 2-2 Superior(A) and posterior (B) view of a lumbar vertebra(Picture from " Anatomie descriptive et fonctionnelle de l'appareil locomoteur",Jean Marc Vital[25]).

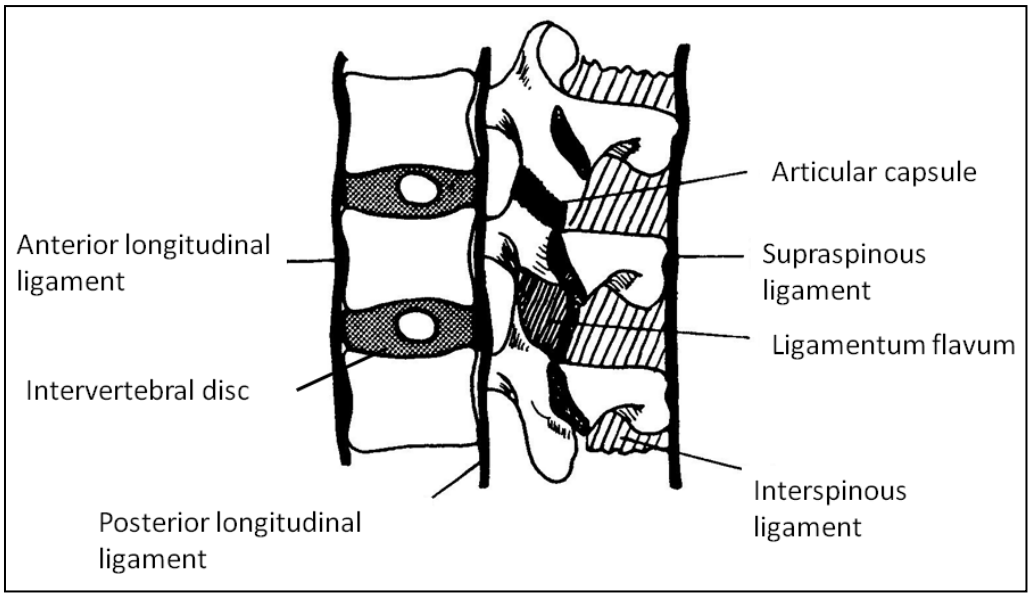

Figure 2-3: Sagittal view of the ligaments and capsule of the spine(Picture from " Anatomie descriptive et fonctionnelle de l'appareil locomoteur",Jean Marc Vital[25]).

2.1.3 PELVIS AND LOWER LIMB

The pelvis regroups several bones (Figure 2-4):

- the sacrum composed of 5 sacral vertebrae fused together, which is articulated with the lumbar spine via an intervertebral disc and two articular processes.
- the coccyx is fixed to the distal part of the last sacral vertebrae
- the coxal bones are articulated with the sacrum with the two sacro-iliac joints. Of note, the sacro-iliac articulation is surrounded by ligaments and there are no muscles.

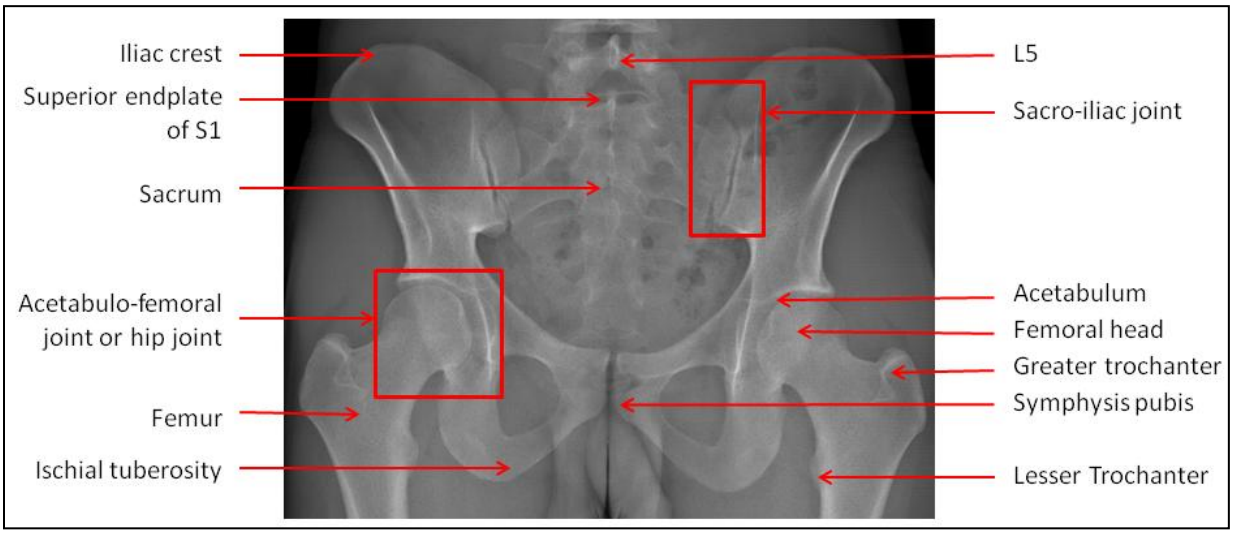

Figure 2-4: Coronal X-ray of the pelvis of an asymptomatic male (24 year old and BMI= 21.3)

The pelvis is articulated with the lower limbs by the acetabulofemoral joint, or hip joint. This articulation is composed by the femoral head and the acetabulum of the pelvis. Its primary function is to support the weight of the body. The femur is then articulated to the patella and the tibia. These three bones formed the knee articulation (Figure 2-5).

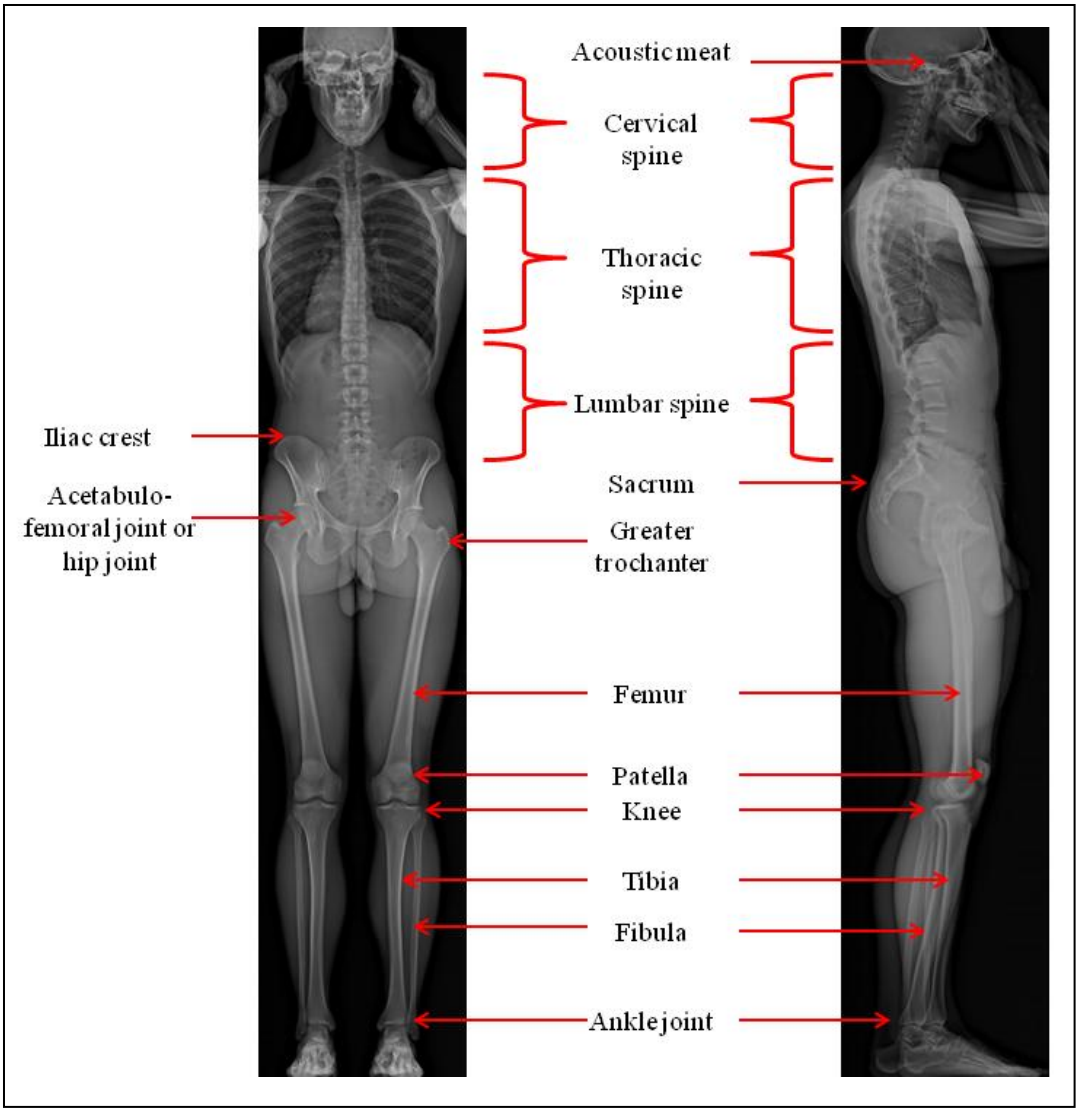

Figure 2-5 Coronal (Left)and Sagittal (Left) full body X-ray of an asymptomatic male (24 year old and BMI= 21.3)

Summary:

The osteo-articular system involved in the posture is composed of the spine, the pelvis and the lower limb (Figure 2-5). At the top of this system, the head, which represents around one eighth of the total weight, imposes a mechanical constraint to the entire system and has to be kept upon the pelvis. The pelvis appears to be the cornerstone of the osteo-articular system in charge of the postural alignment[26].

2.2 MUSCULAR SYSTEM DESCRIPTION

The osteo-articular system described in the previous section, is clothed by a complex muscular system. In this section, only the anatomy of muscles located in the thoraco-lumbar spine, the pelvis and the lower limb area are described. Pelvis trochanter muscles were not included in this description because of their limited involvement in the sagittal imbalance.

2.2.1 LUMBAR AREA

At the thoraco-lumbar spine, three groups of muscles could be distinguished in the axial plane on (Figure 2-6).

- A posterior group: spine erector
- A lateral group: the ilio-psoas and the quadratus lumburom
- An anterior group: rectus abdominis and obliquus groups composed of the transverse, internal oblique and external oblique muscles.

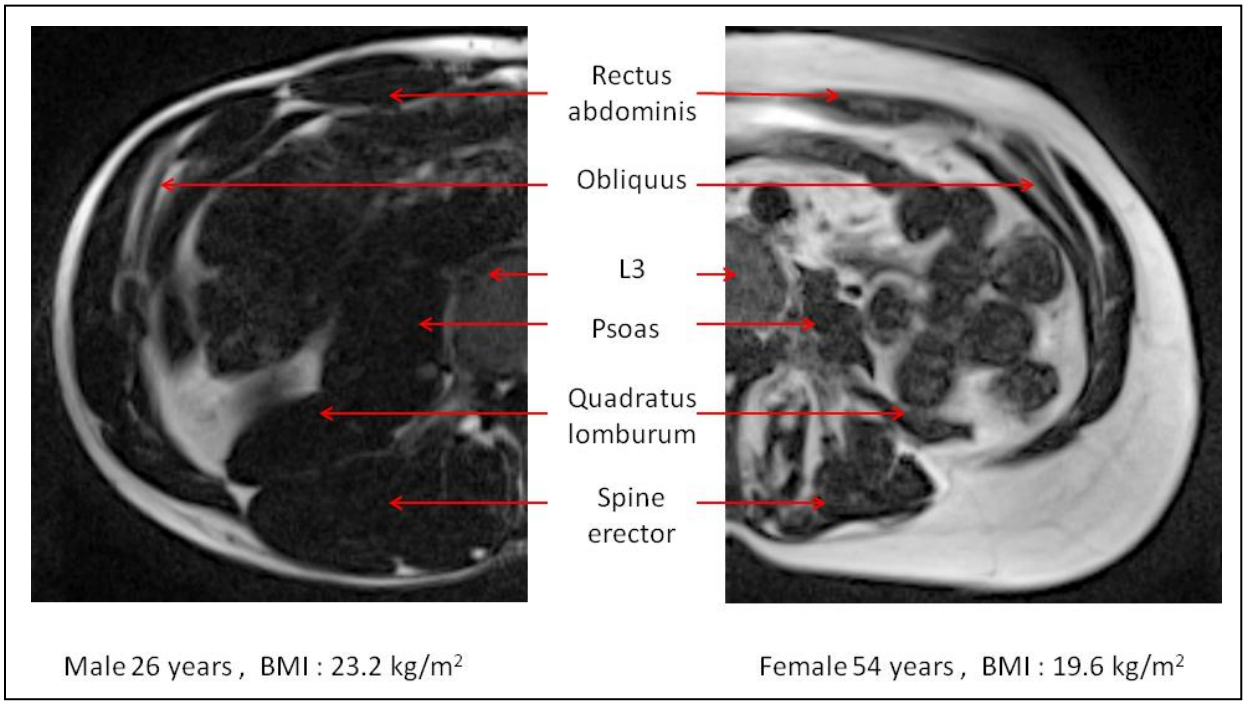

Figure 2-6: Axial MRI section at the level of the L3 vertebrae for a male of 26 years old (left) and of a female of 54 years old (right)

The erector spinae are composed of multiple muscles: interspinales, inter transverse, multifidus, semi-epinous and iliocostalis lumborum. The main action of these muscles is the extension of the lumbar spine.

The lateral group corresponds to the ilio-psoas and the quadratus lumburom. The ilio-psoas is composed by the psoas and the iliacus. The psoas is a long fusiform muscle, which originates from the lumbar vertebrae and the intervertebral discs. Also note that the lumbar plexus lies in the center of the psoas. The origin of the iliacus is the iliac fossa of the pelvis. The distal insertion of the ilio-psoas is the lesser trochanter. This muscle can lead to flexion or lateral rotation of the hip, but also to homo-lateral inclination, contro-lateral rotation, or a hyperlordosis of the spine.

The quadratus lumborum presents an anterior fiber which originates from the lower edges of the last rib and is inserted on the transverse processes of the lumbar vertebrae. The posterior fiber has the same origins, but is inserted on the iliac crest. It can perform four actions: the lateral flexion of the vertebral column, the extension of the lumbar vertebral column, fixes the 12Th rib during forced expiration and elevates the ilium (Figure 2-7).

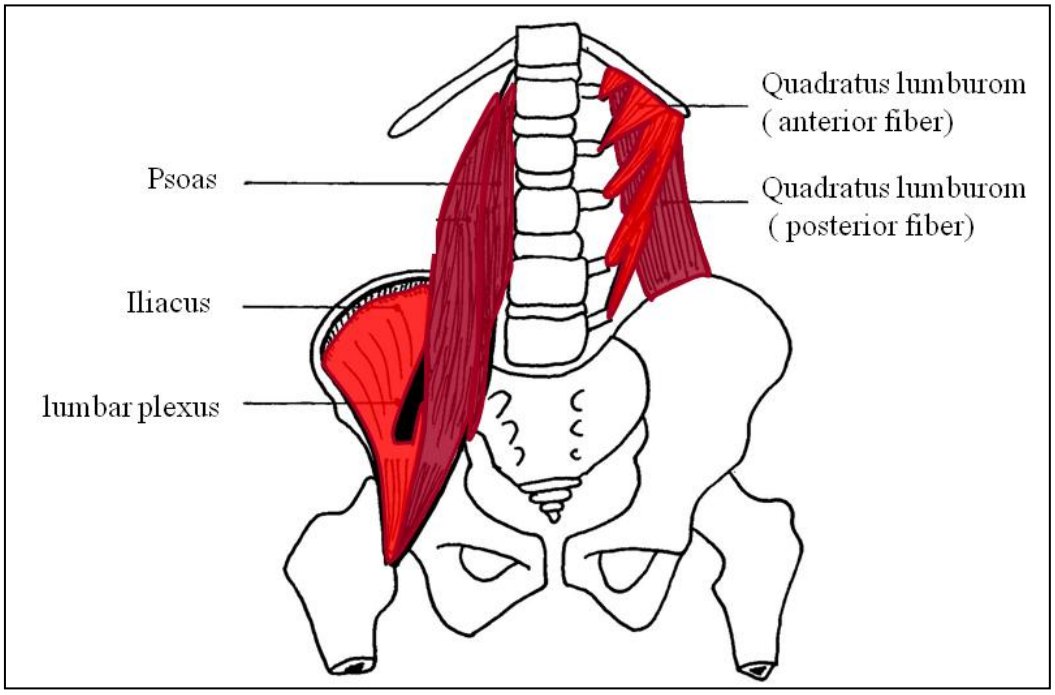

Figure 2-7 Coronal view of lateral groups including the psoas, the iliacus and the quadratus lumburom. (Picture from " Anatomie descriptive et fonctionnelle de l'appareil locomoteur",Jean Marc Vital[25]).

The anterior group presents four muscles which compose the abdominal wall. The rectus abdominis are between the xyphoide appendices and the pubis. The obliquus groups is composed of the transverse, internal obliques and external oblique muscles (from the inside to the outside). The fiber orientation of these muscles are complementary. The fibers from the transverse are transverse, the internal obliques fibers are directed from above and inside and the external obliques fibers from the bottom and inside (Figure 2-8).

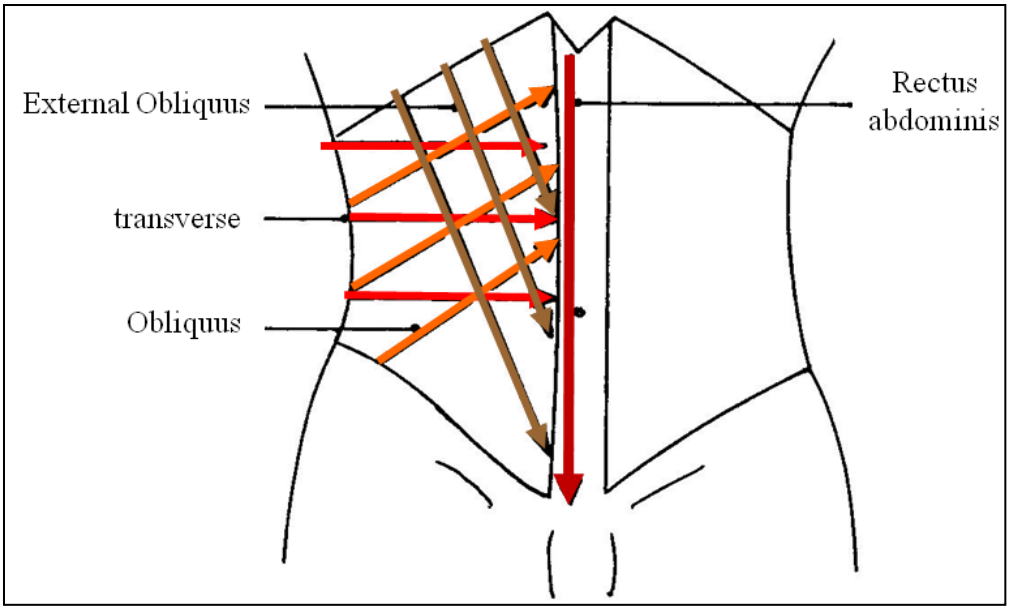

Figure 2-8 Muscle of the anterior groups. (Picture from " Anatomie descriptive et fonctionnelle de l'appareil locomoteur",Jean Marc Vital[25]).

2.2.2 PELVIS AND THIGH AREA

The muscles of the pelvic and the thigh can be described in four groups: anterior, latero-posterior, posterior, and medial.

- The anterior group is composed by the quadriceps and the Sartorius, which is mainly responsible for the knee extension and the hip flexion (Table 2-1: detailed origins, termination and action. Figure 2-9).
- The posterior group corresponds to the biceps femoris, the semitendinous, and the semimembranous. This group has an action of hip extensor and knee flexor in the sagittal plan(Table 2-2: detailed origins, termination and action. Figure 2-9).
- Finally, the medial groups have an action of knee flexor which is composed of the pectinus, the gracilis, and the adductors (long, brevis, magnus) (Table 2-3: detailed origins, termination and action, Figure 2-10).
- The latero-posterior group is composed of the gluteus muscles, the tensor facia lata and the pelvi-trochanter muscles (Table 2-4: detailed origins, termination and action. Figure 2-11).

Anterior Group			
Muscle	**Origins**	**Termination**	**Action**
Sartorius	antero-superior of the iliac crest	medial face of the tibia → Pes anserinus	bi-articular : flexor of the hip and the knee
Quadriceps Rectus femoris	iliac crest exterior surface of the bony ridge on the iliac portion of the acetabulum	patellar tendon	knee extension hip flexion
Quadriceps Vastus lateralis	greater trochanter, upper part of the intertrochanteric line, lip of the gluteal tuberosity, lateral lip of the linea aspera		
Quadriceps Vastus intermedius	antero/lateral of the femur		accessory abductor of the hip
Quadriceps Vastus medial	medial side of the femur		

Table 2-1: Origins, termination and action of the muscles of the anterior group

Posterior group (hamstring)			
Muscle	**Origins**	**Termination**	**Action**
Biceps femoris	*Long biceps* : ischial tuberosity *short biceps* : linea aspera	head of the fibula expansion of posterior lateral condyle of the femur	extensor, adductor, lateral rotator of the thigh
Semitendinous	ischial tuberosity	medial face of the tibia → Pes anserinus	flexor and medial rotator of the thigh extensor of the hip
Semimembranous	ischial tuberosity	posterior lateral condyle of the femur	flexor and medial rotator of the thigh extensor of the hip
	posterior fiber: tuberosity of the ischium		extensor of the thigh

Table 2-2: Origins, termination and action of the muscles of the posterior group

Medial group: Superficial plan			
Muscle	**Origins**	**Termination**	**Action**
Pectineus	pectineal line of the pubis	pectineal line of the femur	adductor and accessory flexor of the thigh
Long adducteur	anterior face of the pubis	middle third of the medial lip of the linea aspera	
Gracilis	lower half of the symphysis pubis	medial face of the tibia → Pes anserinus	

Medial group: Middle plan			
Muscle	**Origins**	**Termination**	**Action**
Short adductor	lower half of the symphysis pubis	proximal linea aspera	adductor of the thigh

Medial group: Deeper Plan			
Muscle	**Origins**	**Termination**	**Action**
Magnus adductor	*anterior fiber*: symphysis pubis	medial linea aspera	adductor and extensor of the thigh

Table 2-3: Origins, termination and action of the muscles of the medial group

Latero-posterior group: Superfical Plan			
Muscle	**Origins**	**Termination**	**Action**
Gluteal maximus	*superficial fiber* : iliac crest, sacral crest, thorcaco-lumbart fascia, gluteal fascia *deeper fiber* : iliac fosse, lateral edge of the sacrum and the coccyx, sacrotuberous ligament	ilio-tibial tractus gluteal tuberosity of the femur	extensor of the hip lateral rotator of the thigh abductor the thigh
Tensor fascia lata	iliac crest, iliac spinous, gluteal fascia	ilio-tibial tractus	flexor, abductor, medial rotator of the thigh tractus ilio-tibial tensor accessory extensor of the thigh

Latero-posterior group: Middle plan			
Muscle	**Origins**	**Termination**	**Action**
Medius gluteal	external ilium face, gluteal fascia	Greater trochanter	adductor and lateral rotator of the thigh monopodal support : maintained pelvis horizontality main factor of stability of the pelvis

Latero-posterior group: Deeper Plan			
Muscle	**Origins**	**Termination**	**Action**
Gluteal minimus	external Ilium face	Greater trochanter	medial rotator of the thigh accessory abductor and flexor of the thigh
pelvi- trochanter muscles			Lateral rotator of the hip

Table 2-4: Origins, termination and action of the muscles of the latero-posterior group.

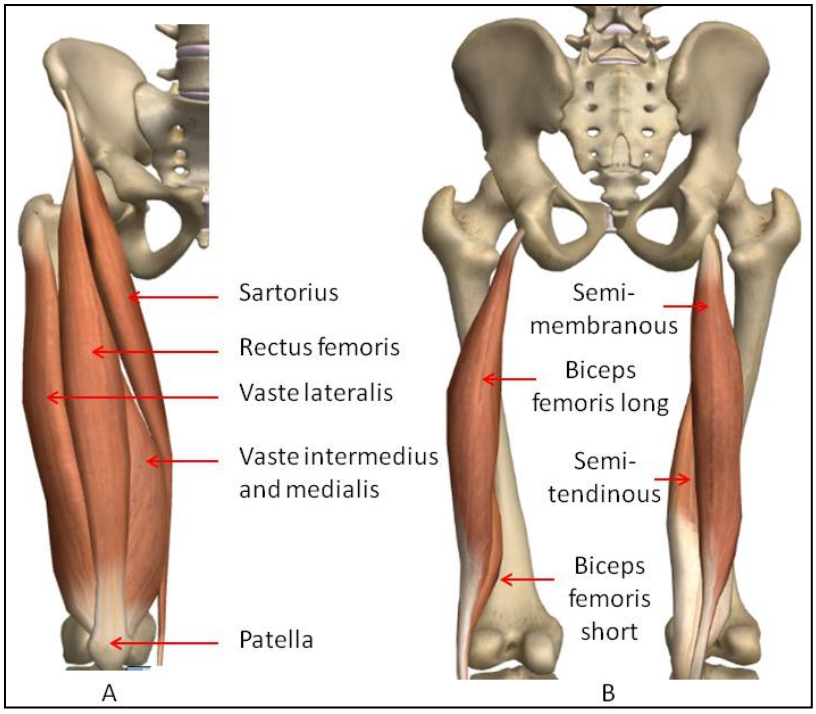

Figure 2-9: A: muscles of the anterior group of the thigh; B: muscles of the posterior groups of the thigh

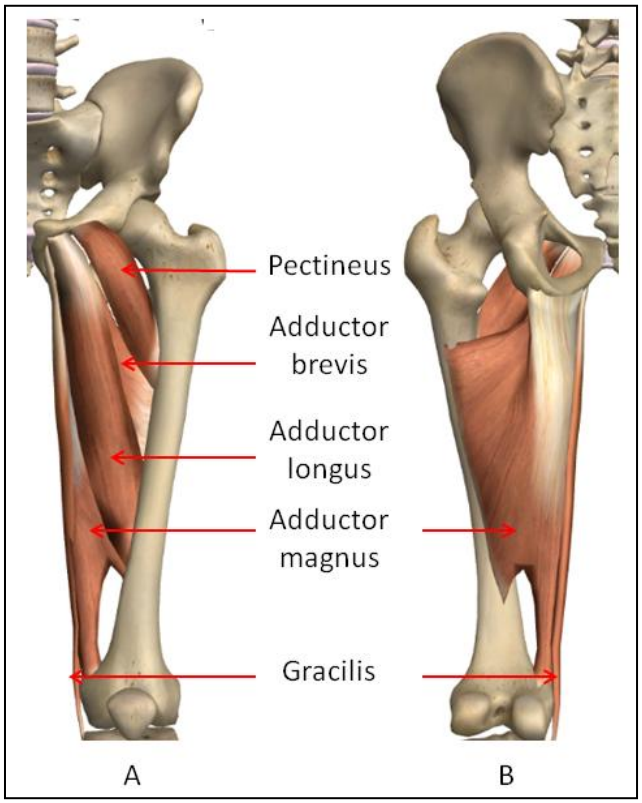

Figure 2-10: Anterior (A) and posterior (B) view of the muscles of the medial group

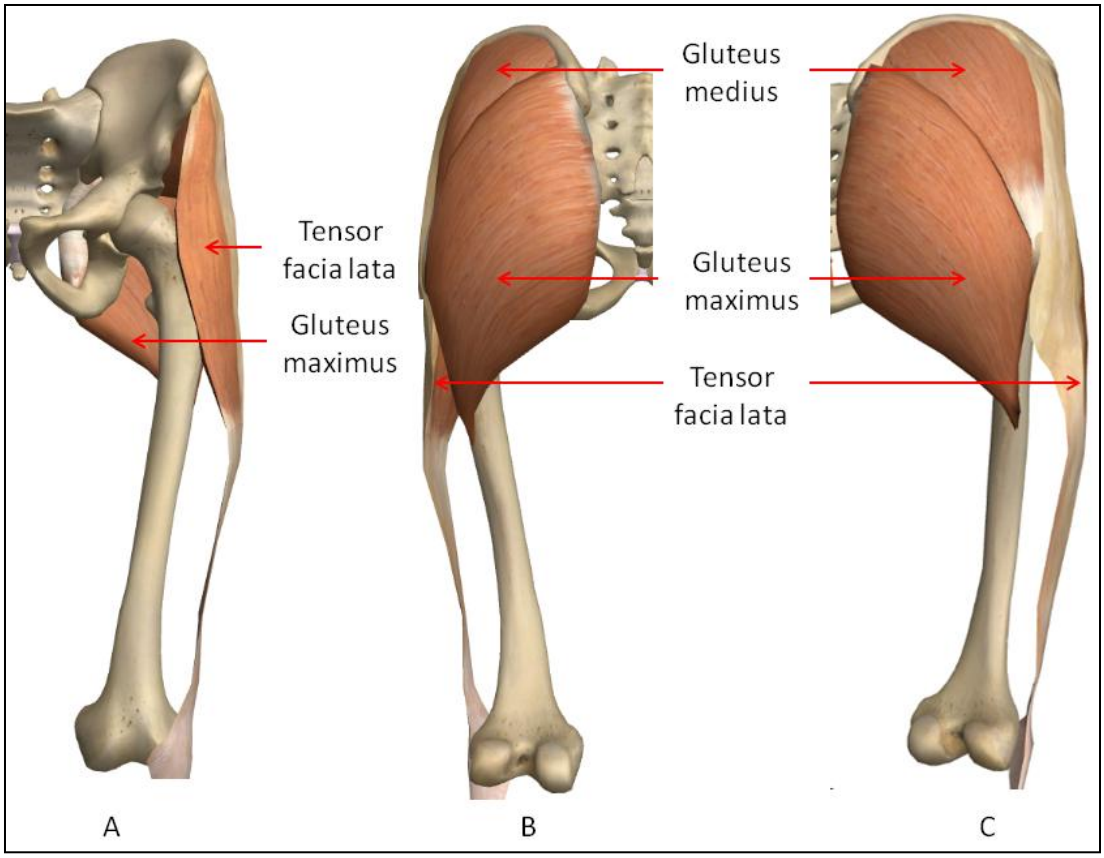

Figure 2-11: Anterior (A), posterior(B) and lareto-posterior view (C) of the muscles of the latero-posterior group

SUMMARY

In addition to the osteo-articular system, the postural alignment is based on a complex network of agonist and antagonist group of muscles, without which the stability of the system will be not reachable.

2.3 DESCRIPTION OF SPINO-PELVIC ALIGNMENT

Radiography has been the key modality permitting the quantification of the alignment in clinical practice. In general, the position of the skeletal is studied in the coronal and the sagittal planes. More recently, thanks to biplanar X-rays and dedicated software, 3D reconstruction of the spine, the pelvis, and the lower limb can be obtained.

2.3.1 CORONAL ALIGNMENT

In the coronal plane, the head, the spine, and the pelvis are vertically aligned in the asymptomatic population as presented (Figure 2-5). However, in the case of pathologic patients, global misalignment can appear, and is measured by the global coronal alignment (GCA), which is the coronal offset of the C7 plumb line and the sacral line (Figure 2-12: Global coronal alignment(GCA)).

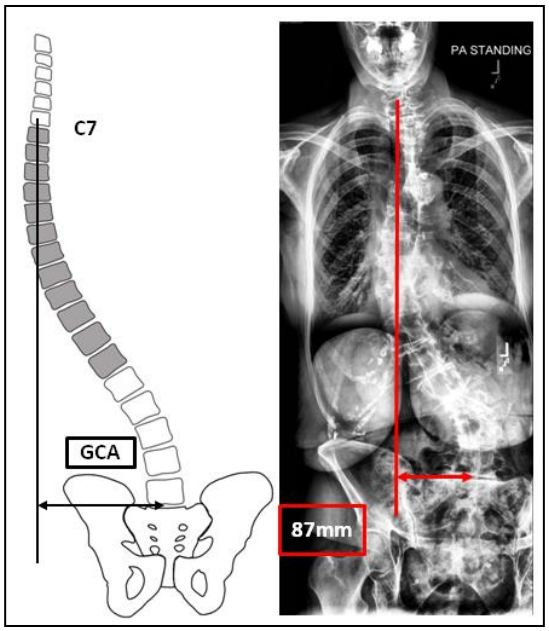

Figure 2-12: Global coronal alignment(GCA)

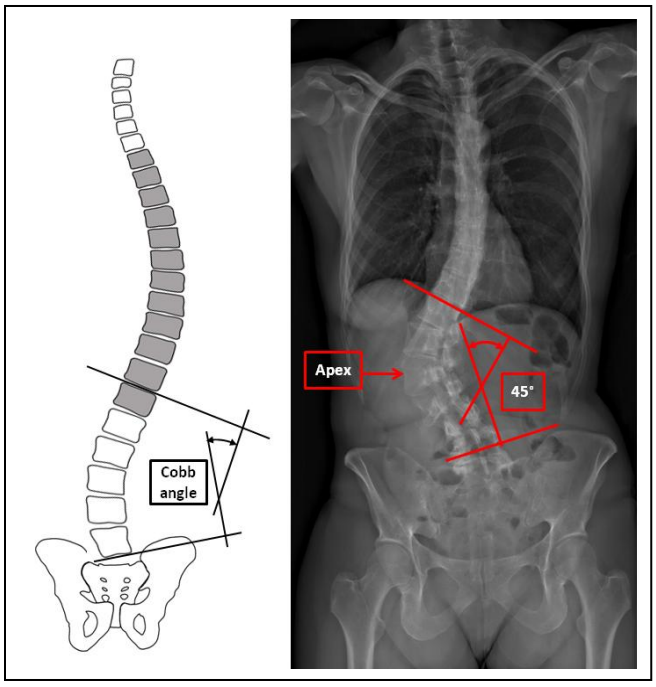

Figure 2-13: Cobb angle in the coronal plane

Despite the fact that the term "scoliosis" refers to a tridimensional deformity of the spine, these deformity are commonly identified on coronal radiography and quantified by the "Cobb" angle[27] measured between the extreme endplates of the most inclined vertebrae(Figure 2-13).

2.3.2 SAGITTAL ALIGNMENT

The analysis of the sagittal alignment is more complex and requires the characterization of several parameters for the spine, the hip and the global alignment.

Pelvic Parameters (Figure 2-14)

The most common pelvic parameters used across different groups, ages and pathologies consist of the pelvic incidence (PI), pelvic tilt (PT), and sacral slope (SS). These three parameters are directly related by the equation PI = PT + SS.

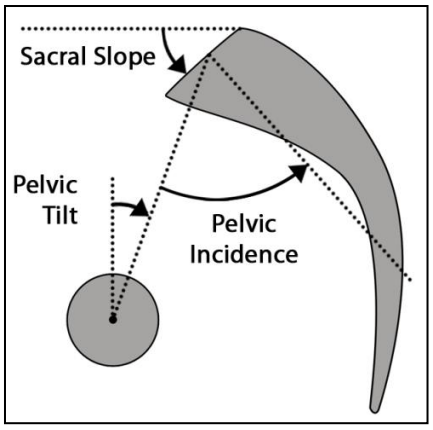

Figure 2-14: Pelvic Parameters (PI = PT + SS), with PI: pelvic incidence, PT: pelvic tilt and SS: sacral slope

Pelvic incidence[26,28] (PI) is the angle created by a line drawn perpendicular to the sacral plate starting from its midpoint, and the line drawn between this midpoint and the femoral heads. This measurement reflects the overall shape of the pelvis which remains fixed within an individual upon skeletal maturity and remains unchanged regardless of the patient position. Duval-Beaupere is credited as the first to define the term “pelvic incidence”[26] as the key factor in regulating sagittal alignment. Hewent on to define values for pelvic and spinal parameters in regards to a “correctly oriented pelvis” and “optimal lordotic positioning”.

Different studies analyzed the sagittal spino-pelvic alignment, and proposed references for key parameters (Table 2-5). Mean value for PI varied between 48° and 52°, lower values around 35°, and higher values near 85°. The Figure 2-15 illustrates three examples of pelvic incidence.

Two positional parameters typically referenced are pelvic tilt (PT) and sacral slope (SS). PT is the angle formed by a line drawn with the vertical axis and a line connecting the midpoint of the femoral heads and the midpoint of the sacral plate. This angle describes the orientation of the pelvis and changes as a lower PT is created by tilting the pelvis forward (anteversion), while a higher PT is created by tilting the pelvis backwards (retroversion). With a higher PT, the sacral endplate becomes more horizontal and the sacrum becomes more vertical. In a normal standing adult individual, the pelvis is in slight retroversion , with a mean PT ranging from 10° to 16° with a standard deviation around 6 °.

The SS is the angle formed from a line drawn with the horizontal and a line drawn along the sacral endplate. The minimal value for SS is 0 degrees (the mean value between 36° to 46° with

a standard deviation around 8°). As seen from the equation for PI, the sacral slope varies inversely with the PT and dictates the position of the lumbar spine (Figure 2-16).

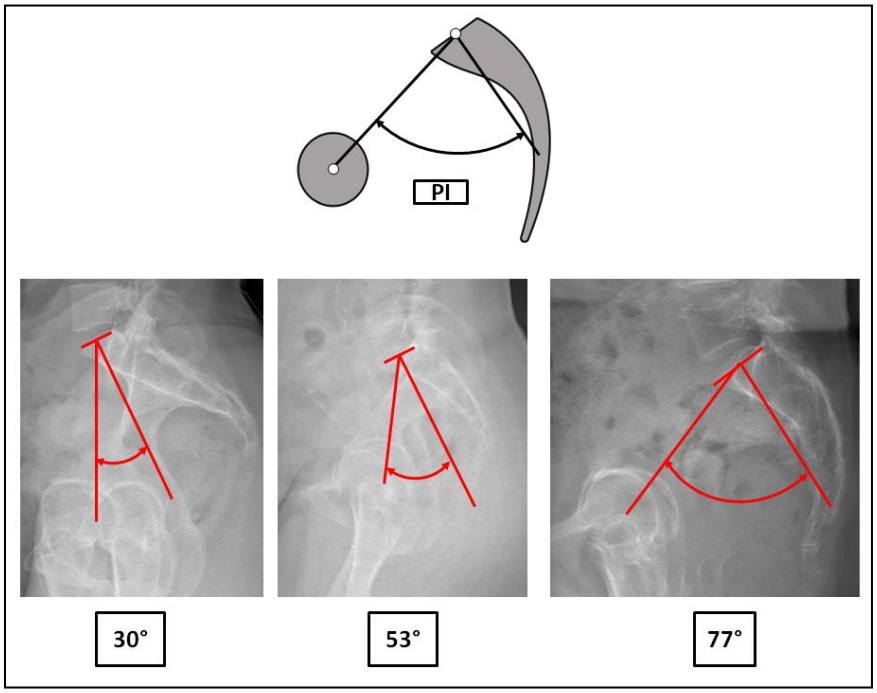

Figure 2-15 three examples of pelvic incidence

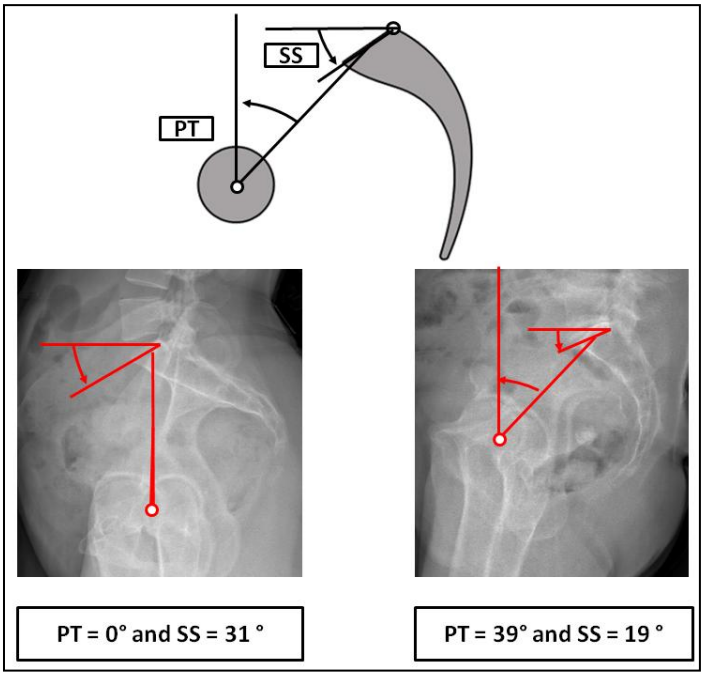

Figure 2-16: Sacral slope (SS) and Pelvic tilt (PT) and two radiographic examples

Spinal Curvatures (Figure 2-17 and Table 2-5)

The spinal curvatures are commonly defined by the lumbar lordosis (LL), the thoracic kyphosis (TK), and the cervical lordosis (CL). The lumbar lordosis (LL) is commonly measured as the angle formed from the lines drawn along the cranial endplates of L1 and of S1. The measure of thoracic kyphosis (TK) is made using the angle formed by the intersection of the lines drawn from the caudal end plate of T12 and the cranial end plate of T4.

Mean reported values for L1-S1 lumbar lordosis on asymptomatic adult subjects varied from 43° to 63° with a standard deviation around 10° and extreme values spanning the 19 ° to 90° range, while the mean T4-T12 thoracic kyphosis was reported between 34° to 44° and ranged from 0° to 76°.

In an effort to define physiological curvatures, Vialle and Roussouly [29,30] used the transitional vertebra, the vertebrae at the junction of the TK and LL, to obtain maximum values for these parameters. The maximum LL is obtained using the cranial end plate of S1 and the cranial end plate of the transitional vertebra and the maximum TK is measured using the angle between the cranial end plate of T4 and the caudal end plate of the transitional vertebrae.

The cervical lordosis is commonly measured from C2 to C7, with reported values on asymptomatic subjects ranging from 15°±10° in young adults to 25°±16° in subjects over 60 years old[31] .

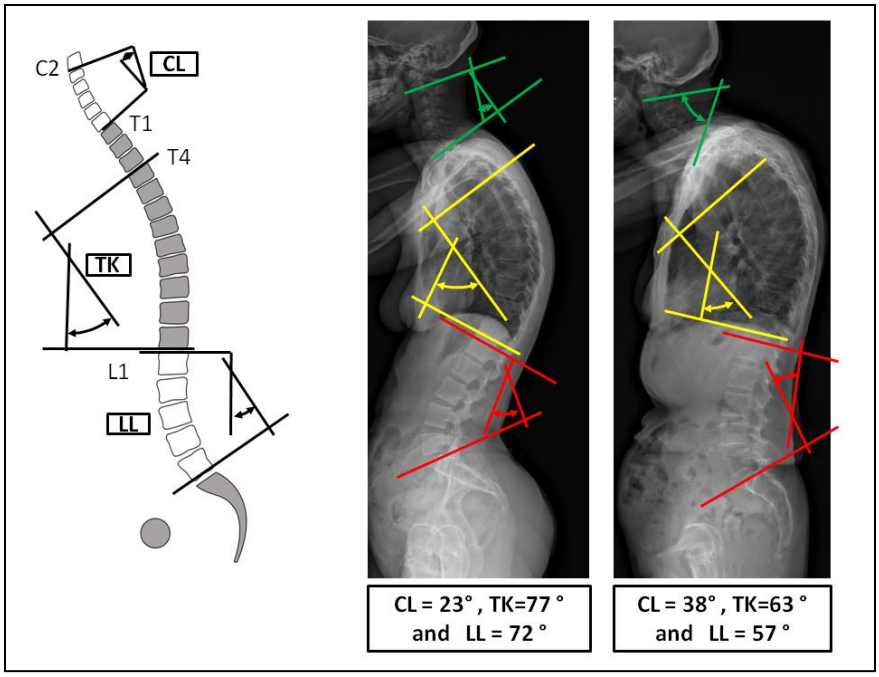

Figure 2-17: Spine curves : Cervical lordosis (CL), thoracic kyphosis (TK) and lumbar lordosis (LL)

Study	Year	N	Age	Spine curve				Pelvis parameters		
				Thoracic kyphosis (°)		Lumbar lordosis (°)		PI (°)	PT (°)	SS (°)
				T4-T12	T4-max	L1-S1	max-S1			
Stagnara[32]	1982	100	[20-29]		37 [7 - 63]					41 [19-65]
During[33]	1985	52	[19-44]					49(8)	10(6)	40 (9)
Gelb[34]	1995	100	57 (11)	34 (11) [9 - 66]						46 (9) [17-68]
Legaye[26]	1998	28 (M)	24 (6) [19- 50]					53 (10)	12 (7)	42 (8)
		21 (F)						48 (7)	10 (5)	38 (8)
Jackson[35]	2000	75	39 [20-63]	39 (12) [17-76]		63 (12) [35-90]				
Vaz[36]	2002	100	27(4) [23-45]					52 (12) [33 -85]	12 (6) [-1 -28]	39 (9) [20- 66]
Guigui [37]	2002	250		41 (9) [7 - 65]	42 (9) [7 - 66]	43 (11) [14- 62]	63 (13) [38-101]	55 (11) [33-104]	13 (7) [-4 - 45]	42 (8) [19- 64]
Duval-Beaupere [38]	2004	47	22					52 (10) [34-78]	12(6) [0-29]	40(8) [25-59]
Roussouly[39]	2005							55 (11) [33-82]	12(6) [-5- 31]	40(8) [21-66]
Vialle[30]	2005	300	35 (12) [20-70]	41 (10) [0-69]	41(10) [7-66]		60(10) [30-89]	55 (11) [33-82]	13 (6) [-5- 27]	41(8) [17-63]
Schwab[40]	2006	25	30 (6) [21-40]	38(12)		60(14)		52 (10)	13 (7)	39(9)
		24	47 (6) [41-60]	37(9)		60(8)		53 (8)	14(6)	40(7)
		22	71 (5) [60- ?]	44(12)		57(11)		51 (9)	16 (6)	36 (9)
Gangnet [41,42]	2003 2006	27	30 (9)	36 (8)		51 (8)		50 (9)	13 (7)	38 (6)
Mac-Thiong[43]	2010	354 (M)	38 (15) [18-81]					53 (10)	13 (7)	39 (8)
		355(F)	36 (14) [18-76]					52 (11)	13 (7)	40 (8)

Table 2-5: Value of the sagittal spino-pelvic radiographic parameters for asymptomatic subjects
Mean (m), standard deviation (STD), minimal (min) and maximal(max) : m, (STD), [min-max]

Global Alignment (Figure 2-18 and Table2-6)

There are numerous published parameters permitting the evaluation of the global spino-pelvic alignment. The most common one is the sagittal vertical axis (SVA)[44], defined as the horizontal offset from a plumb line dropped from C7 (C7PL) to the postero-superior corner of the sacral plate. In a well-aligned spine, the C7PL is located behind or at the posterior edge of the sacral endplate[43]. When the C7 PL is in front of the femoral heads, the spine is misaligned. Normative mean of asymptomatic adult subject varied between -32 mm and 30 mm with a large range varying from -101mm to 77mm. The evaluation of this parameter necessitates calibration of the X-rays.

In line with this parameter, the T1SPi, T1 sagittal spino-pelvic inclination, has also been described in the literature[30,45] as a measurement of the global spino-pelvic alignment. This parameter is defined as the angle between the vertical and the line drawn from the center of the T1 vertebral body to the center of the bicoxofemoral axis. The T1SPi correlates strongly with the SVA and the angular nature of the parameter offers the advantage of not requiring calibrated xrays.

T9 sagittal spino-pelvic inclination (T9SPi) is another parameter reflective of the global alignment of the spine. It was first introduced by Duval-Beaupere[45] as an indicator of the position of the body center of mass[28]. As for the T1SPi, this measurement is the angle between the vertical and the line drawn from the center of the T9 vertebral body to the center of the bicoxofemoral axis. The mean T9SPi is typically 10.5° +/- 3° in asymptomatic adults and correlates strongly with thoracic kyphosis[30].

More recently, and in an effort to evaluate the trunk inclination in regards to the sacral inclination, Roussouly et al[29] introduced the spino-sacral angle (SSA). This parameter is defined as the angle between the C7/S1 line and the sacral inclination. Normative values for SSA were reported by Mac-Thiong et al[43] who established a mean value of 130.4° +/- 8.1 in their study of spinal balance in 709 asymptomatic adults.

The most recent parameter of global alignment is the T1 pelvic angle (TPA)[46]. This is the angle subtended by a line from the femoral heads to the center of the T1 vertebra, and a line from the femoral heads to the center of the sacral endplate. From a geometrical point of view, TPA is equal to the sum of T1SPi and PT. This angular measurement presents the advantage of not being affected by the patient positioning. In a recent study from Protopsaltis et al[46] on adult spinal deformity, it has been demonstrated that TPA correlates with SVA (r= 0.837), PT (r= 0.933), and PI-LL (r=0.889). Based on the work of Vialle et al[30], the average value for TPA was 12° in asymptomatic population.

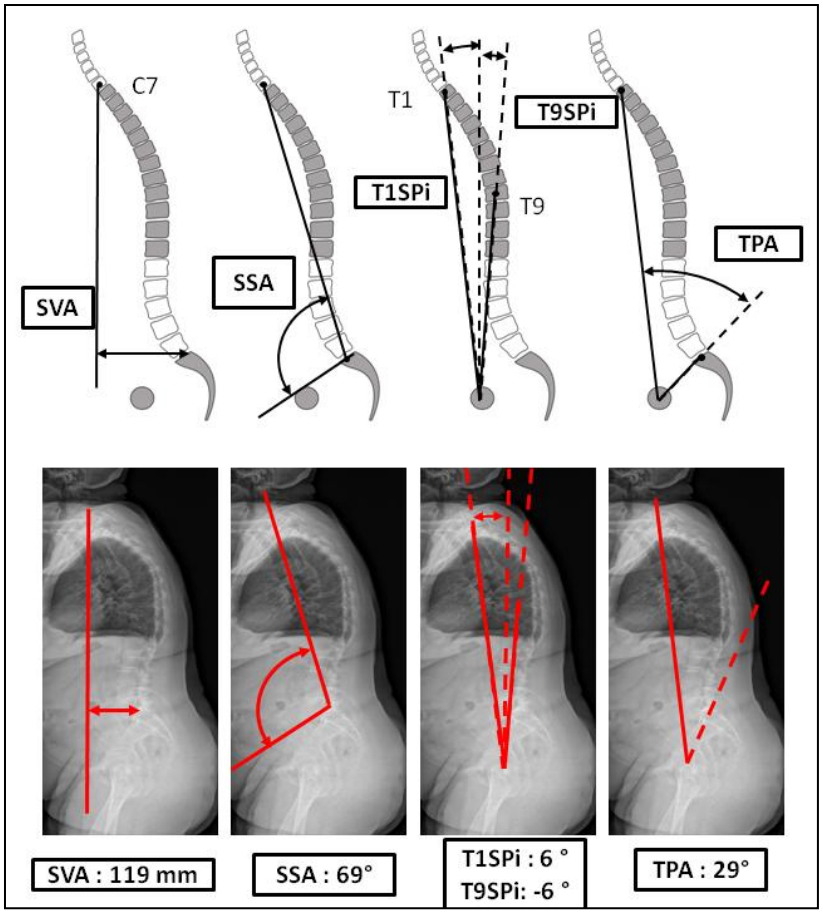

Figure 2-18: Sagittal vertical axis (SVA), Spino-sacral angle (SSA), T1 sagittal spino-pelvic inclination(T1SPi), T9 sagittal spino-pelvic inclination(T9SPi), T1 pelvic angle (TPA)

Of note, the SVA and T1SPi do not take into account the retroversion of the pelvis (pelvic tilt) in their evaluation of sagittal alignment in contrary to the TPA. The SSA take into account the sacral slope in addition to the inclination of T1. However, with only the TPA or SSA it is not possible to evaluate if the patient have an anterior shift due to the possibility of compensation at the level of the pelvis. This mechanism of compensation will be described in the section 0.

With the development of long X-rays, parameters describing the global sagittal alignment and taking into account the position of the head has emerged. The large weight of the head is an essential element of the regulation of the posture. Gangnet et al[41] as well as evaluate the sagittal distance between the middle of the femoral head and the center of the acoustic meati. In order to not be limited to uncalibrated x-ray, Steffen et al[47]introduces the angle between the vertical and the line drawn from the center of the center of the acoustic meati to the center of the bicoxofemoral axis (Figure 2-19).

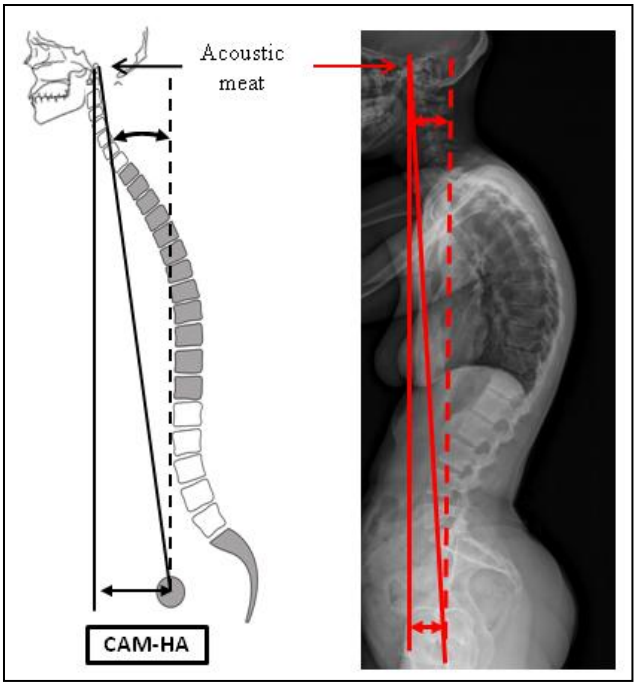

Figure 2-19 CAM: acoustic meat and HA : middle of the femoral head

Study	Year	N	Age	Global sagittal alignment					
				SVA (mm)	T1SPi (°)	T9SPi (°)	SSA(°)	TPA(°)	CAM-HA
Gelb[34]	1995	100	57 (11)	-32 (32) [-101 - 77]					
Guigui[37]	2002	250				-11 (3) [-20-3]			
Duval-Beaupere[38]	2004	47	22			-11(3) [-20-5]			
Vialle[30]	2005	300	35 (12) [20-70]		-1(3) [-9 - 7]			12	
Gangnet [41,42]	2003 2006	27	30 (9)	30 (9)		-9 (3)			[-55-40] (mm)
Steffen[48]	2009	23	18						-3 (2) (°)
Mac-Thiong[43]	2010	354 (M)	38 (15) [18-81]				130 (9) [113-146]		
		355 (F)	36 (14) [18-76]				131 (8) [113-146]		

Table2-6: Value of the global sagittal parameters for asymptomatic subjects
Mean (m), standard deviation (STD), minimal (min) and maximal(max) : m, (STD), [min-max]

Error of measurement

Several software programs are available to measure the different angles or distances[21,40,49–54]. Comparison between manual and computer assisted measurements have been evaluated demonstrating a lower variability for computer methods[49,52]. The error of measurement for angular measurements is comprised between 2-3° with lower error for pelvic angles and greater for spine angle. For distance, the error of measurement is comprised between 2 and 5 mm. For this work, two software have been used: Spineview developed by the Laboratory of Biomechanics Arts et Metiers ParisTech (LBM, Paris, France) and the Laboratory of orthopedic imagery from the superior technology school of Montreal (LIO, Canada)[53,54] and Surgimap developed by Nemaris, New York[21].

EOS system

EOS system® is the results of a collaborative effort between Georges Charpak (Nobel Prize in Physics 1992), the LBM, the LIO and the Saint Vincent de Paul hospital(Paris , France). This system[55] is based on a very sensitive X-ray detector permitting a low radiation dose acquisition [56]. Combined with three-dimensional reconstructions from stereoradiography, the system permits to estimate the personalized geometry of the cervical spine[57], the thoraco-lumbar spine[58], the hip[59] and from the lower limb[60]. This recent technology also permits to evaluate the relative location of the main bones in the setting of an erected posture Figure 2-20.

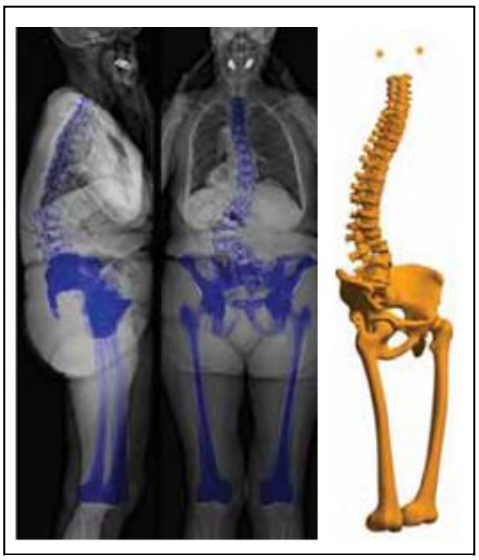

Figure 2-20: EOS system with stereo radiography and three dimensional

SUMMARY

The analysis of alignment with radiographic parameters requires that regional and global parameters in both the coronal and the sagittal planes be taken into account. If the asymptomatic coronal alignment is relatively simple (the head, the spine and the pelvis have to be aligned), the alignment in the sagittal plane is more complex and necessitate more attention. With the development of larger radiographic acquisition fields, there is an ambition to take into account the entire skeletal (head to the feet) into in the alignment analysis.

2.3.3 CORRELATIONS BETWEEN KEY SAGITTAL RADIOGRAPHIC PARAMETERS

The complexity of the sagittal spino-pelvic alignment resides also in the inter-relationship among the different parameters. This specific question has been a topic of research for several teams; findings in the setting of asymptomatic adults are summarized Table 2-7.

	Pelvis parameters		Spine curve		
	PT (°)	SS (°)	Thoracic kyphosis (°)	Lumbar lordosis (°)	
PI (°)	0.54*	0.84*	-	0.60*	Legaye et al[26]
	0.62*	0.81*	-	0.62*	Berthonnaud et al[61]
	0.66*	0.81*	0.04	0.69*	Vialle et al[30]
	0.65*	0.80*	-	-	Roussouly et al[39]
PT (°)		-	-	NS	Legaye et al[26]
		NS	NS	0.21	Berthonnaud et al[61]
		0.13	-0.12	0.26	Vialle et al[30]
		NS	-		Roussouly et al[39]
SS (°)			-	0.86*	Legaye et al[26]
			NS	0.65*	Berthonnaud et al[61]
			0.06	0.86*	Vialle et al[30]
Thoracic kyphosis (°)				-	Legaye et al[26]
				0.21*	Berthonnaud et al[61]
				0.35	Vialle et al[30]

Table 2-7 Pearsons's correlation between sagittal radiographic parameters in asymptomatic adults

Pelvic parameters:

As previously reported, the pelvic incidence is a morphological parameter linked to the pelvic tilt and sacral slope by a geometrical equation PI = PT + SS. In addition to this relation, a strong correlation exist between the SS and the PI (r between 0.80 to 0.84 depending on the studies). The PT also correlates with the pelvic incidence, but the coefficients are not as strong (0.55 to 0.65). Based on these correlations, Vialle et al[30] develops linear regressions connecting the pelvic incidence to the sacral slope on one hand and to the pelvic tilt on the other. Figure 2-21 illustrates these linear regressions for a pelvic incidence varying between 40 and 70°, and highlights the greater variation of sacral slope (range 32 to 51°) compared to variation of pelvic tilt (range 8 to 18°). Of note, no significant correlation was demonstrated between the pelvic tilt and the sacral slope.

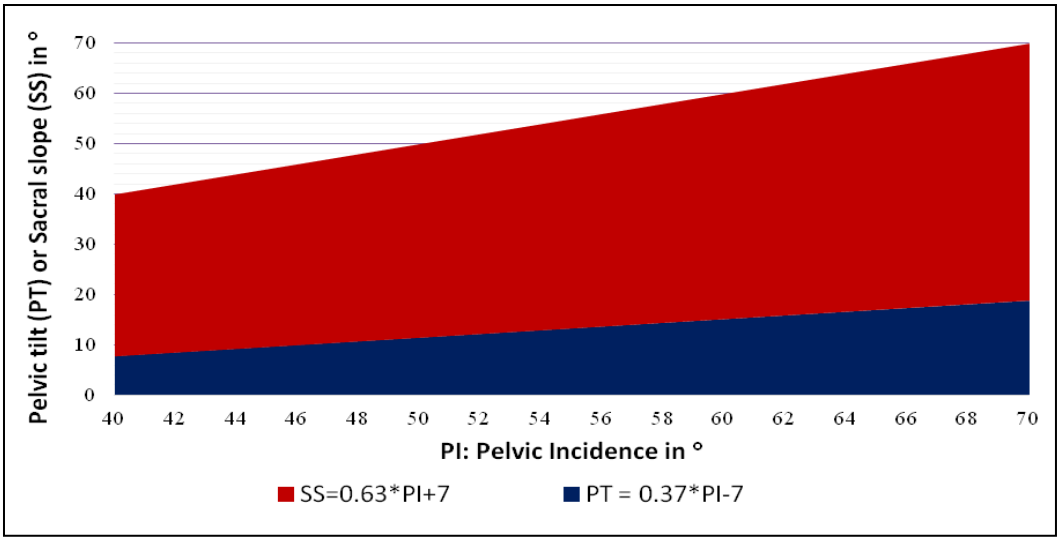

Figure 2-21: Linear regression between the pelvic incidence and the sacral slope on the one hand and the pelvic tilt on the other from Vialle et al[30]

Pelvic parameters and lumbar lordosis

Pelvic morphology and orientation ultimately determines the position of the lumbar spine. In an asymptomatic adult, a high correlation has been demonstrated between LL and SS (r : [0.65; 0.86]), while the correlation between LL and PI is slightly weaker (r:[0.60; 0.69]). No correlation between the LL and the PT was has been reported in the literature.

Based on these findings and, more specifically, the strong correlation between the sacral slope and the lumbar lordosis, Roussouly et al studied a group of asymptomatic volunteers to define four types of lumbar lordosis (Figure 2-22)[39]. The first two types are associated with a low SS (<35 degrees) and low PI; type 3 is a well-balanced lumbar spine with SS ranging from 35-45, and Type 4, is a balanced spine with accentuated curves throughout the thoracic and lumbar spines.

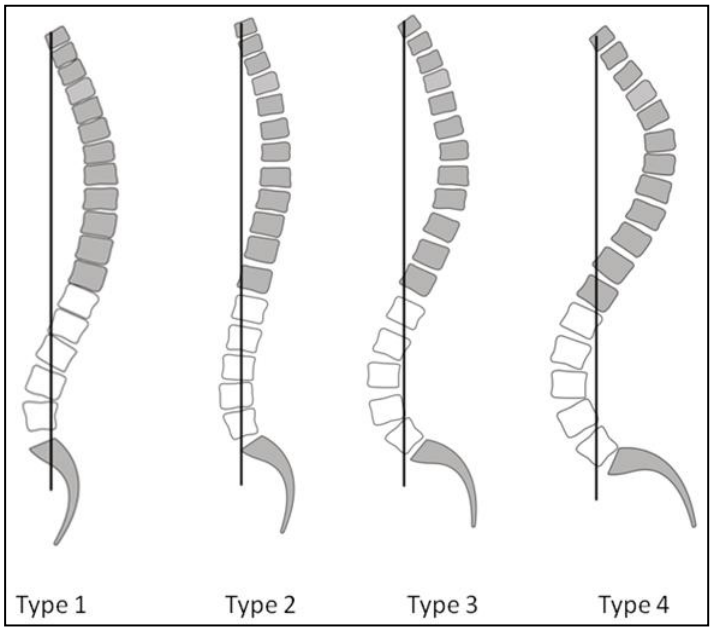

Figure 2-22: Classification of lumbar lordosis according to Roussouly[39]

Thoracic spine:

Contrary to the lumbar lordosis, the thoracic kyphosis seems relatively independent of the pelvic parameters. A weak correlation was found with lumbar lordosis by two studies[30,61].

In an analysis of 300 asymptomatic volunteers, Vialle et al[30] carried out a principal component analysis on sagittal radiographic parameters, and demonstrated that 90% of the variation of the parameters could be explained by three uncorrelated variables. The first variable included the pelvic incidence, the maximum lumbar lordosis and the sacral slope; the second one was the thoracic kyphosis and the third one the pelvic tilt.

SUMMARY:

In asymptomatic population, the sagittal alignment presents a large diversity and is based on the relation between the pelvis and the spine with the objective to keep the head upon the pelvis. The pelvic incidence, main morphological parameters seems to be key parameter, around which the different curve of the spine and the position of the pelvis adapt then with the respect of a certain harmony.

2.4 ADULT SPINAL DEFORMITY

2.4.1 DEFINITION, ETIOLOGY CLINICAL EVALUATION

As previously mentioned, the term "adult spinal deformity" refers to patients with deformation of the spine. This pathology corresponds to radiographic diagnostics of coronal and/or sagittal deformity and is not associated with an isolated etiology.

Etiology

One of the most representative populations are patients with a scoliosis, which is a deformation in the three plane of the space, but generally characterized by the coronal Cobb angle. Two main etiologies of scoliosis could be distinguished:

- Idiopathic scoliosis develop before bone skeletal maturity during childhood and adolescence. The curvature can progress during adult life. These curves can get worse in the older patient due to degeneration of the discs. Additionally, arthritis sets in facets which leads to the formation of bone spurs. This can result in pain and stiffness of the back. In more severe cases, patients may also develop shooting pain and numbness down the legs due to pinched nerves[62].
- "De novo" or degenerative scoliosis which starts after skeletal maturity and is thought to be the result of arthritis or degeneration of the spine, with changes in alignment due to degeneration of the discs and the facet joints, generally in the lumbar spine. It is usually accompanied by straightening of the spine from the side (loss of lumbar lordosis). Pain, stiffness, numbness and shooting pain down the legs are seen in symptomatic patients[63].

In addition to those etiologies, others causes could be observed for scoliosis as congenital malformation[64] (ex: hemi vertebrae), advanced form of tuberculosis[65], trauma or tumor.

Independently of the etiology, scoliosis are 3D deformations, with an axial component and can lead to sagittal or coronal misalignment. In a multi-centric prospective data collection of ASD patients, those scoliotic patients represent around 80% of the ASD population, and 68% of them have in addition a sagittal misalignment[66].

In addition to those 3D spine deformations, the other main deformation types are in the sagittal plane. Those patients represent around 20% of the ASD population[66]. Several etiologies can lead to those sagittal deformities:

- joint ankylose due to specific spondyloarthropathy, where the lumbar lordosis is fused and in generally in a position not adapted to the pelvic incidence which leads the patients to increase its pelvic tilt (retroversion around the hip)[67]
- iatrogenic deformity[68] : this type is seen in patients who had previously undergone spinal surgery either for scoliosis or for degenerative low back conditions. One of the most well know iatrogenic deformation is the flat back syndrome[69] defined as where the lumbar lordosis is fused in a position not adapted to the pelvic incidence (Figure 2-23-A). Another category is “Junctional Kyphosis”[70,71] which is an angular deformity (kyphosis) that develops just above or below a previous spinal fusion
- global hyper-kyphosis where the kyphosis is extend to the lumbar area(Figure 2-23-B).

Figure 2-23: patient with a iatrogenic flatback (A) and patient with global hyper-kyphosis (B)

Clinical evaluation

In regard to the large diversity of deformity and in order to standardize the evaluation of adult spinal deformity (ASD), health-related quality of life (HRQOL) instruments are widely used in clinical practice and the scientific community. In ASD population, the most common questionnaires are the short form(SF)[72–75], the Oswestry Disability Index (ODI)[76,77], and the Scoliosis Research Society (SRS) [78–80].

The SF is considered to be a generic and universal measure of health state and is not disease specific. Therefore, it permits the comparison of clinical impact of different diseases. The objective of the ODI questionnaire[77] is to evaluate how low back pain affects the ability of the patient to function on a daily basis. SRS score[78–80] has been developed to obtain a disease-specific HRQOL instrument for spinal deformity. This questionnaire evaluates four domains (function, pain, self-image and mental health), and includes a global evaluation (SRS Total) as well as a score to evaluate the satisfaction of the patient regarding the treatment received.

Minimal clinically important difference (MCID).

While clinical scores are now widely used, their interpretation is still a domain of active research. In this context the minimal clinically important difference (MCID) is now more and more employed. MCID represents the smallest improvement in a given score considered worthwhile by a patient, and, therefore, it is used to differentiate a statistical difference from a clinical one perceived by the patient.

Several MCIDs are defined in the literature for the SF-12 (range 6.1 to12.6) [18,81–83] and ODI (range 6.8 to 18.8)[18,81–83] in the setting of ASD population. Only one study defined MCID SRS scores[83] for ASD patients (Table 2-8). No MCID were available for the SRS Total and Satisfaction domains.

SRS Pain	SRS Appearance	SRS Activity	SRS Mental
+ 0.587 points/ 5	+ 0.8 points/ 5	+ 0.375 points/ 5	+ 0.42 points/ 5

Table 2-8: MCID value for the SRS domains

Reference values on asymptomatic subject

Scores on asymptomatic population are essential to correctly interpret results obtained in the setting of patients suffering from different pathologies. This is specifically true in the setting of ASD population where patients are covering a large range of ages (> 18 years old without any limit in the elderly population).

As previously explained, the SF score measures health values that are not age, treatment, or disease specific and can therefore be applied on a population of asymptomatic subjects. In addition, Baldus et al[84] published their work on 1346 asymptomatic adult subjects. The results were stratified by age and sex.

SUMMARY

Adult with spinal deformity is defined with radiographic criteria and regroups a broad spectrum of etiology. For the clinical evaluation of those patients, to the development of HRQOL scores, useful tools as MCID and normative values on asymptomatic subjects are available for their interpretation. Despite active research, there is no guideline to evaluate clinical effectiveness of treatments in the setting of ASD patients. Therefore, a part of the personal work was dedicated to develop an innovative method to clinically evaluate the treatment of ASD patient.

2.4.2 MALALIGNMENT, PAIN AND DISABILITY

Symptoms developed by ASD are mostly a combination of back pain, radicular symptoms (radiating leg pain, weakness, and numbness), neurogenic claudication unrelieved by lumbar flexion or sitting, loss of upright posture, increased disability, bowel and urinary dysfunction, and even cauda equina syndrome[85]. These symptoms may be severe enough to blight quality of life as cancer or diabetes[5].

As demonstrated by Bess et al [86], pain and disability determine treatment modality (operative or conservative), while deformity guides treatment for younger patients with idiopathic scoliosis. The developement of a multi or monocentric database including not only HRQOL scores but also radiographic parameters that have permitted a better understanding of the relashionship between clinical outcomes and radiographic alignment. While the interest for sagittal alignment is not new, these databases have permitted clearly identified parameters of interest and highlighted their relevance[26,87].

Coronal Plane

Historically, the coronal Cobb angle has been considered the most important parameter for the diagnosis and management strategy of patients with ASD. However Schwab et al[88] on 95 ASD patients and then Glassman et al[13] on 352 ASD patients, revealed that there was no significant correlation between the magnitude of the Cobb angle (or the number of vertebrae involved in the coronal curve) and pain or disability of patient. Nevertheless Glassman et al[13] demonstrated that thoracolumbar and lumbar curve generate less favorable clinical scores than thoracic curves.

More recently on 492 patients, Schwab et al[14] reported a poor correlation between clinical score and Cobb angle (ODI, r= 0.201 and SRS, r=0.128). If these results have reduced the clinical interest for the Cobb angle, it remains a gold standard radiographic parameters and still play an important role in the description of spinal deformity. According to the SRS-Schwab classification, the threshold for pathological Cobb angle in the setting of adult spinal deformity is 30°[89].

Glassman et al[13] also noticed that coronal misalignment, evaluated with the GCA, greater than 4 cm was associated with deterioration in pain and function scores for un-operated patients, but not in patients with previous surgery.

Sagittal Plane

The most common and important results of studies evaluating the relation between patients reported outcomes in alignment related to the importance of the sagittal plane.

Across all the studies, global sagittal misalignment seems to be the radiographic parameters which contributes the most to the clinical deterioration of the patients. Glassman et al found a linear relationship between the severity of symptoms and the quantity of positive sagittal alignment measured by the SVA[90]. Lafage et al[16] demonstrated that SVA and truncal inclination (T1SPi) were two of the 3 radiographic parameters that most highly correlated with clinical outcomes; the third one was the pelvic tilt. The same team in another study[14] of 492 patients demonstrated that the SVA was the parameters that most correlated with the ODI (r=0.469).

The lack of lumbar lordosis has also been identified as a clinically relevant parameter. Glassman et al demonstrated that lumbar kyphosis was very poorly tolerated by patients[13]. This relation between loss of lordosis and a clinical deficit was then highlight by Schwab's team[14]; they reported that the lack of harmony between pelvic incidence (PI) and lumbar lordosis (LL), quantified by the "PI minus LL (PI-LL)" mismatch was significantly correlated with pain and disability, (PI-LL) (Figure 2-24). Correlation with clinical scores was evaluated at r=0.450 for the ODI and r=0.377 for the SRS. Independently neither the lumbar lordosis nor the pelvic incidence were correlated to clinical outcomes in this study, reflecting that a crucial element of the posture is the harmony between the pelvis and the lumbar spine. More recently, and in line with this concept, Boissiere et al[91] introduced the ratio between the lumbar lordosis and the pelvic incidence (LL/PI) and demonstrated that this parameter can guide the surgeon's decision in the case of surgical treatment.

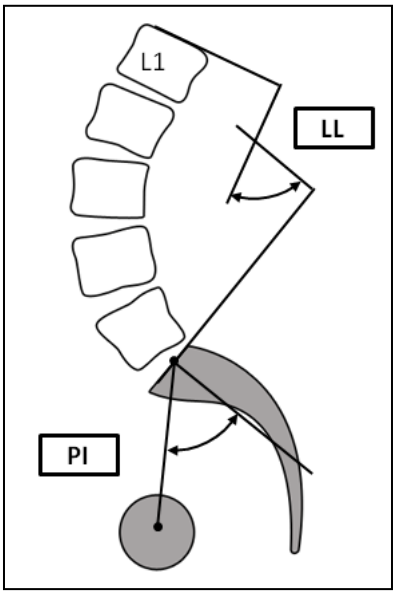

Figure 2-24: PI: Pelvic incidence; LL: Lumbar lordosis evaluate between the superior endplate of L1 and the sacral slope

Of note in both instances (i.e. PI-LL and LL/PI), the lumbar lordosis was evaluated between the superior endplate of L1 and the sacral endplate, and did not take into consideration the possible variation in the lordosis shape[39].

As previously reported, pelvic tilt is also one of the radiographic parameters the most highly correlated with clinical score[14,16,92]. An increase in pelvic tilt (i.e. retroversion) is associated with a worsening of patients reported outcomes.

More recently the parameter combining the sagittal misalignment and the pelvic tilt as the TPA[46] or the SS as the SSA and has been also correlated with the deterioration of the patients.

The knee flexion has been also associated with a worsening of the pain and disability in a retrospective study of patients who underwent a full body EOS images[93].

Restoration of sagittal alignment and clinical outcomes

In addition to these correlations, several studies have demonstrated that the correction of the sagittal misalignment implies a clinical benefit for the patients[18,94,95]. Blondel et al[18], on 76 ASD patients underlined that the correction of the SVA improves the clinical outcomes of patients at 2 years. This improvement was even more substantial if the restoration of the sagittal global alignment was complete. More recently, in an analysis of 341 patients who received conservative or surgical treatment, Smith et al[95] demonstrated that patients who sustained a correction of PT, SVA, or PI-LL were significantly more likely to achieve minimal clinically important difference for ODI, SF-36 physical component score (SVA and PI-LL only), SRS activity, and SRS pain (PI-LL only) than patients who did not.

SUMMARY

The collection of clinical outcomes and radiographic measurements together have highlighted the importance of sagittal alignment and its restoration in the treatment of ASD patients. The primary parameters identified as clinically relevant are:

- SVA: global assessment of the sagittal alignment
- PI-LL: regional harmony between the pelvis and the lumbar lordosis
- PT : retroversion of the pelvis, major compensatory mechanism at the level of the pelvis

That is why, in the personal work, the efficiency of the surgical treatment to restore those parameters has been explored.

In the following section, the different mechanism used by patient to maintain a functional posture despite sagittal malalignment would be described.

2.4.3 COMPENSATION MECHANISMS OF SAGITTAL MALALIGNMENT

In total, around 75% of the ASD patients present a sagittal malalignment[66]. Independently of the etiology, the erected posture is characterized by a horizontal gaze with the objective of maintaining the head aligned with the pelvis in the most economic way to conserve a high level of functionality.

Dubousset et al[87] developed the concept of "polygon of sustentation" and "conus of economy"(Figure 2-25). The "polygon of sustentation" is defined as the surface where the gravity line of the body moves around when the subject is in the standing position. The "conus of economy" is defined as the cone in which the body can stay balanced within the surface of the "polygon of sustentation" with minimum muscle action.

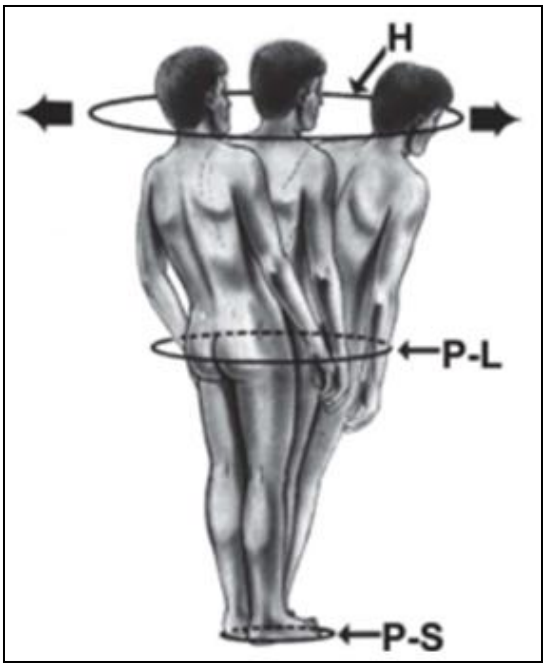

Figure 2-25: Illustration of the "conus of economy", P-S : polygon of sustentation, P-L: pelvic level, H: Head[87]

Patients with spinal deformity will recruit different mechanisms of compensation in an effort to maintain the gravity line within the "conus of economy" despite a sagittal misalignment. Independently to the etiology, those mechanisms of compensation are common to most of ASD patients[15,16]. These mechanisms can occur in the spine, the pelvis and in the lower limb area and it is fundamental to take them into account during the evaluation of the sagittal spino-pelvic alignment [15].

Cervical lordosis

The ability of increasing the cervical lordosis to reduce the sagittal misalignment between the head and the pelvis is still controversial. Moreover, if this reduction is effective, compared to the others mechanisms, the effect on sagittal alignment would be limited. However this increase of the lordosis could permit to maintain the horizontal gaze despite a sagittal misalignment[96].

Thoracic kyphosis

In young patients with a flexible spine, reduction of the thoracic kyphosis permit to limit the anterior shift[15,97–99]. However, it seems that in the case of rigid spine, the patient is not

able to reduce his kyphosis[99]. Of note there is not study demonstrating correlation between HRQL scores and flattening of the thoracic kyphosis.

Lumbar lordosis

The hyperextension of adjacent segments in the lumbar area can limit the consequence of the loss of lordosis[44,100]. However, this mechanism can increase the stresses on posterior structures, be associated with retrolisthesis, and may result in accelerated facet joints arthritis, inter-spinous hyperpressure (Baastrup's disease), and sometimes isthmic lysis[15].

Pelvis

One of the most efficient mechanisms to reduce sagittal misalignment is through pelvic retroversion (i.e. backward rotation) [16,44,92,97]. Maximal pelvic retroversion is limited by hip joint extension and, when insufficient, can be associated to knee flexion in order to displace the proximal femurs posteriorly. Theoretically, subjects with low pelvic incidence have a more marked anterior opening of the acetabulum, with hips naturally in more extension, which result in a weaker capacity to adapt to sagittal misalignment [101]. In pathological conditions, as lumbar lordosis decreases (Figure 2-26-B), the pelvis retroverts (Figure 2-26-C), permitting a reduction in truncal inclination.

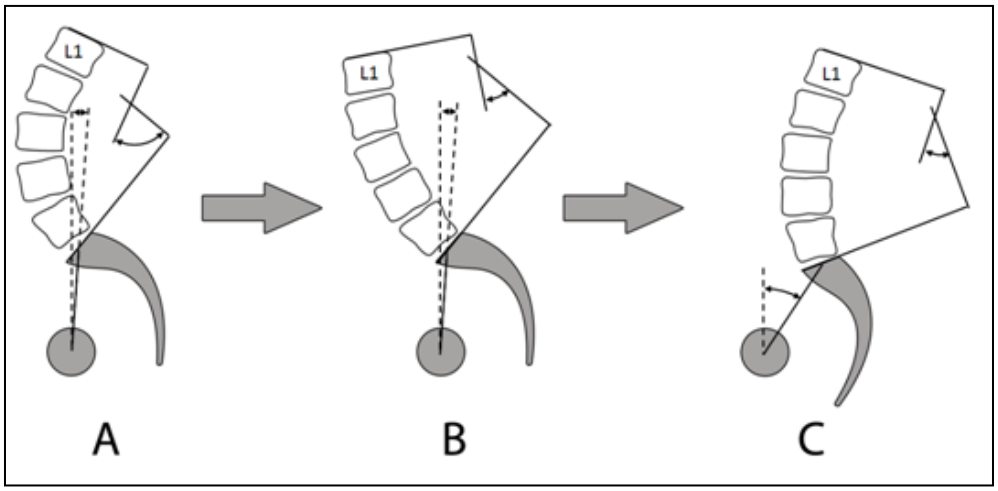

Figure 2-26: asymptomatic lumbar and pelvic tilt position(A), loss of lumbar lordosis (B), pelvic retroversion (C)

Knee

Another common compensation for spinal sagittal misalignment is knee flexion and has been described in several studies[17,102,103]. It implies recruitment of the anterior muscles of the thigh, additionally affecting gait pattern with increased energy expenditure and decreased walking autonomy. It generally appears after the exhaustion of compensatory mechanisms at the level of the spine and the pelvis[99]. Moreover previous studies reported the "knee-spine

syndrome" and proposed the loss of lordosis in the lumbar area as a compensation for a degenerated knee with a loss of extension[104,105]. It seems hard to distinguish between the primary and secondary pathology in this paradigm but in a study[99] it is suggested that spinal alignment is linked to knee flexion and both should be properly evaluated if either is abnormal.

Ankle

Finally, ankle extension (plantarflexion) is also a mechanism of compensation to maintain the gravity line of the body as close as possible to its natural position within the cone of economy. The gravity line is an extension of the body's center of gravity projecting onto the ground, and should remain between the feet, even in the case of an increased SVA [106].

As presented, the mechanisms of compensation are numerous, and to take them into account in the sagittal alignment analysis is not obvious.

The Figure 2-27 represents a patient with a sagittal misalignment due to a loss of lumbar lordosis. It also shows the various compensatory mechanisms: flattening of the thoracic kyphosis, retroversion of the pelvis, and knee flexion.

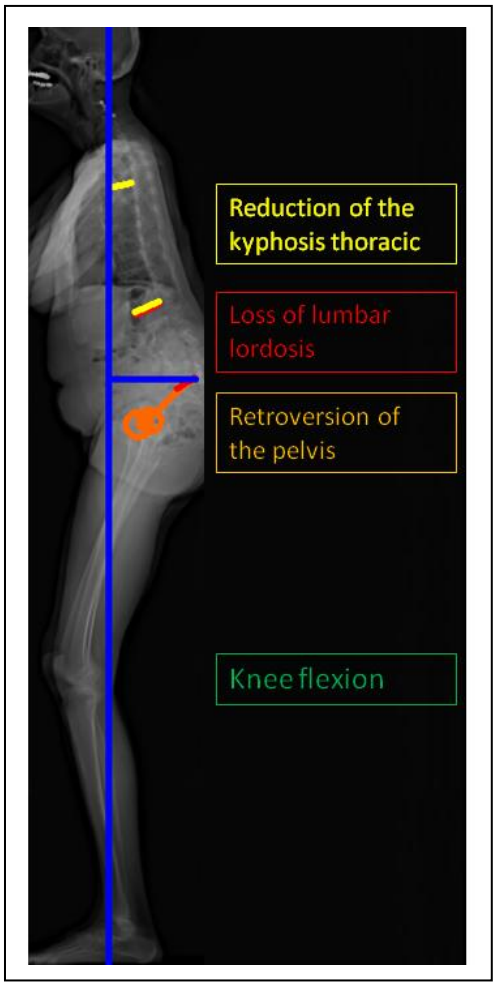

Figure 2-27: Patient with a sagittal malalignment (SVA: 134mm) due to loss of lumbar lordosis (LL=2° with a pelvic incidence of 77°). To compensate, patient reduces its thoracic kyphosis(TK=14°), retrovers its pelvis (Pelvic tilt=47°) and flexes the knee

As presented, compensatory mechanisms involved in the sagittal misalignment caused by ASD are numerous. Taking these mechanisms into account when evaluating the ASD patients is challenging. Moreover the diversity in the amplitude of physiologic curves highlighted in the section 2.3.3, makes it difficult to show the distinction between adapted curves and compensations. Therefore, Barrey et al[15] described a three step algorithm to determine if the subject has asymptomatic alignment or a pathologic alignment define as either the presence of a compensatory mechanisms or a sagittal misalignment. The 3 steps of the algorithm are the following:

1. Evaluation of the pelvis incidence to determine the theoretical values for spino-pelvic positional parameters via the use of abacus of

asymptomatic radiographic measurements.

2. Evaluation of the global sagittal alignment using SSA and SVA/SFD ratio (SFD,sacro-femoral distance, the horizontal distance between the vertical bi-coxo-femoral axis and the vertical line passing through the posterior corner of the sacrum)[29]
3. Evaluation of the presence of compensatory mechanisms
    - Analysis of the regional spinal curvatures (lordosis and kyphosis) to identify the presence of compensatory discopathy and retrolisthesis.
    - Analysis of the pelvic retroversion in regards to the pelvic incidence. The presence of horizontal sacral plate is highly suspected of pelvis tilt mechanism.
    - Analysis of the knee flexion and to distinguish whether it demonstrates a primary local pathology or secondary to the knee recruitment to compensate for spinal sagittal misalignment.

However, if all the mechanisms have to be investigated, they are rarely all presented on one subject. At this point it is not clear why some patients do or do not recruit specific mechanisms. For instance, some patient presents a sagittal misalignment and do not retrovert the pelvis[107]. The analysis of the potential of compensation, which could be defined as the maximum utilization of all the mechanism of compensation for one subject, is still an area of active research and will probably require inclusion of the analysis of soft tissues which explains the high interest of it the following work on the muscular component.

SUMMARY

For ASD patients, common mechanisms of compensation exist to limit the sagittal anterior shift. Those mechanisms have been described for the spine, the pelvis, and in the lower limbs, but their recruitment and amplitude is still not clear and should require a better understanding of the muscles.

2.4.4 CLASSIFICATION OF ASD PATIENTS

ASD includes a large diversity of etiology and curve patterns with multiple mechanism of compensation; as a consequence, several efforts in developing a classification system for ASD have been reported in the literature [108–113]. The overall objectives of these classifications is to define a common language, provide organization to pathologic conditions, and provide guidance regarding treatment. In addition, the classification system needs to have a high reliability and reproducibility.

In the case of an adolescent with idiopathic scoliosis(AIS), the King Moe classification[114] and also its improvement by Lenke et al[115] is widely adopted as it provides treatment guidelines based on the curve types. Since these classifications rely mainly on coronal radiographic parameters, they are not adapted to ASD patients where sagittal alignment is the main radiographic driver of pain and disability.

There are two different approaches reported in the literature regarding ASD classification. The first approach focuses on the cause of the pathology [110] and a second focuses on radiograph analysis[111–113].

Cause classification: Aebi classification (Table 2-9)

The Aebi classification system[110] is composed of four Types (I, II, IIIa and IIIb) representing different possible etiologies. The Aebi classification has the advantage to be quite simple and clear[108] however the classification does not integrate pattern of deformity and therefore lack in providing treatment guidelines. Moreover, with the exception of the manuscript describing the classification, there is no publication based on the Aebi classification.

Type	Description	Cause
I	Primary degenerative scoliosis; Most commonly has curve apex L2–3 or L4	Disc degeneration (asymmetric); Facet joint degeneration
II	Idiopathic scoliosis that has progressed; Lumbar and/or thoracolumbar	Progression of idiopathic scoliosis (present since childhood) caused by degenerative disease and/or mechanical/bony reasons
IIIa	Secondary adult scoliosis; Typically thoracolumbar or lumbar-lumbosacral	Secondary to an adjacent curve of idiopathic, neuromuscular or congenital origin; Obliquity of pelvis caused by leg length discrepancy or hip abnormality; Lumbosacral transitional anomaly
IIIb	Deformity resulting from bone weakness (e.g., osteoporotic fracture)	Metabolic bone disease, osteoporosis

Table 2-9 Aebi adult deformity classification

Radiographs analysis classification:

Three classifications are based on coronal and sagittal radiographic analysis:

- Kuntz classification[111],
- SRS Lowe classification[112],
- SRS Schwab classification[113] (Figure 2-28)

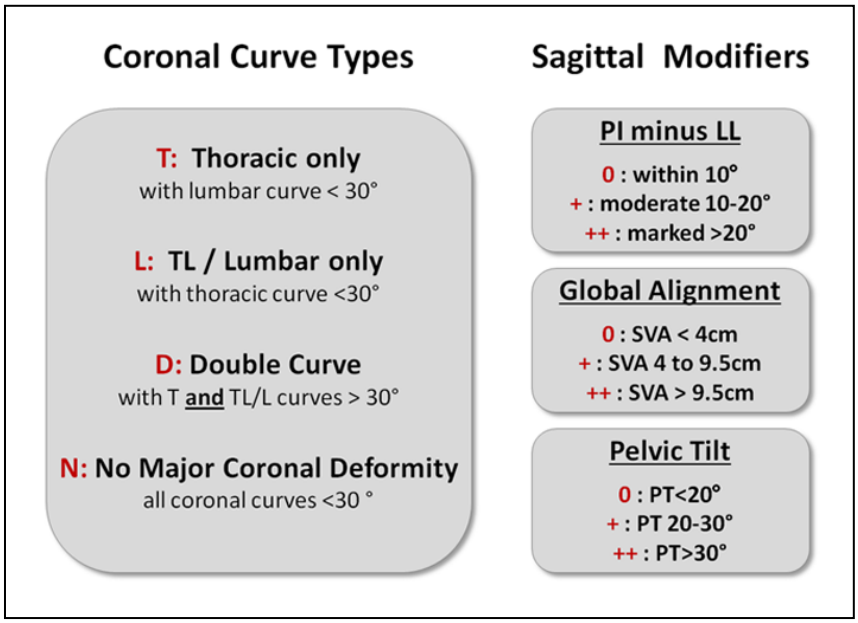

Figure 2-28:SRS-Schwab classification[113]

In these three classifications, the coronal plane is described with the number of curves and the position of the apex, with more or less details. Only the SRS Schwab did not include the coronal misalignment. All three classifications focus on sagittal alignment and include a global parameter as SVA. Both Kuntz and SRS Lowe classifications provided a detailed analysis on the kyphosis and lumbar curve. In addition, the Kuntz classification included descriptors for the cervical curve. The SRS Schwab classification did not include parameters for the kyphosis, due to lack of clinical relevance[14] and it being considered the lumbar lordosis in relation to the pelvic incidence. It is the only one which includes the pelvic incidence. Both Kuntz and Schwab classifications included the pelvis retroversion (pelvic tilt). The three classifications provide inter and interobserver reliability with a Kappa comprised between 0.67 and 0.83.[112,116,117]. The greatest reliability was for the SRS Schwab classification.

The specificity of the Kuntz classification is to provide normative values defining "neutral upright spinal alignment" for 4 groups of age (Juvenile, Adolescent, Adult and Geriatric).

However, this classification is complex, time-consuming and does not provide recommendation regarding treatment[116].

The SRS Lowe classification is an adaptation of the Lenke classification for AIS. For each parameter, pathologic threshold are defined, but their clinical relevance are not currently defined clearly.

The SRS Schwab was developed in a joint effort with the Scoliosis Research Society, and is the result of several years of active research and refinements [7,89,109,118,119]. The objective was to provide a simple classification based on the established correlations between patients reported outcomes and radiographic parameters. While the two other classifications include more than 20 parameters, the SRS Schwab classification is based on one descriptor for the coronal curve and 3 sagittal modifiers (SVA, PI-LL and PT). The three modifiers correspond to the 3 radiographic parameters the most correlated with clinical outcomes, and each modifier can assume three grades (0, + and ++). Thresholds between non-pathologic (grade 0) and pathologic (grade +) were obtained via regression analysis with ODI and are defined as: SVA>40 mm, PI-LL> 10°, and PT>20°. Smith et al [95], on 341 ASD patients, operative and nonoperative, demonstrated that sagittal modifiers grade are responsive to change in pain and disability and reflect significant changes in patient-reported outcomes.

SUMMARY

Although SRS Schwab classification has some limitations (little consideration for clinical state of patient, primary/revision, coronal misalignment), it provides a simple, reliable and clinically relevant classification. This classification is more and more used in research and clinical community[89,95,117,120], and has been validated and used on non US population[121,122]. Despite the fact that guidelines between the different curve types and a specific treatment is not clearly defined in contrary to Lenke classification of AIS, Terran et al[89] demonstrated an association between SRS Schwab classification and the choice of operative versus non operative treatment. Moreover, the decrease in SRS-Schwab modifier grade have been linked to clinical benefit[95]. Those advantages have led to the utilization of the SRS-Schwab classification in the personal work.

2.4.5 SURGICAL TREATMENT AND PLANNING

Like any other orthopedic conditions, treatment for ASD patients could be either conservative or operative. These two treatment options share a common objective of decreasing the pain and disability[86,123,124]. However, indications for surgical treatment are not clearly defined. The surgery should be contemplated for patients who develop intractable marked pain and unacceptable disability despite exhausting non-surgical management options. As previously mentioned severe radiculopathy, radicular weakness, and greater sagittal imbalance are likely in favor of surgical treatment[85]. Surgery is rarely indicated for relieving low back pain only[125]. Surgical options include decompression to relieve the pressure on one or many pinched nerves, and fusion improves the stability of the spine and restores the alignment.

In a case of rigid spine or when large realignment is required, several surgical methods have been described. The first method consists of lengthening the anterior column with cage or graft (Figure 2-29). The other methods, and the most commonly used, consist in shortening the posterior column with vertebral resection (osteotomy, Figure 2-30).

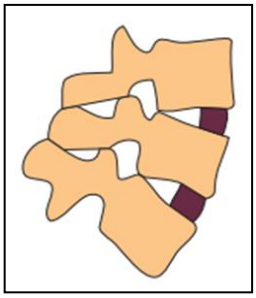

Figure 2-29: lengthened of the anterior column with cages.

Vertebral osteotomy

The objective of these procedures is to reduce the posterior column in an effort to either increase the lumbar lordosis or decrease the thoracic kyphosis. Several methods and range of osteotomy have been described in the literature. In order to offer a common language for patient care and continued research, Schwab et al.[20] developed an anatomical classification that offers 6 grades of resection reflecting an increase degree of destabilization and thus potential angular correction ability. The Grade 1 corresponds to partial facet resection which correspond to Smith Peterson osteotomy[126], and can achieve a deformity correction of around 5 degrees. Grade 2 corresponds to complete facet resection (Ponte osteotomy[127]), and can achieve an even greater degree of correction around 5 to 10 degrees. Grade 3 and 4 correspond to pedicle and partial body resection (pedicle subtraction osteotomy), compare to grade 3, there is a disk resection in the grade 4. Deformity correction of about 25-35 degrees can be achieved. Indication for pedicle subtraction osteotomies have been described as pseudoarthrosis, sharp angular kyphosis, severe global positive sagittal misalignment, concomitant coronal deformity, or previous multilevel circumferential fusions[128–130]. The correction of Grade 5 and 6 correspond to complete body resection and disk resection. Those osteotomies permits a 3-plane correction but in the practice of surgical realignment of ASD patient grade 5 and 6 are rarely used.

	Anatomical Resection	Description	Figure
Grade 1	Partial Facet Joint	Resection of the inferior facet and joint capsule at a given spinal level Correction : ~5°	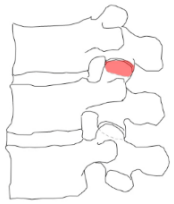
Grade 2	Complete Facet Joint	Both superior and inferior facets at a given spinal segment are resected with complete ligamentum flavum removal; other posterior elements of the vertebra including the lamina, and the spinous processes may also be resected Correction : ~5-10°	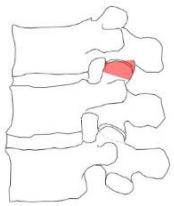
Grade 3	Pedicle/Partial Body	Partial wedge resection of a segment of the posterior vertebral body and a portion of the posterior vertebral elements with pedicles Correction : ~20-25°	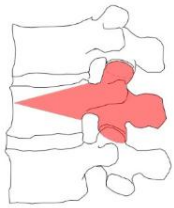
Grade 4	Pedicle/Partial Body /Disc	Wider wedge resection through the vertebral body; includes a substantial portion of the posterior vertebral body, posterior elements with pedicles and includes resection of at least a portion of one endplate with the adjacent intervertebral disc Correction : ~20-25°	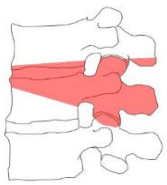
Grade 5	Complete Vertebra and Discs	Complete removal of a vertebra and both adjacent discs (rib resection in the thoracic region)	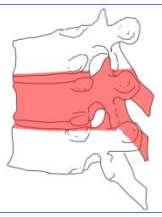
Grade 6	Multiple Vertebrae and Discs	Resection of more than one entire vertebra and adjacent discs. Grade 5 resection and additional adjacent vertebral resection	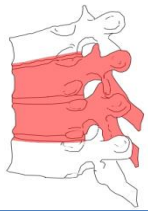

Figure 2-30: Spinal Osteotomy classification[20]

Surgical realignment and planning

The objectives of realignment procedures are to restore the harmony between the lumbar lordosis and the pelvic incidence, and to release the recruitment of compensatory mechanisms such as pelvic retroversion and knee flexion.

The analysis of the literature reveals a large disparity of these radiographic objectives, with several studies reporting only on global alignment and regional spinal curvatures [131–133], while others also included the pelvic orientation [21–23,134,135] (Table 2-10 and Table 2-11). Only two teams took into account the alignment from the head to the knee[24,48].

It is fundamental to understand that surgeons do not control directly the alignment, but only the region of the spine covered by the arthrodesis. The position of the unfused segments, generally a part of the thoracic spine, the cervical spine and the pelvic, are the results of the correction in the fused segments and the adaptation of the patient. The surgical planning exercise consists of not only defining a procedure (extend of the posterior fusion, interbody fusion, use of osteotomy, ….), but also anticipating reciprocal changes in the unfused segments. Therefore, numerous methods have been described to evaluate preoperatively the correction needed to reach a correct sagittal alignment. These methods could be distinguished in two groups: the numerical methods and the combined methods which incorporated numerical and graphical evaluation.

Numerical methods are based on the relations between radiographic measurements (Table 2-10). In the work from Bridwell's team [131,135], the authors provide alignment objectives in terms of regional curvature; these findings are based on the comparison between patients who reached a correct alignment and those who did not. More recently Lafage [23,134] developed and validated predictive models of alignment (SVA and PT) based on linear regressions among radiographic parameters of ASD patients; Lafage did not provide an alignment objective but permit to estimate post-operative alignment. Smith et al[136] evaluated the ability of these models in predicting postoperative SVA after grade III osteotomy on 147 ASD patients and demonstrated that the Lafage formulas[23,134], had the greatest accuracy in predicting postoperative SVA.

These methods are independent of the surgical strategy and are solely based on the anticipated changes in regional sagittal curvatures. This could represent a limitation because, as reported by Lafage et al[137], and more recently by Rousseau et al[138] because the location of the osteotomy affects the correction of the PT, with more caudal osteotomies providing larger PT correction. Other limitations relate to the fact that these methods have only been validated retrospectively, and are not necessarily user-friendly for clinical routine use.

The combined methods are based on geometric constructions performed on X-rays(Table 2-11) and depends of the surgical procedure. The anatomical part taking into account for the planning are different following the methods. Aurouer et al as well as of Steffen et al[48] consider the alignment between the head and the knee in order to consider all the mechanism of compensation. Akbar and Lehuec[22] methods include the thoracic and the lumbar spine as well as the pelvis. Ondra's et al method[132] is limited to the thoracic and the lumbar spine without any consideration to pelvis adaption.

Three methods were analyzed prospectively[22,24,48], and on those three only Autouer[24] and Steffen et al[48] presented the comparison between the preoperative planned measurement and the postoperative. Moreover, the small number of patients was always a limitation to confidently apply these method as standards of surgical planning(6[48] and 11[24] ASD patients).

Steffen et al[48] is the only team presenting an analysis in three dimensions. This methods was based on 3D reconstruction, obtained thanks to the system EOS. The method of Van Royen et al[133] was only applied on patients with specific pathologies (Ankylosing Spondylitis) for which the thoracic kyphosis are generally complete fused.

A common limitation to all the described methods is that they do not provide guidance on reciprocal changes in the unfused segments of the spine. Lafage et al[21] reported a reciprocal increase of 13° in the thoracic kyphosis after lumbar Grade III osteotomy and suggested that it is more common in patients with a higher PI, a greater preoperative sagittal misalignment, and an older age.

Coronal alignment

In regards to the coronal alignment, the objective of realignment is to align the head over the pelvis. In the case of rigid or fused spine, asymmetric coronal osteotomy could be performed [139,140]. In the case of the Cobb angle, there is no guide line for the surgical correction.

Summary

In order to decrease the pain and the disability of patients, the objective of surgical treatment is to restore a harmony alignment. One of the difficulties of those procedures is to anticipate reciprocal changes in the unfused segments (including pelvis and lower limbs). Several methods have been develop to provide assistance to surgeons in the plan of those procedures; however, none have been validated in large set of patients. One part of the personal work has been to evaluate the Akbar method with Surgimap software (Nemaris, New york) on a large ASD population.

	Authors	Objectives or models	Parameters included in the models or methods						Study sample and validation of the method	Results (#)	Comment
			Global sagittal alignment	Head cervical spine	Thoracic + lumbar spine	Pelvis	Knee	multiple osteotomy simulation			
Numerical methods	Kim [131]	LL> TK + 20°			X			Yes	80 ASD patients (retrospective)	63%	
	Rose [135]	LL + PI + TK ≤ 45 °	SVA		X	X (PI only)		Yes	40 ASD patients (retrospective)	72%	
	Lafage [23,134]	SVA =–52.87 +5.90xPI –5.13x LL_{max} –4.45xPT – 2.09xTK_{max} +0.566xAge PT = 1.14 + 0.71xPI – 0.52 xLL_{max} –0.19xTK_{max}	SVA		X	X		Yes	multi-linear model based on 179 ASD patients, validated on 40 ASD and 99 ASD patients (retrospective)	89%	age included in the model

Table 2-10: Numerical models or methods for the simulation of surgical realignment for adults with spinal deformity (ASD). PI: pelvic incidence, PT: pelvic tilt, LL: lumbar lordosis, SVA: Sagittal vertical axis, TK: thoracic kyphosis, LL: lumbar lordosis. # prediction accuracy (percentage of correct alignment prediction)

	Authors	Objectives or models	Parameters included in the models or methods						Study sample and validation of the method	Results	Comment
			Global sagittal alignment	Head cervical spine	Thoracic lumbar spine	Pelvis	Knee	multiple osteotomy simulation			
Graphical methods	Ondra [132]	resection angle atan (SVA/Z)	SVA		X			No	15 ASD (retrospective)	No data	
	Van Royen [133]	No data	SVA		X			No	2 patients	No data	ankylosing spondylitis: software: ASKyphoplan
	Le huec [22]	resection angle C7TA+FOA+PTCA	SVA		X	X		No	18 ASD (retrospective) 8 ASD (prospective)	No data	
	Aurouer [24]	CAM-HA € [-20 -20mm] PT= 0.37xPI - 7; LL= 0.54xPI + 32.56	CAM-HA	X	X	X	X	Yes	11 ASD (prospective)	CAM-HA: 32±38 mm PT: 7°±7 #!	software: Spineview
	Akbar [21]	Pi-LL < 10° ; PT < 20°; SVA < 40mm	SVA		X	X		Yes and cage	No data	No study	software: Surgimap
	Steffen [48]	resection angle PT-0.37xPI+ CAM-HA°+10	CAM-HA	X	X	X	X	No	6 ASD (prospective)	CAM-HA: 3.4˚± 1.6˚ PT: 3,5˚± 8˚ #!	3D reconstruction EOS system

Table 2-11: Combined methods for the simulation of surgical realignment for adults with spinal deformity (ASD). PI: pelvic incidence, PT: pelvic tilt, LL: lumbar lordosis, SVA: Sagittal vertical axis, TK: thoracic kyphosis, LL: lumbar lordosis, CAM-HA: distance between center of the acousitic meati and the center of femoral head, C7TA: Angle of C7 translation, FOA: Angle of femur obliquity, PTCA: Angle of tilt compensation, Z: horizontal distance between C7 and the osteotomy, #! Difference between prediction and postoperative results

2.5 MUSCULAR ANALYSIS

As mentioned, the alignment is a key element of ASD treatment. However, with only radiographic analysis, the muscular system, which has an essential role in the maintenance of the posture, is not included in clinical practice. Even in research, investigation of relationships between the muscles and postural pathologies such as adult spinal deformity, has been limited.

As illustrated in the section 0, spinal disorder in ASD population impact the hip and knee position. Therefore the analysis of the muscular system for this population has to take into account not only the muscles involved in the maintenance of the spine, but also those involved in the hip and the knee stabilization. Several tools or methods have been described to understand the muscular system in a research purposes:

- histological analyses[141–144],
- measurement of muscular strength[145–148],
- measurement of electromyographical signals[149–151],
- ultrasound : measurement of the muscle cross-sectional areas [152],
- CT scan: measurement of the muscle cross-sectional areas [151,153–155] and measurement of muscular density [151,153–156],
- MRI: measurement of the muscle cross-sectional areas [147,157–164] and measurement of muscular signal [146,147,160,161,163–165] .

Histological, evaluation of muscular strength and electromyographical signals are not adapted to evaluation of multiples muscles. In the same way ultrasound measurement are not applicable for a large number of muscles and especially for deeper muscles as psoas.

An image based system, like CT scan and MRI, can provide a large field of acquisition permitting quantitative and qualitative characterization of muscles. While MRI acquisition presents the advantage to being radiation free, the inhomogeneity of the magnetic field renders the quantification of the muscular signal less reliable[166] than the measurement of muscular density with CT scan. While the clinical evaluation of a limited number of MRI/CT slices is common in clinical routine, little is known regarding the correlation between individual slice-specific findings and the variability in volume of an entire muscle slice[167]. To address these limitations, recent methods of 3D muscles reconstruction have been developed based on axial slices of MRI and CT-scan.

2.5.1 **3D RECONSTRUCTION OF MUSCLES**

A possible method to obtain the 3D reconstruction of the muscles based on the axial slices of CT scan or MRI is to manually segment all the slices where the muscles appear. Even for research purposes, this method has been reported to be time consuming[168]. In order to decrease the time of manual segmentations and to obtain relevant tools for clinical practice, several methods have been developed and are presented Table 2-12. Two groups of methods could be distinguished: automatic and semi-automatic methods.

Authors and year	**Modality (slices thickness)**	**Number of subject**	**Anatomical part**	**Reconstruction methods**	**Volumetric / point-to-surface-error**
Cordier et al [169] 1998	CT-scan (No data)	No data	Arm	Segmentation with active outline and deformation of a generic model	No data
Jolivet et al [170,171] 2007	CT-scan (No data)	5	Hip and thigh	DPSO method	5-12% 2RMS =5.8 mm
Sudhoff et al [172] 2009	MRI (10 mm)	10	Hip and lower limb	DPSO method	For 7 slices : <3-12% <6.5mm
Gilles and Magnenat-Thalmann [173] 2010	MRI (2.4 et 10 mm)	7	Hip and lower limb	Manual initialization (2min) and automatic segmentation based on a generic model	No data 0.8±1mm
Baudin et al [174] 2012	MRI (1 mm)	15	Thigh	Automatic segmentation based on a generic model	No data
Li et al[175] 2014	MRI (2 mm)	6	Cervical	DPSO method	No data
Jolivet et al[176] 2014	MRI (10 mm)	4	Hip and lower limb	DPSO method and optimization of non segmented slices	for 5 slices: <5% 2RMS<2.6 mm

Table 2-12: Semi-automatic and automatic methods for 3D reconstructions. Manual segmentation of a limited number of outline with deformation of a parametric model (DPSO method)

Only one study described an automatic method[174] which is based on the deformation of a generic model. This method was only developed on muscle of the tight and was not adapted to other area as the pelvis or the lumbar spine.

Only one semi-automatic method developed by Gilles and Magnenat-Thalmann[173] did not used manual segmentation, but an operator needed to proceed in the identification on the image with a limited number of parameters. This method necessitated specific MRI acquisition and is based on a generic model of hip and lower limb muscles, and so it cannot be directly applied on muscles of the spine. Moreover, it has not been validated on pathologic populations.

In general, semi-automatic methods are based on the manual segmentation of a limited number of slices. Based on those manual segmentations, a generic[169] or a parametric[170–172,176] model is then deformed. To our knowledge, the method, developed by Cordier et al[169] and based on manual segmentation and a generic model, has been only applied on muscles of the harms.

In the method developed by Jolivet et al [170–172,176], named deformation of parametric specific objects (DPSO), the construction of the parametric model is based on the interpolation of ellipses evaluated with the manual segmentation. For each muscle, a subset of MRI or CT scan axial slices (MSS: manually segmented slices) is manually segmented. Using contrast differences, these manual segmentations are then optimized (Figure 2-31.A). The contours are then approximated by ellipses (Figure 2-31.B) and cubic spline interpolation is used to interpolate ellipses in all non-outlined slices covering the muscle (Figure 2-31.C). These interpolated ellipses generate a 3D parametric object (Figure 2-31.D). Finally, using a kriging algorithm[177], the parametric object is deformed non-linearly using the manual segmentations of MSS as control points (Figure 2-31.E). Contrast enhancements were used to optimize the segmentation at each slice. Once all muscles are reconstructed, a geometry-correction algorithm can be applied to eliminate muscle segmentation interpenetration. Finally, 3D meshed reconstruction of each muscle is obtained. In a recent publication by Jolivet et al 2014[176], the authors present an improvement of the method by adding, image processing to optimize the segmentation of non-manually segmented slices. The great advantage to this method with parametric models is that it is easily reproducible on other muscles with the difference of generic model.

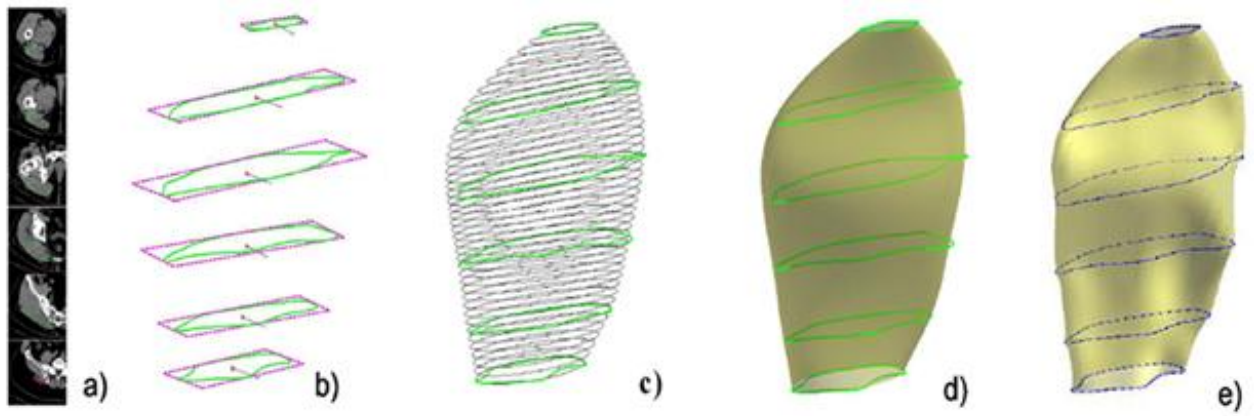

Figure 2-31: Overview of the deformation of parametric specific objects (DPSO) method[170–172,176] . A) Sub-set of MRI axial slices with manually segmented axial sections. B) Contours approximated by ellipses [represented on the figure by a green rectangle whose length and width correspond to the major and minor axes of the ellipses]. C) Cubic spline interpolation used to interpolate ellipses in all non-outlined slices covering the muscle. D) Interpolated ellipses generated a 3D parametric object. E) Non-linear deformation of the parametric object using the manual segmentations.

This method has been evaluated on the following muscles: gluteus maximus, gluteus medius, gluteus minimus, sartorius and tensor fascia lata on the CT scan of 98 subjects. On 30 of those subjects, Jolivet et al.[171] reported errors (two standard deviations around the mean volume) of 5-12% in a reproducibility analysis (3 operators). The DPSO methods has also been applied by Sudhoff[172] on 13 muscles involved in the knee joint motion with MRI acquisition. The authors compared the muscular volume of ten asymptomatic young men, to 5 young men waiting for an ACL reconstruction. In this study, they reported 6% error in muscle volume when compared to 3D reconstruction obtained from the manual segmentation of all the slices where muscles were present. They also evaluate the reproducibility of DPSO method between 2 and 12 % depending on the muscles (2 operators). The point to surface error was ranged from 3 to 6.5 mm.

The main objective of these methods is to reduce the time of manual segmentation and identification performed by the operator. The DPSO method[170,172,176] offers a significant reduction of operator time, a low error of measurement, and the ability to be applied at all of the muscles.

2.5.2 FAT AND CONTRACTILE COMPONENT CHARACTERIZATION OF MUSCLES

As previously mentioned, the inhomogeneity of the MRI magnetic field can be challenging in the setting of quantification of fat infiltration. Therefore, Dixon et al[166] developed an acquisition protocol based on the slight difference in the Larmor frequency of fat and water protons (chemical shift). By acquiring the signal at different echo times, the modulation of the signal intensity can be fitted and the fat and water content can be separated. With this method named two-points Dixon methods, two images are then obtained: one in which the intensity of each voxel is correlated with the quantity of fat and the other in which the intensity of each voxel is correlated with the quantity of water (Figure 2-32)

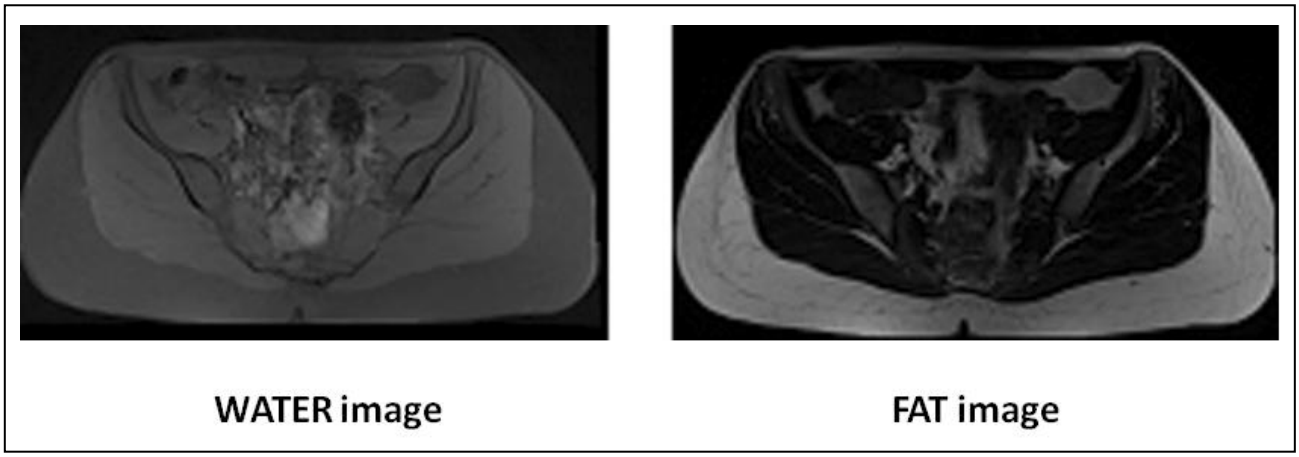

Figure 2-32 Example of water (left) and fat (right) images with Dixon methods on a 64 year old female ASD patient

The evaluation of the fat infiltration using the two points Dixon method has already been applied to investigate different organs (liver[178,179], bones[180] and muscles[181,182]). This method was then improved by Glover et al[183] and named the three-points Dixon method. Contrary to the two points Dixon methods the decay in signal intensity between the in-phase and opposed phase images due to T2* is taken into account[179]. However, recent studies have shown that the two point Dixon without T2* has excellent concordance with spectroscopy measured in the spine, bones[180], liver[178], or spine muscles[182].

Summary

This literature review illustrates the lack of relevant tools or protocol to accurately analyze the muscular system in the setting of ASD population. A clinically relevant method should not only permit the quantitative and qualitative evaluation of a large number of muscles, but also be non-invasive for the patients, and be associated to a reasonable post-processing time.

The combination of MRI acquisition with the Dixon method and the methods of reconstruction based on the work of Jolivet et al[170,172,176], could be a realistic method to evaluate the muscular system in ASD patients.

2.6 INTRODUCTION TO THE PERSONAL WORK

This bibliographical synthesis has highlighted different issue regarding the treatment of ASD patients particularly related to the clinical evaluation, the restoration of the alignment, and the muscular evaluation.

Although the reduction of pain and disability are the main expectation of those patients, there is no clear and precise methodology to clinically evaluate the treatment in ASD population. Therefore, the first article (section 3.1, page 69) presents an innovative method for clinical evaluation including SRS scores, MCID and age and sex matched normative scores with 2-years follow-up. The objective of this manuscript was twofold: to provide a description of a new method of evaluation, and analysis of the clinical effectiveness of surgical treatment.

In regard to the relations described between the restoration of the sagittal alignment and the clinical benefit of ASD patients, the objective of the second article (section 3.2, page 85) was to determine the effectiveness of the surgical treatment to restore the alignment of main radiographic parameters.

Results of the first two manuscripts brought to light suboptimal clinical and radiographic outcomes in the setting of surgical treatment of ASD, and the necessity to evaluate on a large ASD population method for pre-operative planning, but also to consider intra-operative reconciliation of the planning. Therefore, the third manuscript presents the results of a prospective monocentric (NYU) study combined a new protocol of data collection, including surgical planning and intra-operative evaluation (section 3.3, page 98).

In addition, the lack of relevant tools for muscular evaluation is a break to the improvement of ASD treatment and could explain the difficulty to better understand the degeneration of the alignment as well as its restoration.

Therefore, a new protocol, including 3D reconstructions of muscles obtained with DPSO methods and Dixon acquisition, has been validated and the error of measurement has been quantified (section 4.1, page 115).

This protocol has been applied on an ASD population composed of 19 patients. The description of the spino-pelvic musculature was presented in term of volume and fat infiltration (section 4.2 page 131).

Finally, even with the DPSO method, the protocol described in the section 4.1 was too time consuming to be applied in a clinical routine. Therefore, the last article (section 4.3, page 147) described a new method based on multi-linear regression to assess the fat infiltration and the volume of main muscular group of the spino-pelvic musculature with a smaller number of manual segmentations.

3. SURGICAL TREATMENT AND ADULT WITH SPINAL DEFORMITY

3.1 CLINICAL IMPROVEMENT THROUGH SURGERY FOR ADULT SPINAL DEFORMITY: WHAT CAN BE EXPECTED AND WHO IS LIKELY TO BENEFIT MOST?

The first two manuscripts are based on a retrospective analysis of a multicenter consecutive database of ASD patients. This database was developed by the International Spine Study Group and includes, among other parameters, pre-operative and post-operative clinical and radiographic evaluation.

The following article includes 223 patients treated surgically with a follow up of 2 years. The clinical evaluation includes SRS scores, MCID and age and sex matched normative scores.

This article has been submitted to the SRS journal in Mai 2014.

Authors: Bertrand Moal, Frank Schwab, Christopher P. Ames, Justin S. Smith, Devon Ryan, Praveen V. Mummaneni, Gregory M. Mundis Jr., Jamie S. Terran, Eric Klineberg, Robert A. Hart, Oheneba Boachie-Adjei, Christopher I. Shaffrey, Wafa Skalli, Virginie Lafage, International Spine Study Group

3.1.1 **INTRODUCTION**

To standardize the evaluation of adult spinal deformity (ASD), health-related quality of life (HRQOL) instruments are now widely used in clinical practice and the scientific community[76,80,184]. The Scoliosis Research Society instruments (SRS-22) were validated to provide a disease-specific health questionnaire.[185]. While its use is now common, the interpretation remains an area of active research[18] .

In a study on normative data, Baldus et al.[84] reported significant differences for SRS scores among sex and age groups, suggesting that HRQOL evaluation should account for normative data instead of solely relying on generic scales.

The interpretation of HRQOL scores changes following treatment and involves considerations beyond simple numerical improvement. Literature on HRQOLs advocates the use of the minimal clinically important difference (MCID) concept in order to differentiate a statistical improvement from a clinical one, perceivable by the patient[12,18,83,95,186]. While the use of MCID can enhance clinical relevance, it does not take into account the absolute values of HRQOL scores. Two patients experiencing the same improvement may not have the same outcome if they started at different baseline scores.

The present study aimed to assess clinical outcomes for ASD treated surgically, with an emphasis on the baseline evaluation to include initial clinical state, age, body mass index (BMI), history of previous surgery, co-morbidities and type of spinal deformity. In contrast to previous studies, the outcomes assessment is based on comparisons with normative data, matched based on age and gender, reported as multiples of MCID.

3.1.2 MATERIALS & METHODS

This is a retrospective analysis of a consecutive series of ASD patients (age > 18 years) enrolled in a prospective multi-center study. Patients were drawn from the International Spine Study Group (ISSG) prospective database, derived from 10 clinical sites across the United States. Patients were enrolled through an Institutional Review Board-approved protocol by each site. The radiographic inclusion criterion for the ISSG database was at least one of the following: Cobb angle ≥ 20°, sagittal vertical axis (SVA) ≥ 5 cm, pelvic tilt (PT) ≥ 25°, or thoracic kyphosis (TK) ≥ 60°. Patients with inflammatory arthritis, tumor, or neuromuscular disease were excluded.

Specific inclusion criteria for the present study included operative treatment, availability of SRS-22 scores, and availability of X-rays at baseline and at 2-years follow-up. Age, BMI, medical history, and co-morbidities (Charlson score[187]) were collected. X-rays were analyzed at baseline using validated software [53,54] (Spineview®, Laboratory of Biomechanics Arts et Metiers ParisTech, Paris) to obtain the following parameters: Cobb angle and apex location, PT, pelvic incidence (PI), L1-S1 lumbar lordosis (LL), PI-LL mismatch, and SVA. Each patient was classified according to the different type of curves derived from the SRS-Schwab classification (Figure 2-28, page 51)[89,95,109,117], distinguishing 8 groups based on deformity pattern (Table 3-1).

Type of Curve Groups	Acronym	Coronal Criteria	Sagittal Criteria
Thoracic	T	Type T	All modifiers at grade 0
Thoracic / Sagittal	TS	Type T	At least one modifier at grade + or ++
(Thoraco)-Lumbar	L	Type L	All modifiers at grade 0
(Thoraco)-Lumbar/ Sagittal	LS	Type L	At least one modifier at grade + or ++
Double	D	Type D	All modifiers at grade 0
Double Sagittal	DS	Type D	At least one modifier at grade + or ++
Sagittal only	S	Type N	At least one modifier at grade + or ++
Unclassified	U	Type N	All modifier at grade 0

Table 3-1: Description of the different type of curves derived from the SRS-Schwab classification for adult spinal deformity.

Clinical Classifications

At baseline and 2 year follow-up, Activity, Pain, Appearance, and Mental SRS-22 domains were expressed as differences from normative data (age and gender-matched)[184]. For each patient individually, the differences were normalized using thresholds of MCIDs (Table 2-8,page 41,

Equation 4.1). Since normative data and MCID are not available for the SRS Satisfaction domain and the Total SRS score, these scores were not included in the study.

$$Diff_{norm}{}^{patient}_{domain} = \frac{SRS^{patients}_{domain} - SRS^{normative}_{domain}}{MCID_{domain}} \quad \text{(Equation 4.1)}$$

Each patient was classified for the four domains into one of five groups reflecting clinical change from baseline to two-year follow-up as follow:

- **Consistent**: $Diff_{norm}$ less than 1 MCID at baseline and at 2-year follow-up.
- **Deterioration**: deterioration between baseline and 2-year follow-up greater than 1 MCID.
- **No improvement**: $Diff_{norm}$ at baseline greater than 1 MCID and improvement at 2-year follow-up less than 1 MCID.
- **Improvement**: $Diff_{norm}$ at baseline greater than 1 MCID, improvement greater than 1 MCID and $Diff_{norm}$ at 2-year follow-up greater than 1 MCID.
- **Excellent**: $Diff_{norm}$ at baseline greater than 1 MCID, improvement greater than 1 MCID and $Diff_{norm}$ at 2-year follow-up less than 1 MCID.

The analysis revealed that Pain and Activity were the two domains of primary complaints. These domains were combined to classify the clinical condition of patients at baseline and the overall clinical treatment effectiveness.

At baseline, 4 groups were defined using the distribution of the $Diff_{norm}$ as illustrated in Figure 3-1:

- **Worst**: $Diff_{norm}$ above the 75th percentile (i.e. greater difference) for Activity and Pain domains.
- **Severe**: $Diff_{norm}$ between the 25th percentile and 75th percentile for both Activity and Pain domains.
- **Poor**: $Diff_{norm}$ between the 25th percentile and 75th percentile for one of the domains and less than the 25% percentile for the other domains.
- **Moderate**: $Diff_{norm}$ below the 25th percentile for both domains

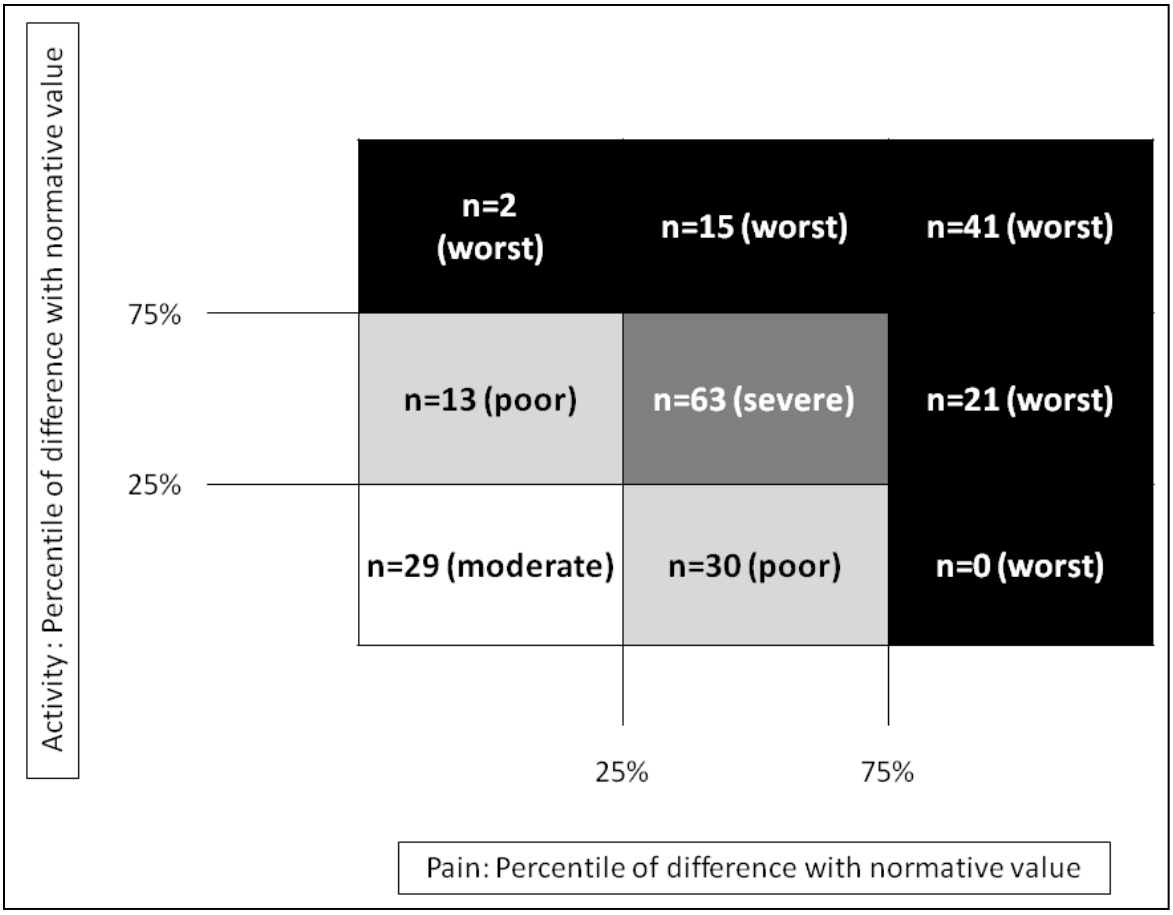

Figure 3-1: Classification of baseline clinical state based on Pain and Activity SRS-22 domains.

To evaluate the overall treatment effectiveness, clinical scores in Pain and Activity were combined to establish the 4 following groups (Figure 3-2):

1. **Optimal**: *excellent* in at least one domain + *consistent or excellent* in the other domain.
2. **Satisfactory**: *improvement* in at least one domain + *consistent or excellent* in the other.
3. **Mediocre**: *no improvement* in one domain + *improvement or excellent* in the other .
4. **No improvement or deterioration**: *deterioration* OR *no improvement* in at least one domain + *consistent or no improvement* in the other.

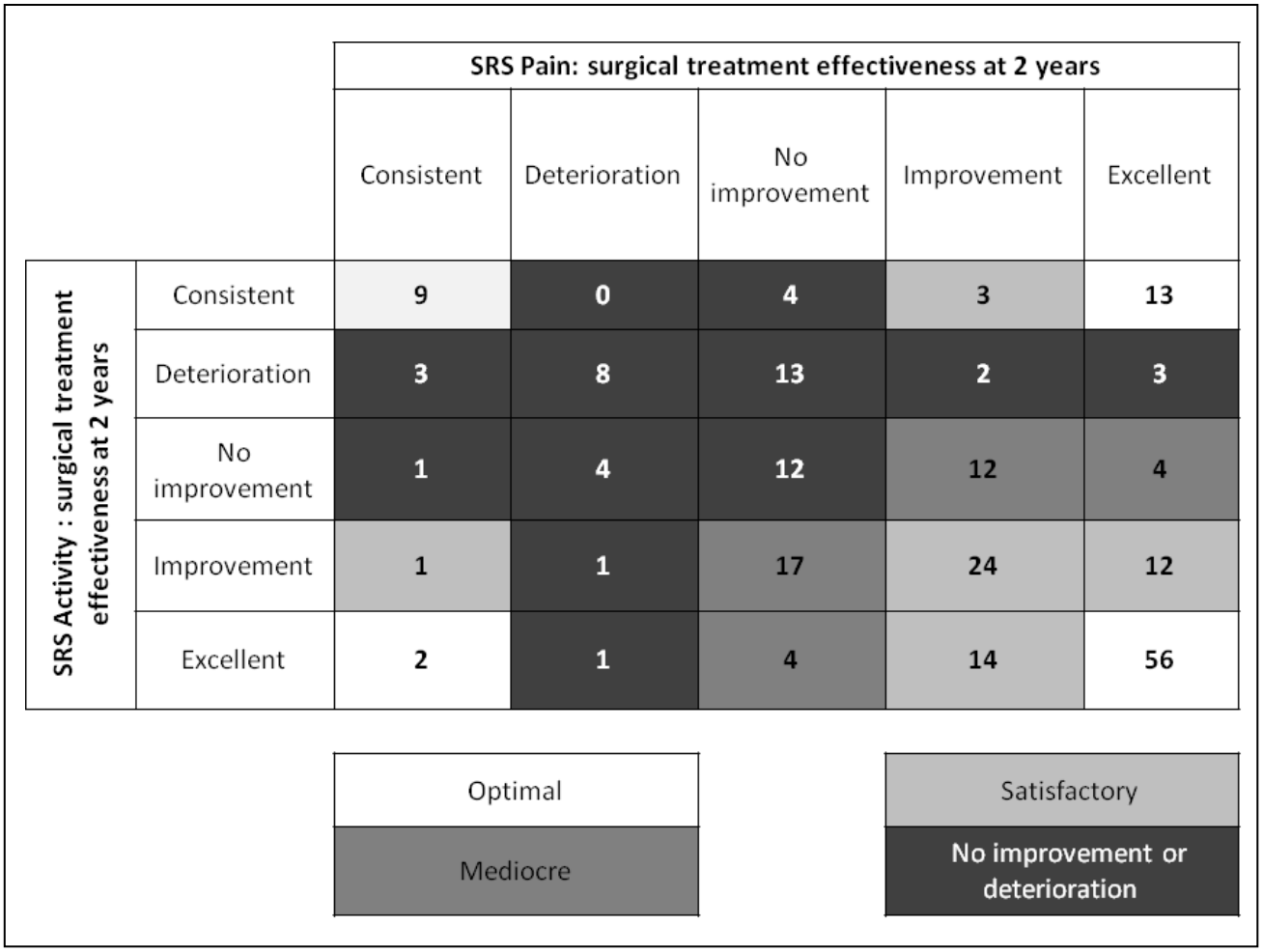

Figure 3-2: Stratification of global clinical effectiveness of surgical treatment for adult spinal deformity at 2 year follow-up based on SRS Activity and SRS Pain domains.

Statistical Analysis

HRQOL scores were summarized by means and standard deviations (SD). The distributions of patients according to the clinical treatment classification were expressed. Comparisons across the baseline clinical classification and overall clinical treatment effectiveness classification were performed using ANOVA t-test. Cross comparison between baseline clinical classification and overall clinical treatment effectiveness classification was analyzed using Chi square. The significance level was set at 0.05.

3.1.3 **RESULTS**

Enrollment (Table 3-2)

Between 1/1/2008 and 12/31/2011, 689 patients were eligible, and 327 were enrolled. 310 patients had adequate baseline radiographs and SRS scores. Out of these patients, 223 (35 men and 188 women) had adequate baseline and 2 years radiographs and SRS scores and thus were the only ones included in this study.

		SITE									
Number of patients	**Total**	**A**	**B**	**C**	**D**	**E**	**F**	**G**	**H**	**J**	**K**
Enrolled between 2008-2011	327	6	15	34	54	25	14	18	62	59	40
Enrolled and adequate baseline radiographs and SRS scores	310	6	15	34	47	25	14	17	54	58	40
Enrolled, adequate baseline and 2-years follow up radiographs and SRS scores	223	6	13	29	39	14	6	10	27	47	32

Table 3-2: Number of patients enrolled, number of patients with adequate baseline radiographs and SRS score, number of patients with adequate baseline radiographs and SRS scores and 2-years follow up and number of patients with adequate baseline and 2 years radiographs and SRS scores by site.

Mean age was 55 years (SD: 15) and mean BMI was 27.3 (SD: 5.9). 42% of the patients had a prior history of spine surgery.

The distribution of patients by curve type at baseline (Table 3-3) identified that 75% of patients had a coronal Cobb angle greater than 30° (T, TS, L, LS, D and DS), and 73% had a sagittal deformity (TS, LS, DS and TS). A total of 7 patients (3%) were unclassifiable due to a difference between the inclusion criteria for the database (Cobb>20°) and the SRS-Schwab classification (Cobb>30°). These patients were removed from the following analysis.

	U	T	L	D	TS	LS	DS	S
Number of patients	7	10	22	21	5	59	51	48
% of patients	3%	4%	10%	9%	2%	26%	23%	22%

Table 3-3: Distribution of patients by curve type at baseline. U: Unclassified, T: Thoracic, TL: Thoracic Sagittal, L: (Thoraco)-Lumbar, LS: (Thoraco)-Lumbar Sagittal, D: Double, DS: Double Sagittal and S: Sagittal

Analysis by domains

At baseline, significantly larger $Diff_{norm}$ were found for Pain (-3.08±1.44 MCID) and Activity (-3.27±2.38 MCID) domains when compared to Appearance (-2.14±0.96 MCID) and Mental (-1.54±2.24 MCID) domains ($p<0.001$) (Table 3-4). The principal domain of complaint, defined as the domain presenting the largest $Diff_{norm}$, were Activity (43% of the population), and Pain (34%).

		SRS score							
		Activity		**Pain**		**Appearance**		**Mental**	
		Mean	**SD**	**Mean**	**SD**	**Mean**	**SD**	**Mean**	**SD**
$Diff_{norm}$	**Pre-Op**	-3.27	2.38	-3.08	1.44	-2.14	0.96	-1.54	2.24
	2 Year	-1.64	2.75	-1.44	1.89	-0.56	1.15	-0.58	2.19
Improvement in MCID		1.63	2.26	1.64	1.84	1.58	1.23	0.97	1.98

Table 3-4: Difference by domains with normative values(Diffnorm) expressed in minimum clinically important difference (MCID) for the entire population, at baseline, 2 year and in terms of improvement.

Post-operatively, the mean MCID difference was -1.64±2.75 MCID for Activity domain, -1.44±1.89 MCID for Pain, -0.56±1.15 MCID for Appearance, and -0.58±2.19 MCID for Mental. On average, Mental domain was the one in which patients experienced the smallest improvement (+0.97±1.98 MICD).

The Activity domain had the highest rate of deterioration (14%), with a rate of optimal effectiveness equal to 36% (Figure 3-3). The Pain domain had a rate of optimal effectiveness of 41% and had the greatest percentage of patient without improvement (23%). Appearance was the domain with the greatest rate of optimal improvement (56%) and smallest rate of deterioration (4%). Mental domain had the greatest percentage of consistent patients (39%) and smallest percentage of optimal results (23%).

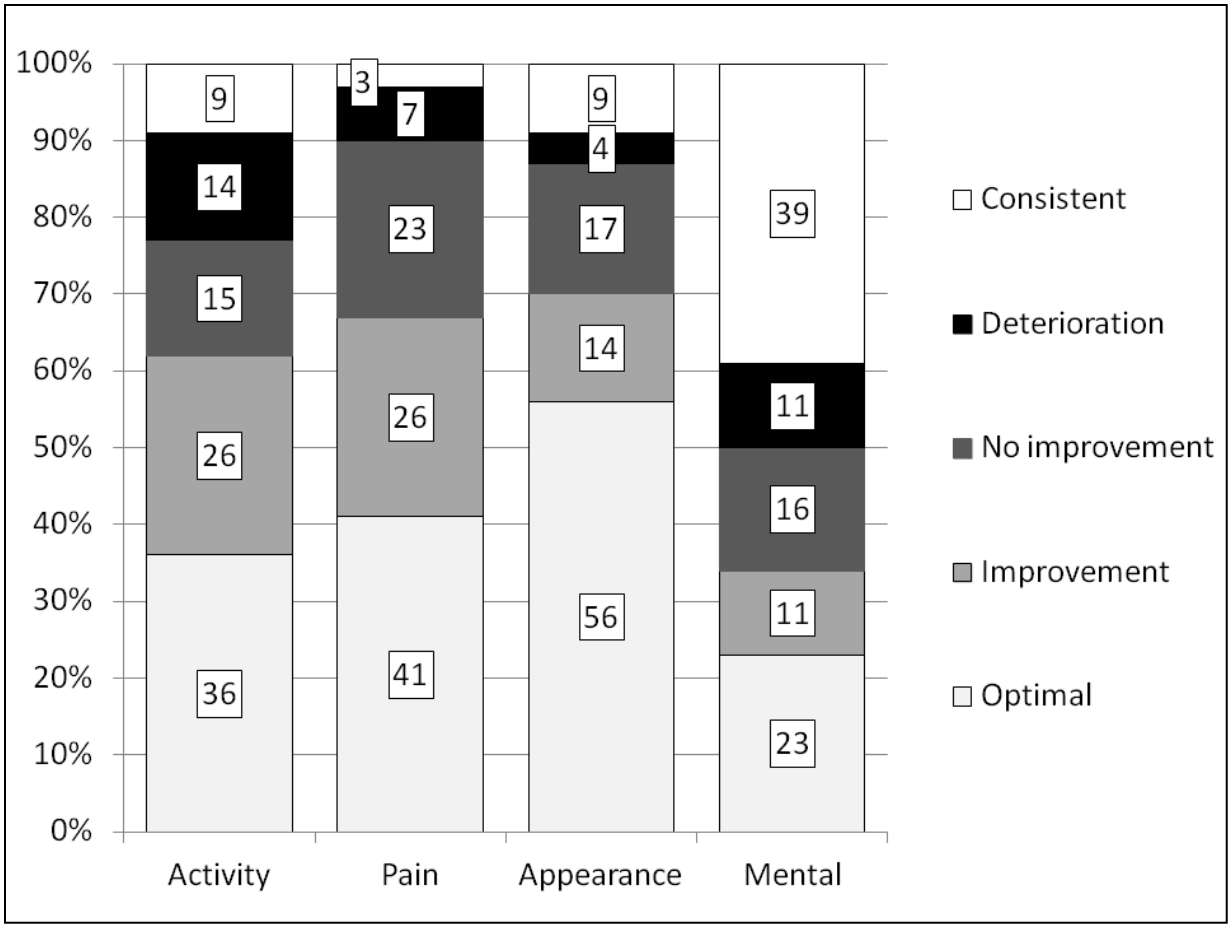

Figure 3-3: Percentage of treatment effectiveness by SRS domains (Activity, Pain, Appearance and Mental).

Clinical condition of patients at baseline

The threshold used in the baseline clinical group for the Pain and the Activity domains were based on the percentiles for the $Diff_{norm}$ for the entire population at baseline (Table 3-5)

	$Diff_{norm}$ at baseline			
Percentiles	**Activity**	**Pain**	**Appearance**	**Mental**
25.00	-5	-4	-3	-3
50.00	-3	-3	-2	-1
75.00	-2	-2	-1	0

Table 3-5: Percentile for the difference by domains with normative values (Diffnorm)expressed in minimum clinically important difference (MCID) for the entire population at baseline

36% (n=79) of the patients were classified as being in the "worst" state, 28% (n=63) as "severe", 19% (n=43) as "poor", and 17% (n=38) as "moderate" (Figure 3-1).

"Worst" (59±10 years) and "severe" (59±14 years) patients were significantly older than "moderate" patients (44±17 years; p=0.001) (Table 3-6). "Worst" patients also had more severe Charlson co-morbidity scores than "poor" and "moderate" patients (p=0.014). "Moderate" patients had a significantly lower BMI (23.0±3.5) than "poor" and "worst" (respectively 27.3±6.7; and 29.2±5.9; p=0.001) patients. Patients presenting with a history of previous spine surgery were more likely to be classified in the "worst" category (p=0.004). The proportion of females classified in the "moderate" category was significantly greater than the proportion of males (p=0.001).

		Demographic						Prior surgery* %		♂	♀
		Age		BMI		Charlson score					
		Mean	SD	Mean	SD	Mean	SD	Yes	No	%	%
Baseline Clinical Classification	Moderate	44*	17	23.0*	3.5	0.55*	0.95	11	22	19	6
	Poor	52	18	26.2	4.3	0.88	0.91	15	23	19	20
	Severe	59*	14	27.3*	6.7	1.30*	1.49	24	31	28	29
	Worst	59*	10	29.2*	5.9	2.10*	1.79	51	24	34	45

Table 3-6: Comparisons among the baseline clinical classification groups in terms of demographic data, gender, co-morbidities and history of prior surgery, *BMI = body mass index, SD = standard deviation, *: p<0.05*♂: female, ♀male.

The sagittal deformity only group (S) had the largest proportion in the "worst" category (54%) while no patients fell into the "moderate category", Table 3-7). The group with double curve without sagittal deformity (D) had the smallest percentage of patients in the "worst category" and the greatest percentage of patients in the "moderate category".

	T	**L**	**D**	**TS**	**LS**	**DS**	**S**
Moderate	40	18	43	20	12	22	0
Poor	20	23	33	0	15	24	15
Severe	0	32	19	40	29	33	31
Worst	40	27	5	40	44	22	54

Table 3-7: Distribution of patients by curve type and by baseline SRS-Schwab classification. U: Unclassified, T: Thoracic, TL: Thoracic Sagittal, L: (Thoraco)-Lumbar, LS: (Thoraco)-Lumbar Sagittal, D: Double, DS: Double Sagittal and S: Sagittal.

Overall treatment effectiveness

33% of the patients perceived an “optimal” improvement, 25% a “satisfactory” improvement, 17% a “mediocre” improvement, and 24% did not perceive an improvement or were deteriorated (Table 3-8). Only 9 patients had less than 1 MCID of $Diff_{norm}$ in the Pain and the Activity domains at baseline and no deterioration at 2-year follow-up (group “consistent” for Pain and Activity; they were not included in the following analysis).

			Demographic									
		%	Age		BMI		Charlson score		Prior surgery %		♂ %	♀ %
			Mean	SD	Mean	SD	Mean	SD	Yes	No		
overall treatment effectiveness classification	No improvement or deterioration	24	53	13	26.5	6.2	1.37	1.56	20	28	25	21
	Mediocre	17	57	14	30.0	5.6	1.76	1.59	24	12	16	27
	Satisfactory	25	58	15	27.8	5.3	1.70	1.81	26	24	25	27
	Optimal	33	55	16	26.1	5.8	1.08	1.27	30	36	34	27

Table 3-8: Distribution and assessment of demographic data based on global clinical treatment classification. BMI = body mass index, ♂: female, ♀male.

There were no significant differences between the clinical treatment effectiveness groups based on age, gender, Charlson co-morbidity score, or history of previous surgery (Table 3-8). Patients with a "mediocre" treatment effectiveness had a significantly greater BMI than the patients with an "optimal" treatment effectiveness.

Depending on curve type (Table 3-9), 15 - 30 % of the patients did not perceive an improvement or reported symptoms indicating deterioration. Between 22 and 44% perceived an optimal improvement. Patients with only sagittal deformity had the lowest percentage of optimal improvement.

Patients’ distribution was significant difference combining the baseline clinical classification and the global clinical treatment effectiveness classification ($p<0.001$,Figure 3-4). 20% of the “worst” patients had no improvement or had deteriorated, whereas 41% of “moderate” patients had no improvement or had deteriorated. Only 19% of “worst” patients had “optimal” results, and 59% of “moderate” patients had “optimal” results. Worst patients had also the greatest percentage of "satisfactory" results.

	T	L	D	TS	LS	DS	S
No improvement or deterioration	22	25	30	25	29	25	15
Mediocre	33	5	5	50	14	17	25
Satisfactory	0	40	25	0	19	23	38
Optimal	44	30	40	25	38	35	22

Table 3-9: Cross-comparison of patient distribution based on pre-operative curve type (SRS-Schwab classification) and global treatment outcome classification. U: Unclassified, T: Thoracic, TL: Thoracic Sagittal, L: (Thoraco)-Lumbar, LS: (Thoraco)-Lumbar Sagittal, D: Double, DS: Double Sagittal and S: Sagittal.

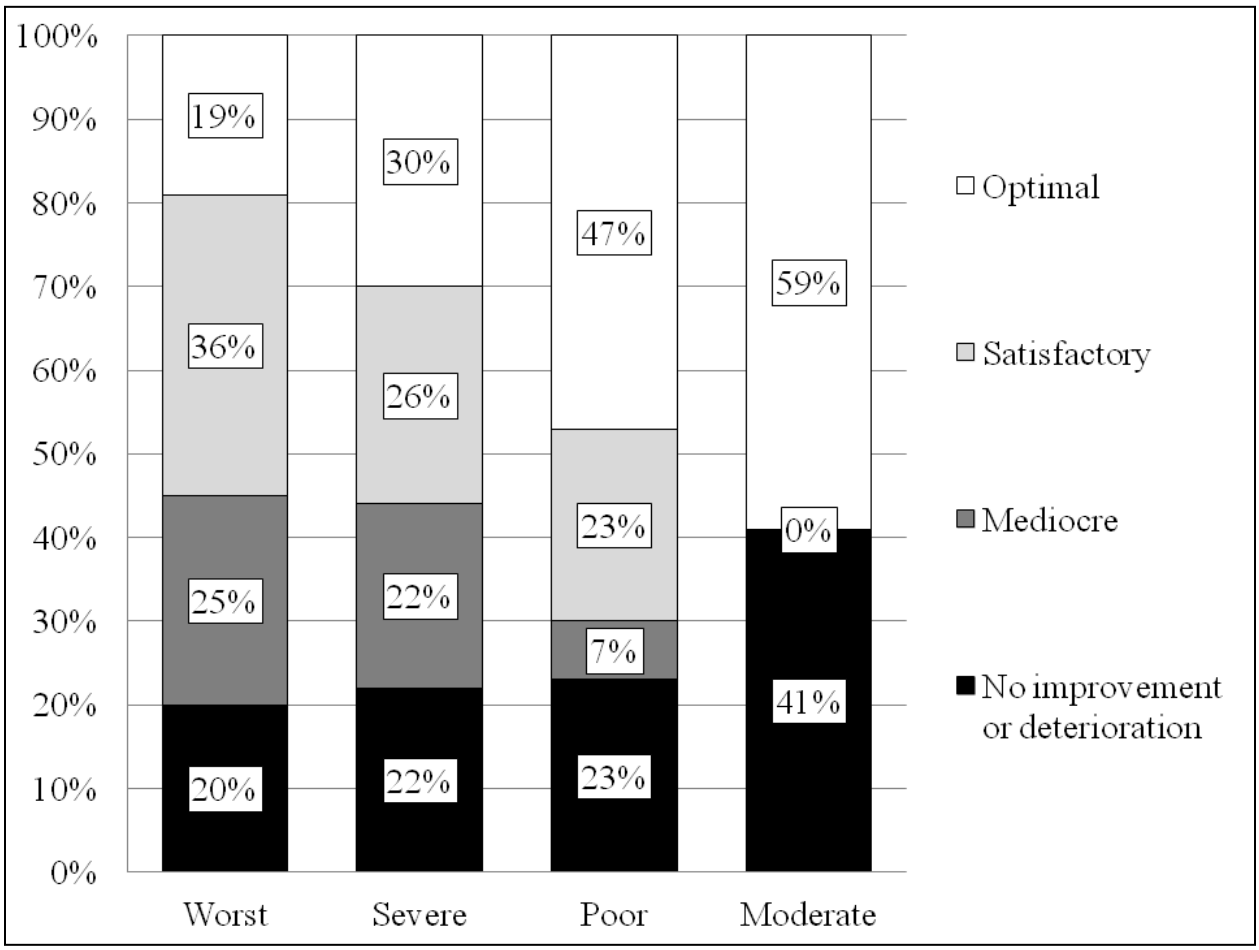

Figure 3-4:Cross-comparison of patient distribution based on baseline clinical classification and overall treatment effectiveness classification.

3.1.4 **DISCUSSION**

Utilizing MCID, this study aimed to evaluate the clinical effectiveness of spine surgery for ASD using a normative population comparison group (stratified by age and sex).

Assessing surgical efficacy using age- and sex-matched normative data avoids bias in the analysis due to gender and age, especially in this sample population with a large age range, (19 to 84 years old). It also assists in setting realistic expectations among age groups. Soroceanu et al[188] highlighted that patient outcomes were strongly correlated with the preoperative expectations. However, the main limitation of this approach relates to the distribution of normative data, with standard deviations (0.31 to 0.79) for each gender and age group approaching MCID thresholds (0.375 and 0.8). To our knowledge, comparison of HRQOL scores with normative data has only been reported in a study published by Blondel et al.[18] that aimed to evaluate the clinical impact of restoring sagittal alignment.

A unique feature of this study's methodology is the use of MCID. While MCIDs have been used in several studies for the clinical assessment of ASD patients[12,95,186], MCID values are traditionally used as thresholds but not as a scale which would require validation. Moreover MCID was developed to differentiate between statistical improvement from clinical improvement but was not validated for deterioration. To our knowledge, no studies exist that evaluates MCID thresholds for deterioration with SRS score. This deficiency was noted by Gum et al[189] on a population of 722 patients who received posterior lumbar fusion for back and leg pain. The authors concluded that ''A threshold for clinical deterioration was difficult to identify" and that "patients may interpret the absence of change as deterioration". In light of these findings, our approach consisted of combining patients with no improvement with ones who sustained a perceived deterioration.

Nevertheless, we believe that a common MCID scale can permit an easier and more relevant clinical interpretation. It also permits comparison of different domains of the SRS instrument, which would not otherwise be possible. Another benefit of the presented methodology is that it combined the evaluation of change in clinical outcomes to the analysis of post-operative outcomes with regards to an age and sex-matched normative population.

Comparisons between Patients and the Normative Population

At baseline, for 77% of the patients, the Pain and Disability domains were the two domains most highly affected. These results are in line with those reported by Bess et al.[86], who postulated that pain and disability were the main drivers of surgical treatment in the ASD population. Those results explained the focus on those domains in the baseline classification, as well as for the global

treatment efficiency classification. For the baseline classification, thresholds for the Pain and Activity were chosen based on percentiles and simple thresholds.

Treatment Effectiveness

The evaluation of treatment effectiveness took into account the most impacted pre-operative and post-operative domains (Pain and Activity), clinical improvement, and deterioration from baseline to follow-up. 33% of the patients had a clinical improvement in their deficient domains that was sufficient to reach less than 1 MCID difference from normative data. However, 24% had no clinical improvement or were clinically deteriorated. The greatest percentage of deterioration was observed in the Activity domains (14%).

The Mental and Appearance domains have been identified as second order compared to Pain and the Activity domains. The two domains were treated independently and were not incorporated into the overall classification so that clinical evaluation is not further complicated. The Appearance domain was the one most likely to show an “optimal” improvement (56%) and the least likely to deteriorate (4%), while the Mental domain was the least likely to show an “optimal” improvement (23%).

Baseline Classification versus Treatment Effectiveness

Two different aspects of the relation between clinical baseline state and treatment effectiveness could be distinguished. Only 19% of patients with the greatest clinical deficit at baseline reached an optimal result postoperatively (for the other groups, the percentage was between 30% and 59%). However, 36% of these patients had a “satisfactory” result, potentially reflecting that for these patients the aim of reaching a score matching the normative population post-operatively may not be realistic. Alternatively, only 20% of these patients did not have an improvement or deteriorated, whereas 41% with a “moderate” deficit did not perceive an improvement or were deteriorated, highlighting two potential issues when indicating patients for surgery: First, performing surgery on patients with a less measureable negative impact may inherently limit the possible benefits that can be derived from intervention. Second, surgeries that were performed at an earlier time point in the disease process may also inherently suffer from an inability to demonstrate large differences in clinical improvement.

Demographic Data

In the ASD population, prior studies demonstrate that older patients reported worse clinical scores than younger patients but did not specifically assess whether this difference could be attributed to spinal deformity or age[6,86,190]. Baseline clinical classification demonstrated that patients suffering from a major disability and/or severe pain were older, indicating that the negative impact

of spinal deformity was greater among older patients. However, in terms of treatment effectiveness, no association was found with age, which is consistent with findings in other studies.[6,190].

In the present study, patients with greater pain and disability had a greater BMI and higher Charlson co-morbidity scores. BMI and co-morbidities independently decrease quality of life. Like age, the analysis of clinical treatment effectiveness indicated that patients with a greater BMI or high levels of co-morbidities can still expect a significant clinical improvement from surgery. However, the role of co-morbidities and BMI seems to be controversial. Smith et al[191] found in a multicenter spinal deformity database with 2-year follow up that a greater BMI is a predictor of poor outcome. Daubs et al.[190] did not find a correlation between patient outcomes after spine surgery and co-morbidities in an elderly ASD population, whereas Slover et al.[192] found that co-morbidities impact the change in clinical improvement.

Revision versus primary surgery

Patients with previous spine surgery had poorer HRQOLs preoperatively. However, no significant difference was found in terms of treatment effectiveness when compared to primary cases. In contrast, Djurasovic et al.[193] found that revision cases showed only modest improvement and that 38% of the patients reach the MCID threshold. One possible explanation of these different conclusions is the difference in methodology used.

Deformity pattern

Pre-operatively, results demonstrated that patients with sagittal deformity had poorer HRQOL than patients with pure coronal deformity. These results are consistent with published reports regarding the importance of sagittal plane deformity[13,18]. Indeed, great variability was found between curve type and treatment effectiveness, depending on the type of curve the percentage of optimal improvement was comprised between 22% and 44%.

Limits

The follow up rate at 2 years was about 70%, which is a weakness of our study. As mentioned previously, the use of MCID as a scale to quantify improvement and deterioration has not been validated to date. Finally, the relatively small number of patients included in the present study did not permit further analysis such as stratification by deformity pattern, age, complication, indication, or technique. Therefore, this study focused on the preoperative condition of the patients, but further analysis is warranted to investigate other potential factors that could drive surgical outcomes.

Conclusion

Using MCID and normative scores, this study presents an innovative way to evaluate the clinical effectiveness of treatment for ASD patients. 33% of patients reached normative values at 2 years following surgery while 24% did not perceive improvement or experienced deterioration. Clinical state at baseline was a dual factor of treatment effectiveness. Patients with a moderate deficit had a greater chance of having an optimal result but also a greater chance of not perceiving an improvement. Stated alternatively, patients presenting with the poorest HRQOLs were more likely to perceive an improvement but were also less likely to reach optimal levels of functionality.

Radiographic restoration has not been included in this analysis but developed in the following article.

3.2 RADIOGRAPHIC OUTCOMES OF ADULT SPINAL DEFORMITY CORRECTION: A CRITICAL ANALYSIS OF VARIABILITY AND FAILURES

In order to evaluate the effectiveness of the surgical treatment in restoring spino-pelvic alignment, a retrospective analysis of multicenter, prospective, consecutive, surgical case series including 161 patients has been conducted. The radiographic parameters included were the Cobb angle and the global coronal alignment (GCA) in the coronal plane as well as the sagittal vertical axis (SVA), the pelvic incidence minus the lumbar lordosis (PI-LL) and the pelvic tilt (PT).

This article has been published in the SRS journal in 2014

Authors : Bertrand Moal, Frank Schwab, Christopher P. Ames, Justin S. Smith, Devon Ryan, Praveen V. Mummaneni, Gregory M. Mundis Jr., Jamie S. Terran, Eric Klineberg, Robert A. Hart, Oheneba Boachie-Adjei, Christopher I. Shaffrey, Wafa Skalli, Virginie Lafage, International Spine Study Group.

3.2.1 **INTRODUCTION**

Although great diversity of deformity patterns among patients with adult spinal deformity (ASD) exists, one common objective of any realignment procedure is to restore harmonious spino-pelvic alignment in the coronal and sagittal planes.

Several sagittal radiographic parameters define and quantify regional and global spino-pelvic alignment: the sagittal vertical axis (SVA), which assesses the global alignment of the spine versus the pelvis; the pelvic incidence minus the lumbar lordosis (PI-LL), which reflects the harmony between lumbar lordosis and the morphologic pelvic incidence; and the pelvic tilt (PT), which characterizes the extent of pelvic compensation for truncal inclination. Recent studies have identified these three radiographic parameters as the most highly correlated with patient-reported outcomes, and they were, accordingly, incorporated as the key parameters in the SRS-Schwab classification for ASD[1]. This validated classification [2,3] defines the threshold of pathologic values for the three parameters based on correlation with clinical scores: SVA>40 mm, PI-LL> 10°, and PT>20°.

The SRS-Schwab classification defines different coronal curve patterns based on Cobb angle measurement and location of the apex of the coronal deformity (thoracic, thoraco-lumbar/lumbar, or double). Historically, the coronal Cobb angle has been considered the most important parameter for the diagnosis and management strategy of patients with ASD. Glassman et al [4] and Schwab et al [2], however, have suggested in two prospective multi-center studies that the magnitude of coronal deformity is less crucial than the restoration of sagittal alignment in assessing pain and disability, although Glassman et al [4] did demonstrate an association between global coronal alignment (GCA, an offset of the C7 plumbline and the sacral line) of greater than 40 mm in the frontal plane and deterioration in patient outcomes.

From a clinical point of view, interpreting the information from several different radiographic parameters in multiple planes can be difficult; an analysis of individual measurements taken independently may help identify the most important parameters to correct.

The objective of this study was to evaluate the effectiveness of surgical treatment in restoring or correcting SVA, PI–LL, PT, coronal Cobb angle, and GCA.

3.2.2 MATERIALS & METHODS

Patient population and data collection

This study is a retrospective analysis of a consecutive series of ASD patients enrolled in a prospective multi-center study (10 sites) evaluating operative patients with x-rays at baseline and 1 year after surgery. Subjects were enrolled according to an IRB-approved protocol at each site. Inclusion criteria for the database were age greater than 18 years and a radiographic diagnosis of ASD defined as at least one of the following: Cobb angle>20°, SVA>50 mm, PT>25°, or Thoracic kyphosis>60°. Exclusion criteria were presence of inflammatory arthritis, tumors, or neuromuscular disease. Demographic and medical history data were collected. Standing antero-posterior and lateral spine radiographs were analyzed at baseline and 1 year after surgery using validated software[53,54] (Spineview®, Laboratory of Biomechanics Arts et Metiers ParisTech, Paris) to measure Thoracic (T) and Thoraco-lumbar (L) coronal Cobb angles(Figure 2-13, page 27), GCA(Figure 2-12, page 27), SVA(Figure 2-18, page 33), PI-LL(Figure 2-24, page 44) and PT(Figure 2-24, page 44) .For the present study, patients without complete set of X-rays at baseline and one year after the surgery were excluded.

Baseline classification

Each patient was individually classified according to the SRS-Schwab classification of ASD[113] Figure 2-28, page 51), and 8 groups based on deformity pattern were distinguish as in the previous study (Table 3-1, page 71).

Surgical correction of individual parameters

Each radiographic parameter was analyzed at baseline and 1 year post-operatively to identify if it met the following deformity thresholds: Cobb angle>30˚, GCA>40mm, SVA>40mm, PI-LL>10˚ and PT>20˚. The comparison between baseline and 1 year was used to individually categorize patients into one of the following “treatment efficiency” groups for each parameter (Table 3-10): “consistently normal,” “radiographic deterioration,” “persistent deformity,” or “radiographic correction.”

Treatment efficiency group defined for each individual parameter Cobb, GCA, SVA, Pi-LL and PT	Meet deformity threshold at baseline?	Meet deformity threshold at 1year postop?
Consistently normal	NO	NO
Radiographic deterioration	NO	YES
Persistent deformity	YES	YES
Radiographic correction	YES	NO

Table 3-10: Description of the "Treatment efficiency" groups for the 5 parameters: Cobb, Global Coronal Alignment (GCA), SVA, Pi-LL and PT.

Overall effectiveness

At 1 year, the overall radiographic effectiveness of the realignment procedure was evaluated individually by combining the results from the coronal and sagittal planes to make the following 4 groups:

- **No deformity**: patients who do not meet the deformity threshold for any of the 5 parameters
- **Coronal deformity**: patients who met only coronal deformity threshold(s) (Cobb angle and/or GCA)
- **Sagittal deformity**: patients who met only sagittal deformity threshold(s) (SVA, PT, and/or PI-LL)
- **Combined deformity**: patients who meet at least one coronal and one sagittal deformity threshold.

Statistical analysis

Differences in demographic data between deformity classification groups at baseline were evaluated using an ANOVA test. Significance threshold was established at $p<0.05$. At baseline the distribution of patients with sagittal deformity for the different combination of sagittal parameter was expressed. At baseline and 1 year, the proportion of patients in the entire sample with a deformity was calculated for each parameter independently. Then, for patients with deformity at baseline, the fraction of patients in the "radiographic correction" and "persistent deformity" groups was calculated by comparison with 1 year data for each parameter. Similarly, for patients without deformity at baseline, the fraction of patients in the "radiographic deterioration" and "consistently normal" groups was established for each parameter. Finally, the proportion of patients in each post-operative classification group was calculated for the entire population and after stratifying by curve type.

3.2.3 **RESULTS**

Enrollment (Table 3-11)

316 surgical patients were enrolled in this study between 2008 and 2011, 252 had adequate baseline radiograph and 215 patients had adequate baseline radiograph and 1 year follow up. On those 215 patients, 161 had adequate baseline and 1 year radiographs and were the only ones included in this study.

		SITE									
Number of patients	**Total**	**A**	**B**	**C**	**D**	**E**	**F**	**G**	**H**	**I**	**J**
Enrolled	315	59	14	51	6	33	25	15	15	58	39
Enrolled and adequate baseline radiographs	252	55	10	42	6	26	19	15	9	36	34
Enrolled, adequate baseline radiographs and 1 year follow up	215	55	10	42	4	20	10	15	8	21	30
Enroll, adequate baseline and 1 year radiographs	161	51	6	31	4	16	9	10	7	3	24

Table 3-11: Number of patients enrolled, number of patients with adequate baseline radiographs, number of patients with adequate baseline radiographs and 1 year follow up and number of patients with adequate baseline and 1 year radiographs by site.

Demographics and curve type (Table 3-12)

This study included 161 ASD patients (24 males and 137 females) with a mean age of 55±15 years. 80% of the patients had a coronal Cobb angle greater than 30°; patients with thoracic curve (13%) were less common than patients with thoraco-lumbar/lumbar curve (34%) or double curve (33%). The analysis of the sagittal spino-pelvic parameters revealed that 71% of the patients had a sagittal deformity (SVA, PI-LL, or PT meeting deformity thresholds), 54 % of whom had both coronal and sagittal deformity (group TS, LS, DS) and 17% had a pure sagittal deformity (group S). A total of 5 patients (3%) were unclassifiable due to the difference between the inclusion criteria for the database (coronal Cobb angle>20°) and the SRS-Schwab classification threshold for deformity in the coronal plane (Cobb angle>30°). These patients were removed from the analysis of treatment efficiency.

	U	T	L	D	TS	LS	DS	S	Total
% of total sample (number of patients)	3 % (5)	7 % (11)	10 % (16)	9 % (16)	6 % (10)	24 % (38)	24 % (37)	17 % (28)	100% (161)
Age	52±14	31±12	47±13	47±13	47±16	63±8	55±12	67±13	55±15
BMI	24±8	22±5	23±3	25±4	31±15	28±8	27±7	30±7	27±8
Prior surgery (%)	60	0	19	6	60	55	24	57	37

Table 3-12: Demographic data and prior surgery by type of curve: U: Unclassified, T: Thoracic, TL: Thoracic Sagittal, L: (Thoraco)-Lumbar, LS: (Thoraco)-Lumbar Sagittal, D: Double, DS: Double Sagittal and S: Sagittal.

Patients with pure thoracic coronal curves (T) were significantly younger (31±12) than those with other curve types ($p<0.05$). Within the group of patients with thoraco-lumbar/lumbar coronal curves (L and LS), patients with sagittal deformities (LS, age=63±8 BMI=28±8) were older and had a greater BMI than patients without sagittal deformity (L, age=47±13 BMI=23±3) ($p<0.05$). Patients with only sagittal deformity (S, age=67±13) were older than any of the groups with only coronal deformities (T, L, and D) ($p<0.05$). 37% of the patients had a history of prior spine surgery. The rate of history of prior spine surgery varied between 0 to 60% depending of the type of curve. Patients with sagittal deformity (with or without coronal deformity) were more likely to have had prior surgery than patients without sagittal deformity.

Sagittal deformity : distribution of sagittal parameters combinations (Table 3-13)

At baseline, the most frequent sagittal deformity (44%) was a combination of the three parameters (SVA, PI-LL and PT). The second most frequent sagittal deformity was defined by only a pelvic retroversion (20%). 3% of the patients with sagittal deformity had only a mismatch between the pelvic incidence and the lumbar lordosis.

	At base line, the distribution of the patients with sagittal deformity for the different combinations of the sagittal parameters (SVA, PI-LL and PT)							
	SVA	PI-LL	PT	SVA+PI-LL	SVA+PT	PI-LL+PT	SVA+PI-LL+PT	TOTAL
Number of patients	14	3	23	2	8	13	50	113
% of patients with sagittal deformity	12%	3%	20%	2%	7%	12%	44%	100%

Table 3-13: At base line, the distribution of the patients with sagittal deformity for the different combination of the sagittal parameters: Sagittal Vertical Axis (SVA), mismatch between pelvic incidence and lumbar lordosis (PI-LL) and Pelvic Tilt (PT)

Review of individual radiographic parameters

Radiographic treatment effectiveness for the different parameters are summarized in Figure 3-5. Table 3-14 expresses the distribution of patients meeting radiographic deformity thresholds at baseline and 1 year following surgery. Table 3-15 expresses the percentage of patients persistently deformed of the population with deformity at baseline and Table 8 expresses percentage of patient radiographically deteriorated of the population without deformity at baseline.

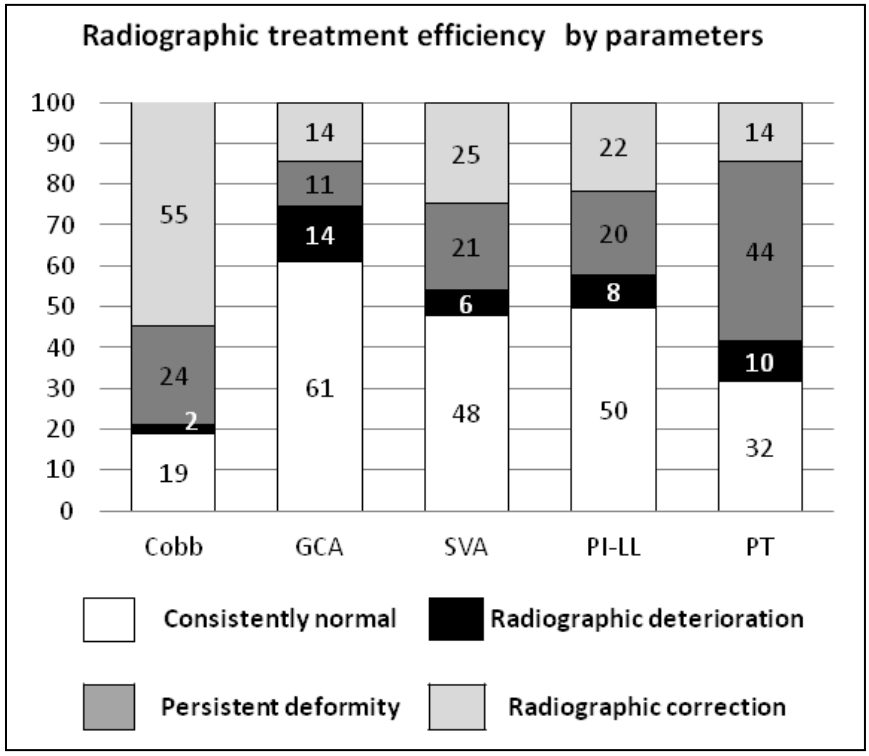

Figure 3-5: Radiographic treatment efficiency by parameters. . GCA : Global coronal alignment , SVA : Sagittal vertical axis, PT: Pelvic tilt, PI: Pelvic incidence, LL: lumbar lordosis

Coronal Cobb angle

At baseline, coronal Cobb angle>30° was the most common deformity (80% of the total population). The Cobb angle was persistently present in 30 % of those cases and so was corrected in 70%, making it also the most consistently corrected parameter. Cobb angle was the parameter that deteriorated least frequently: only 3 patients (9%) had deterioration; all had a preoperative Cobb angle close to 30° and the deterioration was between 3° and 7°. Postoperatively, 26% of patients had a Cobb angle greater than 30°.

	Distribution of patients that met the radiographic deformity thresholds (number of patients)	
	Baseline	**1 Year**
Cobb	80 % / (128)	26 % / (42)
GCA	25 % / (41)	25 % / (40)
SVA	46 % / (74)	27 % / (44)
PI - LL	42 % / (68)	29 % / (46)
PT	58 % / (94)	54 % / (87)

Table 3-14: Distribution of patients that met the radiographic deformity thresholds at baseline and 1 year following surgery for the different parameters: Cobb angle (Cobb), Global Coronal Alignment (GCA), Sagittal Vertical Axis (SVA), mismatch between pelvic incidence and lumbar lordosis (PI-LL) and Pelvic Tilt (PT)

GCA

At baseline, GCA was the least frequent deformity (25%, 41 patients); 93% (38 patients) of these patients had a thoraco-lumbar curve (L, LS, D or DS). GCA was corrected in 54% of those cases. However, GCA was also one of the most likely deteriorated parameters, as 18% of patients with a normal alignment at baseline met the threshold for deformity 1 year following surgery. This led to an overall rate of postoperative coronal misalignment of 25%, the same as the preoperative deformity rate.

SVA

At baseline, 46% of the patients had an SVA that met the deformity threshold. 54% of these patients were radiographically corrected, while 11% of the patients with a normal pre-operative SVA deteriorated. Postoperatively, a total of 27% of the patients had an SVA meeting the deformity threshold.

At 1year, percentage of patients Persistently deformed of the population with deformity at baseline (number of patients)				
Cobb	GCA	SVA	PI-LL	PT
30 % (39)	44 % (18)	46 % (34)	49 % (33)	76 % (71)

Table 3-15: Percentage of patients persistently deformed of the population with deformity at baseline for the following parameters: Cobb angle (Cobb), global coronal alignment (GCA), sagittal vertical axis (SVA), mismatch between pelvic incidence and lumbar lordosis (PI-LL) and pelvic tilt (PT)

PI-LL

At baseline, 42% of the patients had a PI-LL value that met deformity thresholds. 51% of these subjects were radiographically corrected, while 14% of the patients with a normal pre-operative PI-LL deteriorated. Postoperatively, 29% of the patients had PI-LL that met the deformity threshold.

PT

At baseline, 58% of the patients had a PT meeting deformity threshold (i.e. substantial pelvic retroversion); this represented the most frequent deformity among the sagittal parameters. Only 24% of these patients were radiographically corrected, and 24% with a normal baseline PT deteriorated postoperatively. Overall, 54% of the patients had a PT that met the deformity threshold at 1 year.

At 1 year, percentage of patient radiographically deteriorated of the population without deformity at baseline (number of patients)				
Cobb	GCA	SVA	PI-LL	PT
9% (3)	18% (22)	11% (10)	14% (13)	24% (16)

Table 3-16: Percentage of patients radiographically deteriorated of the population without deformity at baseline for the following parameters: Cobb angle (Cobb), global coronal alignment (GCA), sagittal vertical axis (SVA), mismatch between pelvic incidence and lumbar lordosis (PI-LL) and pelvic tilt (PT)

Overall results at 1 years

Table 9 summarizes the overall deformity distribution at 1 year. 23% of the patients had no deformity in either the coronal or sagittal plane, 35% had a deformity only in the sagittal plane, 14% only in the coronal plane, and 27% in both the coronal and sagittal planes. Patients with baseline deformity in the coronal plane only (T, L, or D) were more likely to have complete resolution of their deformity, especially patients with lumbar curves (75%). For patients presenting coronal and sagittal deformity at baseline, this sagittal deformity was not corrected for 68% (DS) to 86% (S) of the patients depending on the type of curve.

Expressed in % by type of curve (number of patients)	T	L	D	TS	LS	DS	S	Total
No deformity	55 % (6)	75 % (9)	38 % (6)	20 % (2)	5 % (2)	16 % (6)	14 % (4)	23 % (37)
Coronal deformity	18 % (2)	13 % (5)	25 % (4)	10 % (1)	13 % (5)	16 % (6)	0 % (0)	14 % (23)
Sagittal deformity	18 % (2)	13 % (2)	25 % (4)	50 % (5)	45 % (14)	32 % (11)	75 % (17)	35 % (57)
Combined deformity	9 % (1)	0 % (0)	13 % (2)	20 % (2)	37 % (17)	35 % (14)	11 % (7)	27 % (44)

Table 3-17: Postoperative categorization, showing the proportion of patients falling into the no deformity (no parameters meeting deformity thresholds), coronal deformity (coronal Cobb angle and/or GCA meeting thresholds), sagittal deformity (SVA, PT, and/or PI-LL meeting thresholds), and combined deformity (at least one coronal and one sagittal parameter meeting thresholds) groups by SRS-Schwab curve type. T: Thoracic, TL: Thoracic Sagittal, L: (Thoraco)-Lumbar, LS: (Thoraco)-Lumbar Sagittal, D: Double, DS: Double Sagittal, S: Sagittal.

3.2.4 **DISCUSSION**

ASD encompasses a broad range of radiographic patterns which makes it challenging to dissociate the intrinsic parameters of the deformity from those related to compensatory mechanisms. Recent reports have brought to light the difficulty in restoring spino-pelvic alignment following three-column osteotomies[194,195]. One common limitation to these studies is that they tend to focus on one single parameter and are often limited to a single plane (coronal or sagittal).

The objective of this study was to evaluate the ability of surgical treatment to radiographically restore spino-pelvic alignment while taking into account the type of deformity. With the exception of the coronal Cobb angle, all radiographic parameters were chosen based on their reported clinical relevance (i.e. correlation with patient reported outcomes), as demonstrated in large cohorts of patients representing the full spectrum of adult spinal deformity[14,90]. Several studies have shown correlation between clinical scores and coronal or sagittal global alignment (GCA/SVA)[14,16,90,196,197]. In an exception to these results, Sanchez-Mariscal et al[198] demonstrated only a low correlation between clinical scores after primary surgery and sagittal misalignment (PT and SVA) in 59 ASD patients. Based on multivariate analysis, the only significant predictor of disability was PT. However, the extent of deformity (i.e. if the patient had sagittal imbalance) and the effect of the surgery were not taken into account. To avoid the former problem, the present study compared radiographic parameters to thresholds of clinical relevance [14].

The present method was, however, limited in that it does not account for the absolute magnitude of surgical correction in regards to the severity of deformity at baseline. As such, a patient with a severe baseline deformity who had significant surgical correction would still be considered under-corrected if he or she did not reach the deformity threshold. The decision to overlook this issue was motivated by two reasons. First, the thresholds were defined by databases that included operative and non operative patients with and without previous surgery. Therefore, those patients with severe baseline deformity and significant restoration have been incorporated into the calculation of thresholds. Second, the objective of this study was to analyze the radiographic effectiveness of the surgery, not the clinical effect[89,109].

Analysis by parameter

The results illustrate that a large number of patients are insufficiently corrected and that deterioration in alignment is not a negligible phenomena; notably, for coronal misalignment (GCA), the number of patients who were corrected was similar to the number of patients who deteriorated (14%, Figure 3-5). While the clinical impact of the Cobb angle remains controversial, scoliosis is nevertheless the most common deformity in ASD surgical patients (80% in this

database). In this study, it was also the parameter with the highest rate of correction. This may reflect a historical bias to predominantly treating the most obvious aspect of ASD, even though sagittal parameters have been shown to be more influential on clinical scores[18,90].

Each sagittal parameter represents a different component of an individual's deformity. While in 44% of the cases the sagittal deformity was a combination of the three sagittal parameters, it also appears that a great variability of combination between the patients exists. The PI-LL represents a regional disharmony between PI, a morphologic parameter, and LL. The surgeon can directly affect this parameter. The considerable rate of inadequate PI-LL correction (48% in total sample) may illustrate insufficient consideration of this important relationship. PT was the parameter that most often deteriorated as well as the one least often corrected. While the surgeon cannot directly modify the PT, several models of PT prediction have been developed[134,194], and complete correction of structural sagittal deformity should obviate the need for pelvic compensation. Results from this study illustrate the gap between the scientific community and clinical practice. The combination of the 3 sagittal parameters revealed that sagittal deformity was present in 71% of patients preoperatively and 62% postoperatively, again perhaps indicating a lack of focus on sagittal imbalance during surgery.

Analysis by curve type

Only 23% of the patients experienced a complete radiographic correction of their deformity. Highly varying rates of correction were observed between the different SRS-Schwab curve types. These differences may relate to differences in overall complexity between curve types and variability in baseline severity of deformity. While patients with baseline deformity in the coronal plane only (T, L, or D) had a greater chance of achieving complete correction than patients with sagittal deformity, there was still substantial variability in likelihood of correction between the coronal groups. In particular, double curves appear to be much more difficult to completely correct than single curves. These results may help identify the risks of radiographic misalignment or deterioration that vary between SRS-Schwab curve types.

Conclusion:

This study represents a detailed analysis of surgical realignment outcomes across ASD patterns and highlight the limited efficiency in alignment restoration.

Combining only a limited number of radiographic measurement in both coronal and sagittal plane, a large diversity of pathologic curve was observed which makes complex the complete analysis of each patient.

The combination of the SVA, PI-LL and PT revealed that sagittal deformity was present in 71% of the patients pre-operatively and 62% post-operatively.

At baseline, 42% of the patients had a PI-LL mismatch that met deformity thresholds. 51% were radiographically corrected while 14% of the patients with a normal pre-operative PI-LL were deteriorated.

At baseline, 58% of the patients had a PT meeting deformity thresholds (i.e. pelvic retroversion); this represented the most frequent deformity among the sagittal parameters; only 24% of them were radiographically corrected.

Deterioration in alignment is not a negligible phenomena, notably, for coronal misalignment; the number of patients corrected was similar to the number of patients deteriorated(14%).

Longer follow up analysis is important to assess variations in compensatory parameters (notably PT) as well as alignment of non-fused portions of the spine. Furthermore, correlation between radiographic correction and clinical benefit requires further analysis.

The following article tends to explained this high rate of suboptimal realignment.

3.3 DISCREPANCIES IN PREOPERATIVE PLANNING AND OPERATIVE EXECUTION IN THE CORRECTION OF SAGITTAL SPINAL DEFORMITIES

The previous article did not identify the reason of failure in the realignment procedure, therefore a prospective, single center study of consecutive adult spinal deformity (ASD) patients undergoing sagittal realignment surgery has been conducted.

41 patients were included with preoperative and postoperative radiography. In addition, the planning was collected and confronted to the postoperative results three months after the surgery.

This article has been submitted to Spine in August 2014 and nominated as best paper at the North America Spine Society Congress 2014

Authors: Bertrand Moal, Virginie Lafage, Stephen Maier, Shian Liu, Vincent Challier, Wafa Skalli, Themistocles S. Protopsaltis, Thomas J. Errico, Frank J. Schwab

3.3.1 **INTRODUCTION**

The correlations between sagittal spino-pelvic radiographic parameters and Health Related Quality of Life (HRQOL) questionnaires[13,14,199–201] have highlighted the clinical relevance of the sagittal plane in the setting of adult spinal deformity (ASD). The sagittal component of the SRS-Schwab classification contains three sagittal modifiers: the sagittal vertical axis (SVA), the pelvic tilt (PT) and the mismatch between the pelvic incidence and the lumbar lordosis (PI-LL). In addition to providing a framework for patient evaluation, this classification also establishes alignment objectives in the sagittal plane[89,95,117].

However, restoration of these key radiographic parameters is challenging[66]. A recent prospective study of 114 surgical ASD patients with a sagittal deformity revealed that 84% of the patients still maintained some components of sagittal misalignment postoperatively[66]. Yet the study did not identify whether this high rate of sub-optimal radiographic outcomes was due to lack of planning, limitation in the execution of a plan, or if the pre-operative plan was in fact deliberately not set for perfect alignment due to patient factors or extent of sagittal deformity.

The objective of this study was to evaluate preoperative planning, and changes in procedure execution, in a root cause analysis of suboptimal radiographic outcomes related to ASD realignment surgery.

3.3.2 MATERIALS & METHODS

Inclusion criteria

This study is a prospective consecutive series of ASD patients who underwent a surgical sagittal realignment procedure. Patients were recruited at one center following IRB approval and treated by the same team of surgeons (4 surgeons, one of them was present for each surgery).

Data collection

Demographic data collected consisted of age, BMI, and past medical history. Preoperative planning was conducted by the surgical team using the Surgimap software (Nemaris, New York, NY)[21]. The software was used to assess key radiographic spino-pelvic parameters and a visual simulation of realignment. Planning included the number of stages, surgical approach, upper and lower instrumented vertebrae (UIV, LIV), use of iliac fixation, use of interbody fusion, and description of level and angle of resection for spinal osteotomies. Grade of resection was defined according to previously described osteotomy classification (Figure 2-30**Error! Reference source not found.**, page 54)[20]. Preoperative and planned maximum thoracic kyphosis (TK, Figure 2-17,page 30), lumbar lordosis (LL, Figure 2-17,page 30), PI(Figure 2-24, page 44), PI-LL(Figure 2-24, page 44), PT(Figure 2-24, page 44), SVA(Figure 2-18, page 33), and thoracic kyphosis within the anticipated instrumented segments (TKins) were collected. Kyphotic angles were reported as negative values, and lordotic angles as positive.

The intra-operative data collection included complications, blood loss, and changes between planning and actual surgical procedures. At the conclusion of the surgical procedure long sagittal cassette X-rays were obtained to measure lordosis of L1-S1, and kyphosis within the instrumented segments.

At 3 month follow-up, the previously described radiographic parameters were measured on sagittal standing full body X-rays, and complications and revision surgeries were noted.

Analysis

Changes between the planned surgical resection procedure and the actual one were stratified into 3 groups:

- More aggressive procedure than planned (MAPTP): the actual procedure included at least one more Grade II osteotomy than the planned one.

- Less aggressive procedure than planned (LAPTP): the actual procedure forewent at least one Grade II osteotomy that had been planned, or one planned Grade III osteotomy was converted into one or two Grade II.

- No change (NC): the actual resection procedure occurred exactly as planned.

Descriptive data was expressed as means, standard deviations, and ranges. A frequency distribution was used to describe the preoperative sagittal modifiers of the SRS-Schwab classification[113] (Figure 2-28, page51). The preoperative planning was described via the frequency of the UIV, LIV, interbody fusion (number and levels), osteotomy (Grade, number, level, and resection angle). The planned radiographic changes in terms of SVA, PT and PI-LL were tabulated and reported using descriptive statistics and by distribution of SRS-Schwab modifiers. Paired t-test and Chi-Square analysis were used to compare the planned radiographic parameters and the post-operative one. Comparisons between postoperative and intra-operative parameters were done using paired t-tests. Finally, changes between the actual and planned surgical procedures were described. Comparisons between patients with LAPTP and NC were done with unpaired t-tests or chi-square analyses.

3.3.3 **RESULTS**

Dataset

Fifty patients were enrolled within a 17 month period (August 2011 to December 2013). Partial data were missing for 9 patients (One with missing postoperative x-rays, four without femoral heads clearly visible on preoperative x-rays, and 4 incomplete preoperative surgical plans), therefore 41 patients were analyzed. There were 29 women and 12 men, with a mean age of 64 years and a BMI of 29 kg/m^2 (Table 3-18). Twenty nine patients presented with a history of previous spine surgery.

	Mean	Std. Deviation	Minimum	Maximum
Age	64	12	20	84
BMI (kg/m^2)	28	7	18	50
Max Kypho (°)	-30	20	-87	-1
TKins (°)	-20	20	-78	5
LL (°)	21	19	-16	69
PI (°)	58	14	34	86
PI_LL (°)	38	18	-3	69
PT (°)	36	13	3	66
SVA (mm)	120	67	19	296

Table 3-18: Demographic and pre-operative radiographic parameters. Max_Kypho (maximum thoracic kyphosis), TKins (thoracic kyphosis within the anticipated instrumented segments), lumbar lordosis (LL), pelvic incidence (PI), pelvic incidence minus lumbar lordosis (PI-LL), pelvic tilt (PT) and sagittal vertical axis (SVA).

Pre-operatively, there was a large variability in sagittal radiographic parameters (Table 3-18) with, on average, a severe sagittal plane misalignment with a mean PI-LL mismatch of 37°±18, a pelvic tilt (PT) of 35°±13, and a SVA of 120mm±67. About 90% of the patients had a SRS-Schwab grade + or ++ in all three parameters (Figure3-6), and none of the patients had all three modifiers at grade 0.

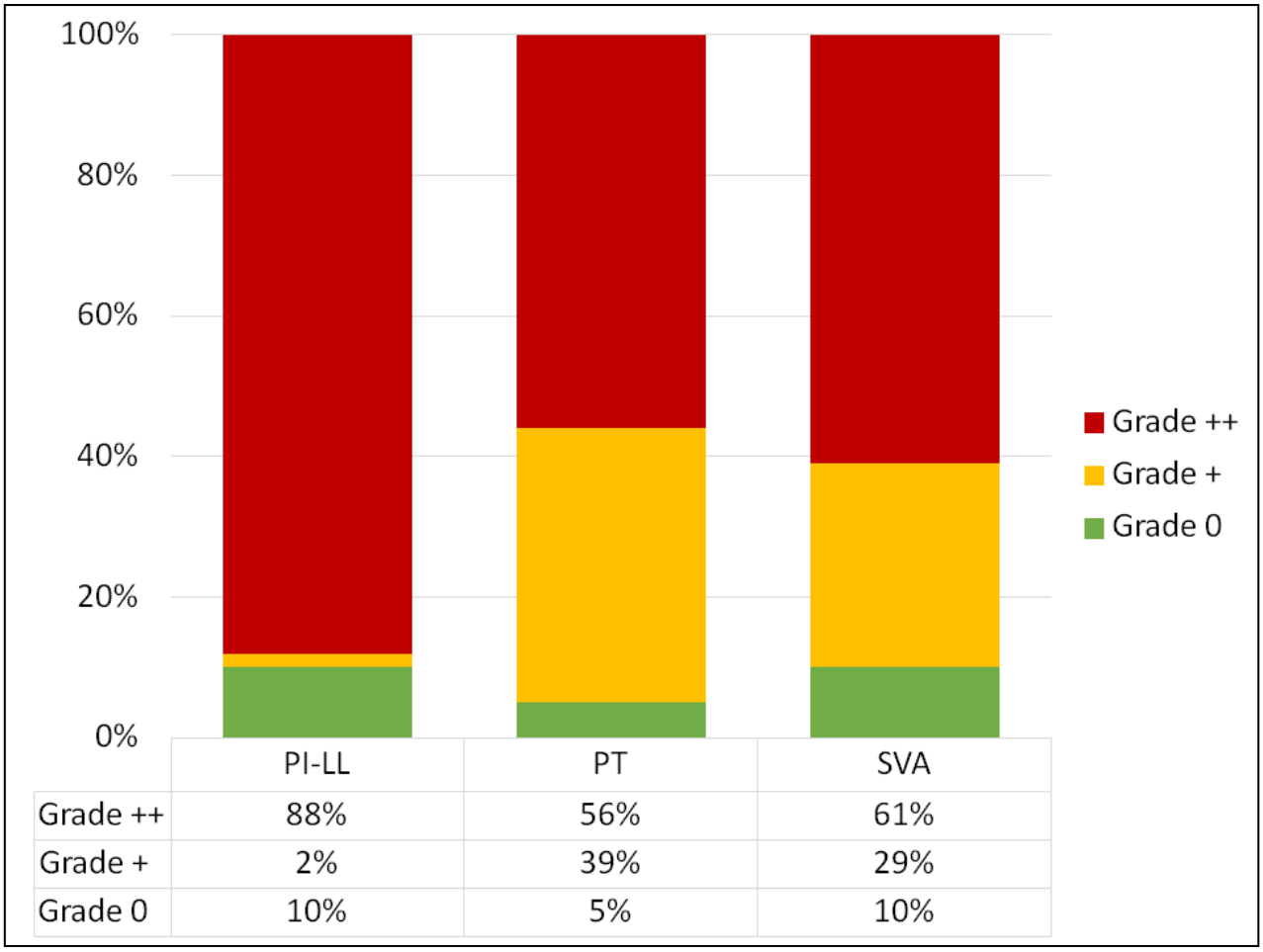

	PI-LL	PT	SVA
Grade ++	88%	56%	61%
Grade +	2%	39%	29%
Grade 0	10%	5%	10%

Figure3-6: Pre-operative distribution of SRS-Schwab modifiers , SVA (sagittal vertical axis), PI-LL (pelvic incidence minus the lumbar lordosis), and PT (pelvic tilt)

Preoperative Planning

All patients were planned for a single stage posterior approach surgery. The most common planned UIV were T10 (n=16) and T4 (n=11), with 51% of the UIV in the upper thoracic area, and 49% in the thoraco-lumbar area. The LIV planning called for a fusion to the ilium for 36 patients, to S1 for 3 patients, and to L5 for 2 patients. Twenty-seven patients were planned for a single Grade III resection (n=20 at L3), and 2 patients for a double Grade III resection. The remaining 12 patients were all planned for at least one Grade II osteotomy. The average planned resection angle was 10°±3 for Grade II resection, and 28°±7 for Grade III osteotomy. Interbody fusion was planned for 24 patients with the following TLIF distribution: 19 L5-S1, 2 L4-L5, and 1 L3-L4.

Planned sagittal alignment (Table 3-19)

On average the surgical planning called for a decrease in PI-LL of -33°±14, PT of -17°±13, and SVA of -85mm±68. The only patient with an S1 osteotomy was planned for an increase in PT (+ 9°). 76%, 62% and 64% were planned to reach SRS-Schwab modifier grade of 0 for Pi-LL, PT and SVA, respectively. There was 14 patients (34%) planned to reach a Grade 0 in the three modifiers; these patients had a smaller PI than the rest of the cohort (51°±8 vs 62°±14), and a smaller PI-LL (30°±20 vs 42°±15).

	Planned changes						
	Mean	Std. Deviation	Minimum	Maximum	Grade 0	Grade +	Grade ++
PI-LL	-33°	14°	-66°	0°	76%	22%	2%
PT	-17°	13°	-48°	9°	61%	32%	7%
SVA	-84mm	69mm	-238mm	37°	63%	29%	7%

Table 3-19: Planned changes for SVA (sagittal vertical axis), PI-LL (pelvic incidence minus the lumbar lordosis), and PT (pelvic tilt)

Post-operative alignment versus Planning

Postoperative alignment by SRS-Schwab modifier (Figure 3-7) revealed that PT was the least corrected parameter (19% of the patients with grade 0), while this grade was reached for ~50% of the patients in PI-LL and SVA. Only 10% (4 patients) of the patients had a postoperative grade 0 in all three modifiers. On average postoperative alignment was under-corrected when compared to the planned procedures in terms of LL (-6° ±11) and PT (+8°±9), and changes in TK and TKins were greater than planned (Table 3-20).

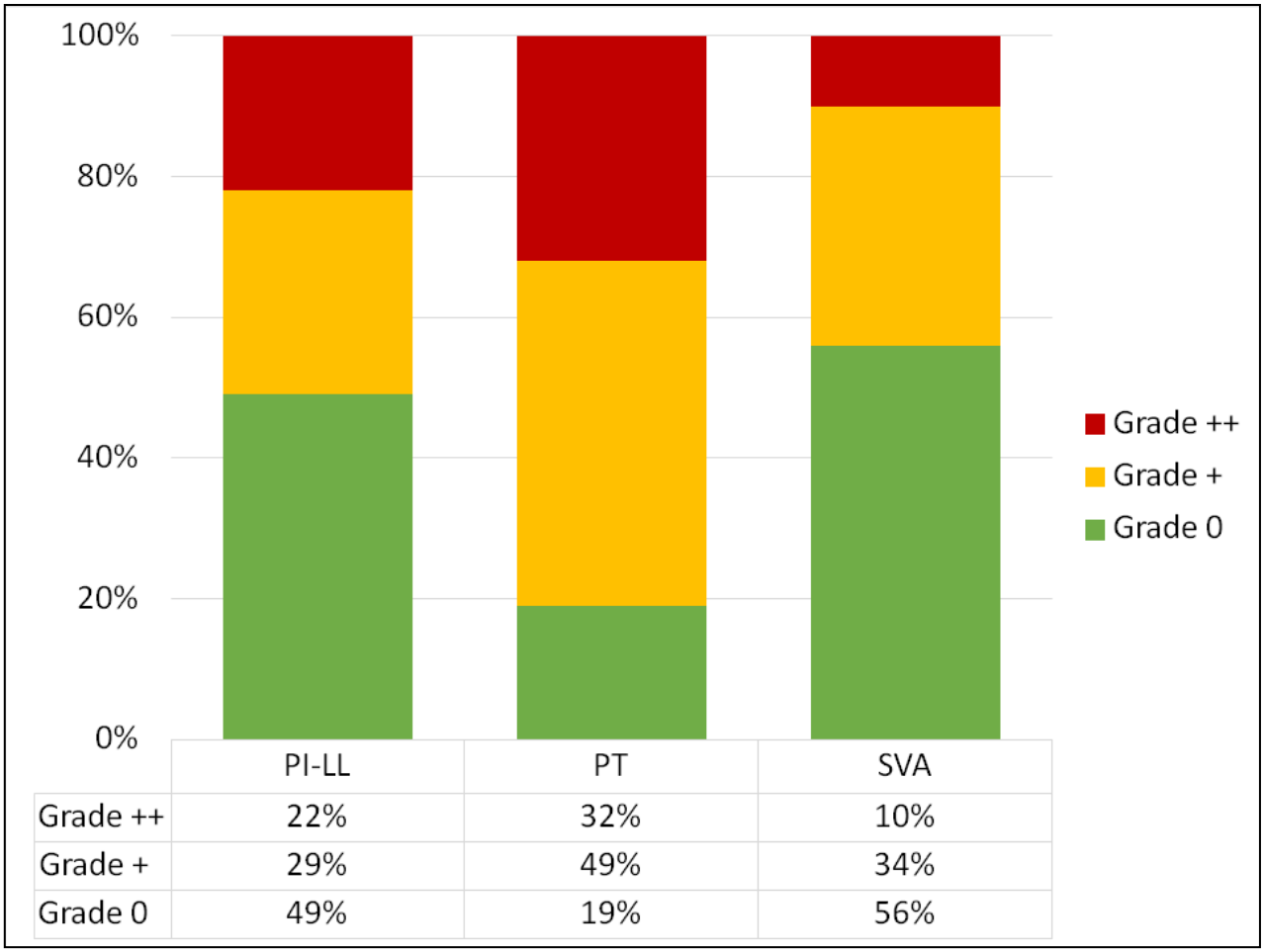

	PI-LL	PT	SVA
Grade ++	22%	32%	10%
Grade +	29%	49%	34%
Grade 0	49%	19%	56%

Figure 3-7: Post-operative distribution of SRS-Schwab modifiers, SVA (sagittal vertical axis), PI-LL (pelvic incidence minus the lumbar lordosis), and PT (pelvic tilt)

Post OP - Planned measurements	Mean	Std. Deviation	Minimum	Maximum	P value
Max_Kypho (°)	-15	13	-44	8	p<0.001
TKins (°)	-11	11	-47	6	p<0.001
LL (°)	-6	11	-31	17	p=0.001
PI-LL (°)	6	11	-11	28	p=0.001
PT (°)	8	9	-14	27	p<0.001
SVA (mm)	-6	51	-110	100	p=0.786

Table 3-20: Difference between planned and postoperative results for the radiographic parameters: Max_Kypho (maximum thoracic kyphosis), TKins (thoracic kyphosis within the anticipated instrumented segments), lumbar lordosis (LL), pelvic incidence (PI), pelvic incidence minus lumbar lordosis (PI-LL), pelvic tilt (PT) and sagittal vertical axis (SVA) were measured preoperatively.

Postoperatively, 51% of the patients reach the same grade than planned for PI-LL, 29% for PT, and 44% for SVA. A greater postoperative grade than planned was reported for 37% (PI-LL), 61% (PT), and 33% (SVA) of the patients; a smaller grade than planned for 12% (PI-LL), 10% (PT), and 23% (SVA). Of note, of the 25 patients whose postoperative PI-LL matched the planned one, respectively 36% and 50% of the patients reached the same grade than planned for the PT and SVA.

There was no significant difference between intra- and postoperative LL, but a larger postoperative kyphosis within the fused segments than intra-operatively (-21± 19, vs -28± 20, $p<0.001$).

Actual Surgical Strategy versus Planned Strategy

The intra-operative UIV differed from the planned one by one level for six patients, with the fusion being shorter in 5 instances. For the LIV, the planning was respected for all but one patient where the iliac fixation was not inserted due to an existing abundant fusion mass. Eight changes in planned interbody fusions (IF) were reported in 7 patients: in five cases, the clinician decided intraoperatively to add an unplanned IF (3 at L5-S1, 1 at L4-L5), and the planned IF was not performed due to existing fusion (3 cases) or excessive blood loss (1 patient).

The level of Grade III resection was changed intra-operatively for 2 of the 27 patients (L2 and L4 osteotomies instead of L3). The type of osteotomy was respected intra-operatively for 25 patients (NC group, example Figure 3-8), 2 patients received a more aggressive procedure (MAPTP group), and 14 received a less aggressive procedure than planned (LAPTP group). For the MAPTP group, 1 patient received one unplanned Grade II resection, and 1 patient received 3 unplanned Grade II resections. In the LAPTP group, the planned Grade III resection was replaced by one or two Grade II resections for 11 patients, and a planned Grade II resection was not performed in 3 patients. Of note two patients suffered of intra-operative hypotension, and the surgeon had to modify the planned sagittal procedure (classified as LAPTP).

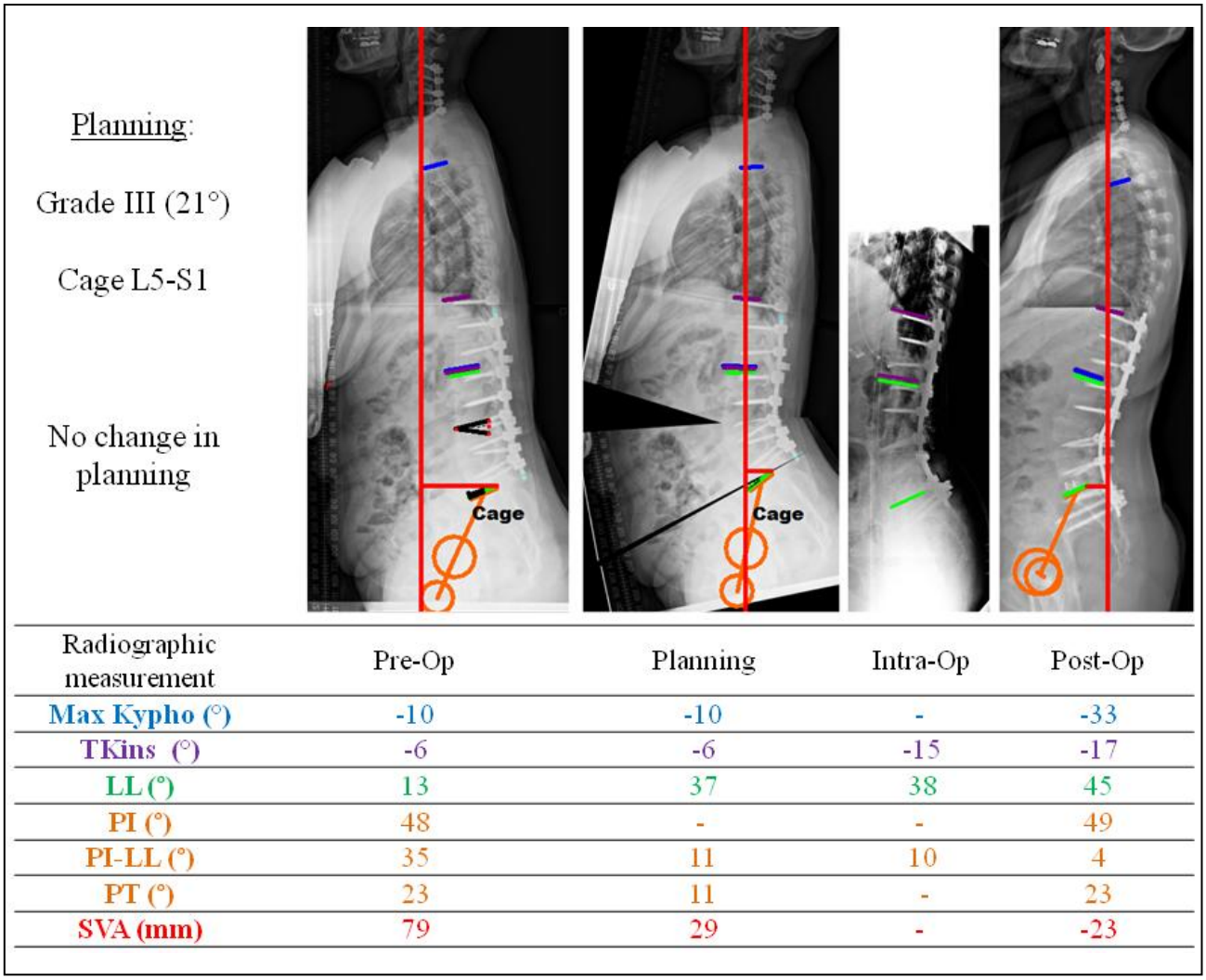

Radiographic measurement	Pre-Op	Planning	Intra-Op	Post-Op
Max Kypho (°)	-10	-10	-	-33
TKins (°)	-6	-6	-15	-17
LL (°)	13	37	38	45
PI (°)	48	-	-	49
PI-LL (°)	35	11	10	4
PT (°)	23	11	-	23
SVA (mm)	79	29	-	-23

Figure 3-8: Example of preoperative, planned , intra-operative and postoperative radiographic for a patient planned for a Grade 3 osteotomy and a cage with no change in the procedure (NC group). Max_Kypho (maximum thoracic kyphosis), TKins (thoracic kyphosis within the anticipated instrumented segments), lumbar lordosis (LL), pelvic incidence (PI), pelvic incidence minus lumbar lordosis (PI-LL), pelvic tilt (PT) and sagittal vertical axis (SVA).

MATP group

The 2 MAPTP patients reached the planned PI-LL grade, both had a greater PT grade than planned. For the SVA, one of them reach the same grade than planned and the other a greater than planned. No revision or complication was reported for these groups.

Comparison between NC and LAPTP groups

No significant difference was found between LAPTP and NC groups in age (LAPTP:65±15 ; NC: 63±9), BMI (LAPTP:28±6 ; NC: 29±7), blood loss (LAPTP: 2333ml ±1638 ; NC: 2966ml ±1337), or in

terms of distribution between long and short fusions (Short fusion, LAPTP: 6/14; NC: 12/25). As illustrated in Table 3-21, more Grade III resections were planned for the LAPTP group (p=0.011) but fewer Grade III resections were actually performed (p=0.048).

	NC	LAPTP
Grade III planned *	16/25	13/14
Grade III done*	16/25	3/14
Number Grade II planned	1.4 ± 2.0	1.7 ± 1.3
Number Grade II done	1.4 ± 2.0	2.8 ± 2.8

Table 3-21: Grade III planned and done as well as number of Grade II planned and done for No change (NC) group and less aggressive procedure (LAPTP) groups. *Indicates p<0.05.

At baseline, LAPTP patients had a greater PI-LL mismatch (50°±11vs 29°±16) and PT (41°±12vs 31°±12) (Table 3-22). These patients were planned for greater change in LL (-42°±11vs 28°±12) and PT (-22°±12vs -13°±11), but also planned for a greater postoperative PI-LL mismatch.. Despite a mean difference of 8°, postoperatively no significant difference was found in PI-LL (16°±10 vs 8°±14, p=0.058). There were no other significant differences in the radiographic parameters investigated. No significant differences were found for the frequencies of complications (NC: 29%, LAPTP: 32%) or revisions (NC: 7%, LAPTP: 8%).

Parameters and time point		Group	N	Mean	Std. Deviation	P value
PI minus LL (°)	Preop	LAPTP	14	50	11	**p<0.001**
		NC	25	29	16	
	Planning	LAPTP	14	8	7	**p=0.044**
		NC	25	1	10	
	Planning - Preop	LAPTP	14	-42	11	**p=0.001**
		NC	25	-28	13	
	Postop	LAPTP	14	16	10	p=0.058
		NC	25	8	14	
	Post - Preop	LAPTP	14	-34	9	**p=0.006**
		NC	25	-19	18	
	Postop - Planning	LAPTP	14	8	10	p=0.658
		NC	25	6	11	
PT (°)	Preop	LAPTP	14	41	12	**p=0.015**
		NC	25	31	11	
	Planning	LAPTP	14	19	9	p=0.664
		NC	25	18	9	
	Planning - Preop	LAPTP	14	-22	12	**p=0.027**
		NC	25	-13	11	
	Postop	LAPTP	14	28	8	p=0.328
		NC	25	25	11	
	Post - Preop	LAPTP	14	-13	11	**p=0.015**
		NC	25	-4	11	
	Postop - Planning	LAPTP	14	9	12	p=0.519
		NC	25	7	8	

Table 3-22: Significant radiographic differences between the LAPTP(less aggressive procedure than planned) and NC(No change) groups. PT : pelvic tilt, PI: pelvic incidence and LL: lumbar lordosis.

3.3.4 **DISCUSSION**

Several methods have been described in the literature to provide tools to guide surgeons in their preoperative planning. Only three studies analyzed their methods prospectively[20,22,126], and on those three only Autouer[22] and Steffen et al[126] presented the comparison between the preoperative planned measurement and the postoperative one with a small number of patients (6[126] and 11[22] ASD patients). However neither of them detailed the surgical procedure as a part of the planning which derives the originality and interest of the present study.

Sagittal realignment planned versus "SRS-Schwab Guidelines"

Results demonstrated that the surgical objectives of PI-LL <10°, PT < 20° and SVA < 40mm were not planned for all the patients included in this study. The required degree of resection and surgical risks associated with larger or multiple osteotomies may have influenced the preoperative plan in this population of older adults (mean age 64, max 84 years old). Recent work has established new age-specific thresholds of sagittal alignment reflecting that a higher SVA, PI-LL may be acceptable in older subjects [202].

Intraoperative change in procedure

In 15% of patients in this case series, change in the upper level of fusion occurred, and in general to reduce the number of levels fused. The amount of deviations from the plan for changing interbody fusion strategies during the surgery can be explained because the quality of fusion or degree of ankylosis between vertebrae is difficult to evaluate at baseline with only coronal and sagittal radiographs[203]. It is nevertheless difficult to evaluate the impact of these changes on sagittal alignment and clinical gain for the patients. The change in vertebral level of osteotomy such as a Grade III resection is rare (2/27), and maybe due to anatomical considerations intraoperatively.

Comparison between the patient NC and LAPTP cohorts

In general, surgeons may be more inclined on reducing aggressiveness of the resection compare to the planning; only 2 patients had a more aggressive surgery. Aggressiveness of surgery compared to the planning was based on grades of posterior correction (ex. Grade II vs. Grade III) and not on the amount of regional alignment change. Of note, LAPTP patients had a greater sagittal misalignment, and were planned for greater correction in lordosis; postoperatively they had a greater correction of the LL, with less Grade III resections and more Grade II resections. These changes in the planning did not have significant effect on the discrepancies between planned and

postoperative sagittal alignment compared to the NC groups. These findings are in line with the one from Cho et al[204] who demonstrated that three or more Grade III resections yielded similar correction than one Grade III resection. These results, specific to a team of surgeons, indicated that when a lordosis correction greater than 30° is needed, deviation in the preoperative plan is a viable option converting from possible Grade III to several Grade II resections.

Under correction of the LL:

On average, the effective change in LL was moderately less than planned, and it was similar for both groups LAPTP and NC (~ 6°), perhaps reflecting either overestimation of the how much resection would be obtained in the OR for a given grade of osteotomy during software simulation/planning, or poor intraoperative feedback on actual correction achieved. In 2 cases, patient factors limited the ability to execute the preoperative plan, as hypotension lead to a reduction in the aggressiveness of the surgery.

Planning and prediction

The correction of LL and the degree of change in kyphosis across fused thoracic levels resulted in reciprocal changes for the PT and kyphosis in unfused thoracic levels. The greater than expected postoperative thoracic change emphasizes the need for a better understanding and anticipation of reciprocal thoracic change, particularly in unfused levels. The overestimated change in PT (~8°) also revealed the limitations of prediction done only on a graphical method. Several other methods using numerical models have been developed to predict the SVA and PT and are detailed in the section 2.4.5, page 53. Smith et al[136], in a comparative study, evaluated the different formulas, and found that Lafage formulas[23], which incorporated PT and spinal compensatory changes, best predicted the SVA. However this model is limited because changes in kyphosis are defined as an input for the prediction.

Several other limitations of the planning method have been highlighted by this root cause analysis method. It appears difficult to account for segmental flexibility et alignment changes applied to the spine, such as the degree of rod bending, facet/disc motion via a purely graphical method. The change due to Grade I resections (facetectomies) were also not integrated in the planning. It is evident that variability in alignment can occur in the spine between preoperative standing position OR position and through the various stages of surgery outside of the formal osteotomy components. .

Intra-operative reconciliation

With the long cassette x-ray, in only 21/41 cases was it possible to quantify the degree of kyphosis in fused thoracic spine, and the quality of the x-ray is sometimes problematic for measuring the LL.

Moreover the intra-operative portable radiograph machine is quite large and lacks agility in an operating room, thus taking up open incision time, and forcing the surgical team away from the operative field. While fluoroscopy can be used with more frequency and agility in the case, it cannot acquire the full image of the lumbar spine to properly assess the lordosis.

Limitations:

This study has significant limitations due to the factors noted above. Furthermore, the variability in operative technique, findings at time of surgery and patient parameters can all heavily influence outcome and are not fully captured in this study.

Conclusion:

The present root cause analysis has identified the limits of the current planning and execution of spinal realignment for severe deformities. In ASD population suffering from severe deformities, planned objectives should take into account age and preoperative deformity. Variation from the planned procedure does not seem to impact sagittal realignment. However, the findings in the study highlight the critical need for developing better tools to predict postoperative standing alignment. Intraoperatively, planning approaches must offer flexibility given the common modification in level and degree of resection required. An additional area of need resides in the intraoperative reconciliation of alignment according to plan.

3.4 SYNTHESIS: SURGICAL TREATMENT FOR ASD PATIENTS

Using SRS score, MCID and normative scores, a new method for the evaluation of clinical effectiveness for ASD patient has been developed. The two main proponents of this method are to use the MCID as a scale and not as a threshold which should permit an easier and more relevant clinical interpretation, and to combine the evaluation of change in clinical outcomes to the analysis of post-operative outcomes with regards to an age and sex-matched normative population.

These methods have demonstrated that if 33% of patients reached normative values at 2 years following surgery, 24% did not perceive improvement or experienced deterioration.

One possible reason for this deficiency in the treatment could be the complexity to restore a correct alignment. As demonstrated, complete restoration of the sagittal alignment was rare and the deterioration was not a negligible phenomenon.

The last part of this work gave preliminary reasons of the issue of alignment restoration. In ASD population suffering from severe deformities, planned objectives should take into account age and preoperative deformity, and an optimal alignment is not always reachable.

It seems obvious that the development of better intraoperative tools to support the surgeons in its surgical correction are an absolute needed condition to reach planned alignment.

In terms of planning methods, our inability to correctly predict change in unfused parts (including the thoracic, the hip and the knee), is a break in the improvement of surgical treatment. New methods have to be developed and the consideration of the soft tissue, and notably the muscles, could certainly improve these methods.

Therefore, the first article of the second section of this work describes a method to assess the muscular system of ASD patients.

4. MUSCULAR EVALUATION AND ADULT WITH SPINAL DEFORMITY

4.1 VALIDATION OF 3D SPINO-PELVIC MUSCLES RECONSTRUCTIONS BASED ON DIXON MRI SEQUENCES FOR FAT-WATER QUANTIFICATION.

The aim of the following article was to evaluate a protocol, including MRI acquisition with Dixon method and the DPSO method, for 3D geometry measurement and fat infiltration of key muscles of the spino-pelvic complex. The reproducibility study included two volunteers for which three operators completed reconstructions three times across three sessions. In addition 3D reconstruction were compared to 3D references obtained on T1 acquisitions identifying the contour of the muscles on all axial images.

This article has been published in Innovation and Research in BioMedical engineering journal (IRBM) in 2014.

Authors : Bertrand Moal, José G. Raya, Erwan Jolivet, Frank Schwab, Benjamin Blondel, Virginie Lafage, Wafa Skalli

Compare to the original version the details related to the DPSO methods has been removed because previously described in the section 2.5.1 page 61

4.1.1 **INTRODUCTION**

The muscular system plays an essential role in the maintenance of postural balance; however, in clinical practice as well as research, investigation into the relationship between the muscular system and postural pathologies such as adult spinal deformity, has been limited.

The current lack of knowledge related to soft tissue stabilizers may be attributed to the absence of a relevant tool to evaluate the muscular system as a whole. The large number of muscles involved in postural maintenance makes a global analysis difficult and time consuming. In the case of adult spinal deformity (ASD), recent research has highlighted the critical role of sagittal spino-pelvic alignment in patient-reported pain and disability[13,14,16,90,205]. Therefore, key muscles involved in pelvic-positioning and lumbar-stabilization are at the forefront of research needs.

Preliminary efforts have been directed towards understanding the muscular envelope of the spine using histological analyses[141–144], measurement of muscular strength[145–147], and measurement of electromyographical signals[149,150]. However, these approaches are not adapted for study of a large number of muscle groups. Other studies, using imaging such as MRI or CT scan, correlated measurement of the muscle cross-sectional areas (via ultrasound, CT-scan or MRI)[153,154,157,158,206], or measurement of muscular density (via CT-scan or MRI)[145–147,153–156,206,207], with chronic back pain or spinal surgery outcome. The limitations of these approaches lie in the difficulty to represent variability in volume of an entire muscle[167].

To overcome these limitations, Jolivet et al[170,171] developed a method of three-dimensional muscle reconstruction via segmentation of a small number of axial images (MRI or CT-scan). This method, based on the deformation of a parametric specific object (DPSO), has been successfully implemented with CT scans for analysis of muscles involved in knee motion[172] and muscle groups around the hip joint[208]. The CT-scan modality presents two advantages: good contrast quality for muscle segmentation and good reliability in terms of fat and muscle density. CT scans allow for both a reproducible analysis of muscle geometry and a quantified evaluation of fat infiltration[171]. Nevertheless, the radiation exposure from CT scans renders it unacceptable as a tool for studies involving ASD patients who are already frequently subjected to radiographic examination. Notably, the DPSO method has also been performed using MRI T1 sequences[172]. However, the inhomogeneity in the magnetic field applied did not allow an accurate quantification of the fat infiltration (without fat infiltration, the muscle volume is an incomplete descriptor).

In order to avoid the problem of inhomogeneity and obtain an accurate quantification of fat infiltration, Dixon et al[166] developed a specific acquisition sequence where two images are

obtained: one in which the intensity of each voxel is correlated with the quantity of fat and the other in which the intensity of each voxel is correlated with the quantity of water. This method was then improved by Glover et al[183]. To our knowledge, the feasibility of 3D muscular reconstruction on MRI with the Dixon method was not studied.

The objective of this study was to evaluate the feasibility of an MRI protocol with dedicated sequences for fat-water quantification to assess the 3D geometry and homogeneity (fat infiltration) of key muscles in the spino-pelvic complex.

4.1.2 MATERIALS & METHODS

Subject Sample

Two asymptomatic female adult volunteers were included in this pilot study: Volunteer A (35 years, 68 kg) and Volunteer B (38 years, 91 kg).

MRI Acquisition

MRI was performed on a 3 T whole-body scanner (Magnetom Verio, Siemens Healthcare, Erlangen, Germany) using a 24-channel spine matrix coil and three 4-channel flex coils from the same vendor. The imaging protocol included a T1-weighted turbo spin-echo (T1 TSE) sequence (TR/TE = 1220/11 ms, acquisition matrix = 512×384, in plane resolution = 0.98×0.98 mm^2, slice thickness = 5 mm, slice gap = 5 mm, parallel imaging acceleration factor (iPat) = 2, 40 slices, flip angle = 150^o, bandwidth = 219 Hz/pixel, turbo factor = 5, acquisition time = 2:15 min) and a T1-weighted TSE sequence for applying the three point Dixon method[166,183,209,210] (TR/TE = 829/15.7 ms, acquisition matrix = 512×384, in plane resolution = 0.98×0.98 mm^2, slice thickness = 5 mm, slice gap = 5 mm, iPat = 2, 40 slices, flip angle = 150^o, bandwidth = 315 Hz/pixel, turbo factor = 3, echo spacing = 15.7, acquisition time = 4:38 min). Water and Fat images were automatically generated by the scanner from the TSE images for the three point Dixon method (Figure 4-1). Both sequences had exactly the same slice position and orientation. Image volume covered the proximal tibia to the lumbar spine (Th12 vertebra) and was acquired in three stages. Total acquisition time was 45 min.

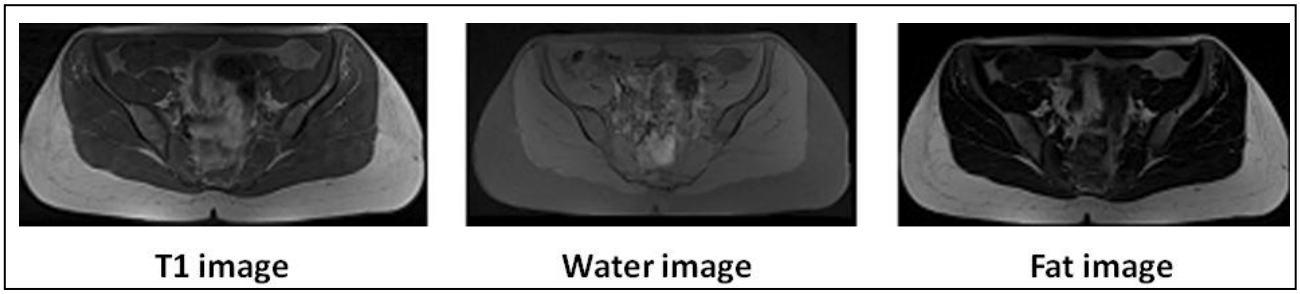

Figure 4-1: Examples of a T1 (right), Water (center), and Fat (right) image.

3D muscles reconstruction

The 3D reconstruction of individual muscles was performed using Muscl'X software, a custom software, (Laboratory of Biomechanics, Arts et métiers ParisTech, France) which permit to apply the deformation of parametric specific objects(DPSO) methods[170,171]. With this method, from a

limited number manually segmented slices (MSS), It was possible to obtain the complete 3D reconstruction of each. The optimal percentage of MSS, (defined as the number of MSS, divided by the total number of slices covering the entire muscle) of each muscle is reported in Table 4-1.

Muscles of interest

Table 4-1 describes the right- and left-sided muscles or groups of muscles analyzed in this study. Muscles were chosen based on their potential role in regulating the position of the pelvis. Because the delineation of certain muscles was difficult and in order to decrease the number of reconstructed muscles, some of the muscles were regrouped. The adductor longus, brevis and magnus were reconstructed into a single group named "Adductor". In addition, the transversus abdominis muscle, internus obliquus, and externus obliquus were considered as a single group named "Obliquus" (they were reconstructed from their caudal insertion up to the liver). The rectus abdominus, the psoas, and the erector spinae were reconstructed from their caudal insertion to the superior endplate of the first lumbar vertebra. The short- and long- heads of the biceps femoris were grouped together ("Biceps femoris"), as were the semimembranosus and semitendinosus muscles ("Semimembranous tendinosus"), and the vastus lateralis and vastus intermedius muscles ("vastus lateralis inter"). In total 18 muscles, right and left, were analyzed.

MR Parameters

Based on 3D reconstructions, the following parameters were calculated for each muscle: mean and maximal axial section (AS), muscle volume, and muscle length. Muscle length was defined as the sum of distances between barycenters of all consecutives slices.

From the Water and Fat images, the relative fat content for each voxel, Fat/Water Ratio, was calculated using equation [4.1.2].

$$Fat/Water\ Ratio = 100 * \frac{SI_{fat}}{SI_{fat} + SI_{water}}$$

[4.1.1]

where SI_fat represents the signal intensity of the fat signal and SI_water represents the signal intensity of the water image. For each muscle, all voxels contained in the muscle outline were identified. The average Fat/Water ratio was calculated over all voxels contained in each muscle allowing a quantification of the fat inside each muscle.

Muscle reconstructed	Percentage of MSS
Adductor	20
Biceps femoris	12
Erector spinae	15
Gluteus maximus	18
Gluteus medius	25
Gluteus minimus	30
Gracilis	10
Iliacus	25
Obliquus	20
Psoas	10
Quadratus lumborum	18
Rectus abdominus	12
Rectus femoris	13
Sartorius	10
Semimembranous tendinosis	11
Tensor Fascia Lata	15
Vastus lateralis inter	15
Vastus medialis	15

Table 4-1: Muscles analyzed in this study, and optimal percentage of MSS slices

MR Parameters

Based on 3D reconstructions, the following parameters were calculated for each muscle: mean and maximal axial section (AS), muscle volume, and muscle length. Muscle length was defined as the sum of distances between barycenters of all consecutives slices.

From the Water and Fat images, the relative fat content for each voxel, Fat/Water Ratio, was calculated using equation [4.1.2].

$$Fat/Water\ Ratio = 100 * \frac{SI_{fat}}{SI_{fat} + SI_{water}}$$

[4.1.2]

where SI_fat represents the signal intensity of the fat signal and SI_water represents the signal intensity of the water image. For each muscle, all voxels contained in the muscle outline were

identified. The average Fat/Water ratio was calculated over all voxels contained in each muscle allowing a quantification of the fat inside each muscle.

Evaluation of the Protocol:

All the operators involved in the protocol evaluation were experienced in reading muscular anatomy on MR images and received training in the use of the software (Muscl'x). For the DPSO method, the first and last slices of each muscle were manually segmented and used as limits for all reconstructions; all operators used exactly the same number of MSS (Table 4-1) while the selection of the actual MSS was left to the operator's discretion.

Evaluation of the DPSO method

For each muscle of the studied volunteers, a reference object (i.e. 3D geometry) was generated on T1 images by manually contouring all MR axial images covering it. Figure 4-2 presents the 3D reconstruction of Volunteer A. This method of reconstruction was named the reference method and the 3D reconstruction objects were named references. The references for Volunteers A and B were obtained by one operator. Using the DPSO method and the number of MSS presented in Table 4-1, this operator reconstructed once on the Fat images and once on the T1 images all the muscles for both volunteers.

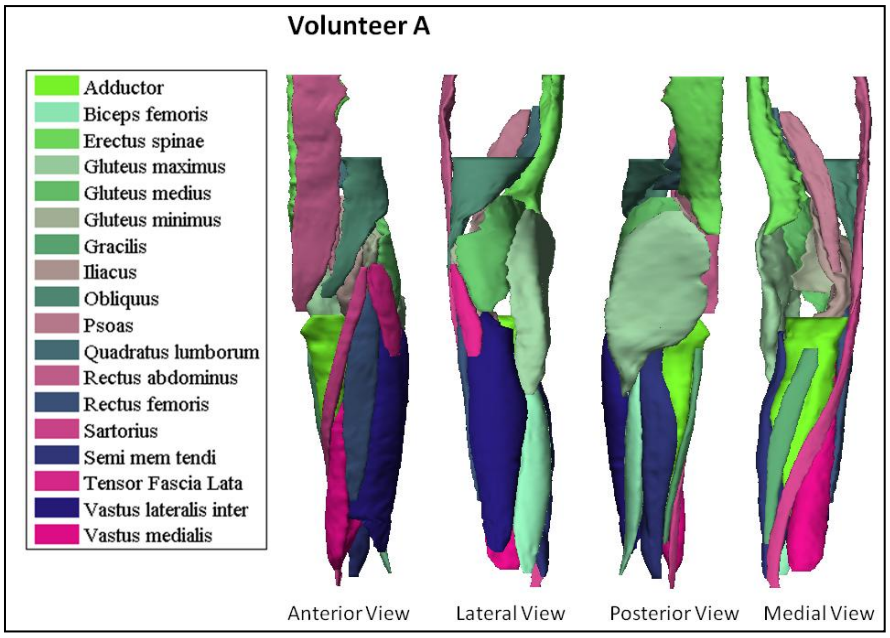

Figure 4-2: Reference reconstruction for Volunteer A including only left muscles; anterior, lateral, posterior and medial views.

The agreement between the DPSO with T1 or Fat images and the Reference method (T1 images) was assessed with the percentage of difference between the methods[211] for the following parameters: maximal AS, mean AS, length, and volume. The mean, standard deviation (STD), maximum and minimum amount of difference between the reference values and the reconstruction values were expressed as a percentage of the reference values. The limits of the agreement were defined by the interval [Mean-2xSTD, Mean+2xSTD].

Reproducibility of the DPSO methods for T1 and Fat images

For this study, the intra- and inter-operator variability of the maximal AS, mean AS, length and volume were calculated in addition to shape accuracy. In this context, three operators using the DPSO methods completed the reconstruction of each muscle for each volunteer three times based on the T1 images ("T1 reconstruction") and three times based on the Fat images ("Fat reconstructions"). Thus, for each muscle of each volunteer, reconstruction was performed nine times for each sequence (3 operators x 3 sessions for T1 and Fat images). The muscular reconstructions for each volunteer were repeated with a minimum interval of 3 days for each operator.

Intra- and inter- variability

For the maximal AS, mean AS, length and volume, the reliability (intra-operator variability) and the reproducibility (inter-operator variability) from the T1 and Fat reconstructions were computed according to the ISO standard 5725-2:1994 (Standardization IIOf. Accuracy (trueness and precision) of measurement methods and results -- Part 2: Basic method for the determination of repeatability and reproducibility of a standard measurement method: 1994) as the coefficient of variation expressed as a percentage. Two different coefficients of variation were calculated: the coefficient of variation of each operator for each volunteer; and the coefficient of variation of the average of the three operators for each volunteer. The intra-operator variability was the root mean square of the first coefficient of variation and the inter-operator variability was the root mean square of the sum of the two coefficients of variation. The intra-and inter- operator variability for the average Fat/Water ratio was calculated only using the Fat reconstructions.

Shape accuracy

In order to evaluate shape accuracy of the reconstructions, the data obtained from the three operators were compared to the reference previously reconstructed for the evaluation of the DPSO method. Differences in shape between the reference and each reconstruction obtained with the DPSO method (T1 and Fat reconstructions) were evaluated by projecting perpendicularly to the reference in three dimensions the points of the reconstructed muscles onto the reference

surface. The 95% confidence interval for the average point-to-surface-distance[212] was evaluated as two times the root mean square (2xRMS). The mean, standard deviation, minimum and maximum values of the 2xRMS distances were calculated separately for the T1 reconstructions and the Fat reconstructions pooling the reconstructions of all operators together.

Statistical analyses were conducted using the software SPSS version 17 (SPSS, Inc, Chicago, IL). Differences between the reproducibility of T1 and Fat reconstructions were investigated using a two-sided paired t-test with a level of significance of 0.05.

4.1.3 RESULTS

Reconstruction time

The time to obtain a reconstruction (including visual verification to correct local geometric errors) of the muscles for one volunteer was 7 hours. For the reference, the time of reconstruction was between 14 and 15 hours.

Individual Results per Subject

The reference values for right muscles of volunteers A and B are presented in Table 4-2. This table includes results of the maximal AS, mean AS, length, volume and Fat/Water ratio (average of all Fat reconstructions) for each muscle.

Right muscles	Max AS (mm^2)		Mean AS (mm^2)		Length (mm)		Volume (mm^3)		Fat/Water ratio	
	A	B	A	B	A	B	A	B	A	B
Adductor	4865	5173	2714	2990	301	327	776222	916293	12.45	18.11
Biceps femoris	1265	1428	632	717	337	352	207257	245682	17.76	21.74
Erectus spinae	2714	2615	1890	1830	261	212	439112	340376	23.27	28.49
Gluteus maximus	3963	5561	2571	3154	289	319	692013	878789	19.63	33.70
Gluteus medius	2728	3040	1653	1673	210	206	287706	298895	12.72	19.12
Gluteus minimus	1647	1161	976	689	133	125	101465	63928	16.71	18.25
Gracilis	367	592	245	396	297	288	69990	107238	10.99	19.36
Iliacus	1336	1341	858	745	245	242	187503	158666	12.82	17.53
Obliquus	3032	2315	1156	1150	263	210	246104	212022	25.00	33.22
Psoas	1356	1185	740	654	255	240	176296	146012	17.03	23.91
Quadratus lumborum	701	567	347	363	159	139	45449	41563	22.20	26.60
Rectus abdominus	816	798	623	594	359	301	214962	172540	22.88	31.46
Rectus femoris	934	1075	546	641	304	326	162332	203609	10.37	15.49
Sartorius	308	406	234	317	470	468	100298	134812	14.02	22.94
Semimembranous tendinosis	1425	2358	906	1283	372	378	329319	459471	16.14	21.48
Tensor Fascia Lata R	567	632	369	427	141	148	50795	58669	17.02	23.96
Vastus lateralis inter R	3608	4675	2212	2762	383	372	794354	964067	11.40	15.16
Vastus medialis R	1598	2123	956	1290	331	308	299664	384815	9.49	13.24

Table 4-2 Results for right muscles of volunteers A and B obtained with Reference method.(except Fat/Water ratio: average on all the Fat reconstructions)

Evaluation of the DPSO method

Table 4-3 illustrates the agreement between the DPSO methods with Fat and T1 images and the Reference methods. The limits of agreement between the DPSO methods with Fat and the Reference methods were [-3.50;7.89] for the volume. For both sequences the maximal AS showed the largest errors. The results demonstrated that for the volume and the mean AS, the agreement between the DPSO method with T1 images and the Reference method was better than the agreement between the DPSO method with Fat images and the Reference. On average, the DSPO method, as compared to the Reference Method, tended to underestimate all parameters (between 0.74% to 2.20%).

on all the muscles and both volunteers	**100 x(Reference Method – DSPO Method)/ Reference Method for one operator and both volunteers**							
	Max AS		**Mean AS ***		**Length**		**Volume***	
	T1	**Fat**	**T1**	**Fat**	**T1**	**Fat**	**T1**	**Fat**
Mean	1.21	1.16	0.74	2.20	0.91	0.44	1.10	2.19
Std	4.87	6.17	2.57	2.82	1.79	2.44	2.50	2.85
Limits of agreement sup (Mean+2xStd)	10.95	13.49	5.87	7.84	4.49	5.32	6.10	7.89
Limits of agreement inf (Mean-2xStd)	-8.53	-11.18	-4.39	-3.45	-2.68	-4.45	-3.91	-3.50
Max	15.43	15.57	6.01	6.92	6.18	10.39	5.92	6.92
Min	-9.41	-17.75	-6.22	-6.50	-2.96	-4.08	-6.62	-6.46

Table 4-3: Variability in percentage between Reference Methods and DSPO methods for T1 and Fat images. (*): Significant difference between Fat and T1

Intra- and inter-operator variability (DPSO method with T1 and Fat images only)

The intra- and inter-operator variability results for the T1 and Fat reconstructions of each muscle are summarized in terms of mean, standard deviation, maximal and minimal values for all the muscles in Table 4-4 and Table 4-5. On average, the intra- and inter-operator variability was less than 5% for all parameters. For both T1 and Fat images, only the gluteus minimus (both left and right) had an intra-operator variability greater than 5% for the mean AS, length, and volume.

The other muscles with an inter-operator variability greater than 5% were the rectus abdominus and the gluteus medius. For the T1 image, the inter-operator variability of the length was equal to 5.87% for the gluteus medius right. On T1 images, the rectus abdominus left inter-operator variability was 5.80% for the mean AS and 5.78% for the volume.

on all the muscles	Max AS		Mean AS		Length*		Volume		Fat/Water ratio
	T1	Fat	T1	Fat	T1	Fat	T1	Fat	Fat
Mean	4.08	3.76	2.16	2.05	1.78	1.26	2.16	2.05	2.23
Std	2.54	2.19	0.87	1.02	2.05	1.02	0.86	1.01	1.25
Max	12.49	10.66	3.81	5.60	9.93	5.16	3.75	5.62	5.56
Min	0.93	1.44	0.94	0.89	0.17	0.10	0.95	0.90	0.82

Table 4-4: Intra-operator variability in % (coefficient of variation). (*): Significant difference between Fat and T1

For the average of Fat/Water ratio, the left and right gluteus minima and the left vastus medialis were the only muscles with an intra-operator variability greater than 5%. Except for the length, no significant differences were found between T1 and Fat reconstructions in terms of intra- or inter-operator variability.

on all the muscles	Max AS		Mean AS		Length*		Volume		Fat/Water ratio
	T1	Fat	T1	Fat	T1	Fat	T1	Fat	Fat
Mean	4.63	4.50	2.56	2.61	1.86	1.42	2.55	2.61	2.98
Std	3.12	3.33	1.09	1.82	2.10	1.27	1.07	1.82	1.76
Max	15.65	19.62	5.80	11.67	9.93	5.93	5.78	11.80	10.59
Min	1.01	1.46	0.94	0.93	0.17	0.14	0.95	0.93	1.24

Table 4-5: Inter-operator variability in % (coefficient of variation). (*) : Significant difference between Fat and T1

Shape Accuracy Analysis

The results of the point-to-surface-distances for the T1 and Fat reconstructions of each muscle are summarized in terms of mean, standard deviation, and minimal and maximal values for all muscles in Table 4-6. The mean 2xRMS values were less than 3 mm (i.e. less than 3 voxels), with significantly smaller values for the T1 reconstructions than for the Fat reconstructions. The minimum 2xRMS was also significantly smaller for the T1 images. The maximal 2xRMS value in terms of point–to-surface-distance was less for the T1 reconstructions (11.30 mmn) than for the Fat reconstructions (16.41mm).

	Projection : distance points surfaces in mm							
	Mean 2xRMS *		Std 2xRMS		Min 2xRMS *		Max 2xRMS	
	T1	Fat	T1	Fat	T1	Fat	T1	Fat
Mean	2.62	2.95	0.48	0.52	1.96	2.36	3.80	4.30
Std	0.73	0.91	0.35	0.53	0.57	0.63	1.85	2.72
Min	1.27	1.32	0.16	0.09	0.88	1.15	1.83	1.57
Max	4.15	5.80	1.98	2.91	3.24	3.76	11.30	16.41

Table 4-6: Distance points surfaces in mm. Mean, Std, Min and Max 2*RMS with the average, standard deviation, minimal and maximal of 2xRMS on all reconstructions of one muscle (9 reconstructions/per muscle), (*): Significant difference between Fat and T1

4.1.4 **DISCUSSION**

As mechanical models and diagnostic protocols can offer significant contributions to the treatment of degenerative pathologies and deformities, the need exists for further research into the role of soft tissue stabilizers in postural balance.

The reproducibility of the DPSO methods with MR images was previously established by Sudhoff et al[172] for the muscles involved in knee motion. Reconstructions were based on volume interpolated breath-hold examination (VIBE) images. In order to obtain good visualization of soft tissue, the authors used T1 images only. The correlation between the intensity of the signal and the quantification of fat was not reliable due to the lack of homogeneity of the magnetic field.

In order to quantify both muscle geometry and fat infiltration, our study utilized the three point Dixon method. As demonstrated by Bley et al[213], this method is robust and, as for CT analysis, permits separation of the fat and water volumes, thus allowing quantification of fat infiltration.

The time needed to complete the 3D reconstruction of all the studied muscles from the thoraco-lumbar region to the patella (Table 4-1), with a systematic outline of every slice (Reference methods), was between 14 and 15 hours, while the time needed to obtain the reconstruction with Muscl'x software and DPSO methods was about 7 hours. The substantial reduction in time renders the software compatible for clinical research but further research should aim at reducing the time needed for reconstruction.

In this study, the reference object was constructed based on T1 images; this sequence was chosen based on the contrast between fat and muscle and for its wide use in clinical applications. The agreement between the two methods (T1 and Fat images) was variable between muscles and comprised between -4.50% and +8.00% for the mean AS, the length and the volume. For the same muscle, it appeared that on average the volume and the mean AS obtained with the DPSO method was smaller (T1:~1%, Fat: ~2%) than the volume obtained with the Reference Method. The difference was significantly greater for the DPSO method with Fat image. This systematic bias could be explained by the use of the contrast optimization which can reduce the AS of the non-manually segmented slices. However this error did not hamper the use of the DPSO method in the 3D geometry assessment of the muscle.

The segmentation of the three point Dixon method had the same quality of segmentation as the segmentation on T1 images. The Fat images had higher Fat/muscle contrast than the T1 images; however, visibility of the epimysium and the bone/muscle contrast were better delineated in the T1 images (Figure 4-3). This may also explain why the systematic error in the agreement between methods was greater for DPSO with Fat images than for DPSO with T1 images.

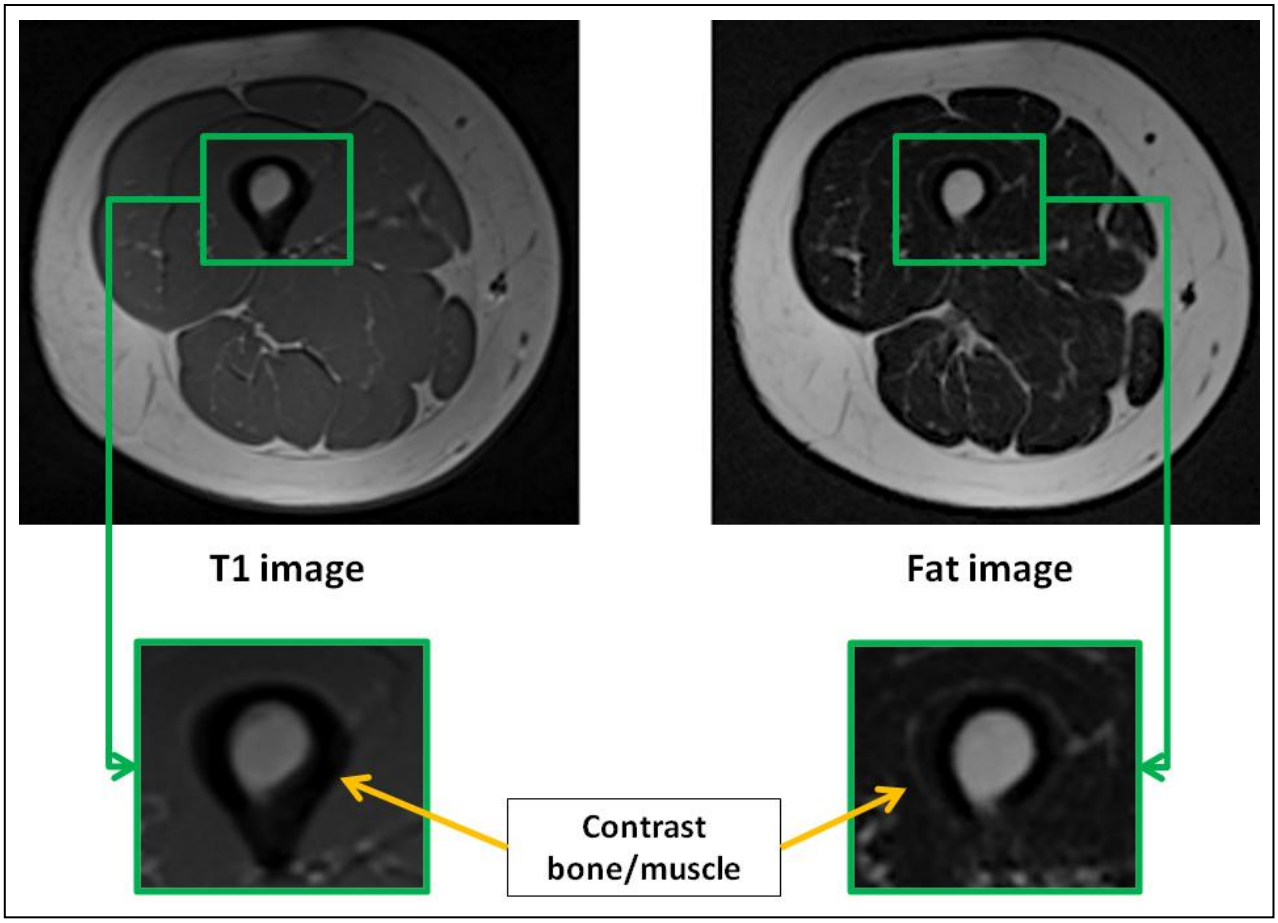

Figure 4-3: Contrast between bone/muscle in T1 and Fat images

An analysis of the accuracy of muscle shape (i.e. comparison of T1/Fat reconstructions with the reference) revealed small point-to-surface-distance errors (mean 2xRMS errors of 2.6 mm and 2.95 mm for T1 and Fat reconstructions, respectively). The references were only constructed on the T1 image, which could explain a greater difference in terms of point to surface on the Fat images. The DPSO method leads to error when a muscle is poorly approximated by an ellipse (e.g. the adductor), or when there are abrupt variations in muscle shape between adjacent slices (e.g. the iliacus). However, errors in terms of shape had little impact on the agreement for other parameters: muscle length, mean AS, and volumes between the two methods. The greatest impact was found on measurement of the maximal AS for which the limits of agreement was [-9 %; 11%] for T1 and [-11%; 13.50%] for Fat.

Point-to-surface errors from this study were comparable to previously published values [171,172]. Sudhoff[172] reported 6% error in muscle volume when compared to a reference object (based on

10 volunteers and 2 operators). Using CT images, Jolivet et al.[171] reported errors (two standard deviations around the mean volume) of 5-12% in a reproducibility analysis of the hip muscles of 30 subjects (3 operators). In the current study, which includes only two volunteers, errors were on average, less than 5% for all parameters. Of note, the current protocol used pre-defined slices to identify the muscle insertion.

The variation of reproducibility among the different muscles may be explained by several reasons. First, independent of the image considered, the distinction between muscles was not always straightforward (e.g. gluteus minimus versus gluteus medius or vastus medialis versus vastus intermedius)—a difficulty previously reported by other authors[172]. Second, MRI acquisitions were acquired in free breathing, which led to motion artifacts in the abdominal region, that may compromise accuracy of segmentation of the abdominal muscles (e.g. the rectus abdominus and obliquus).

Conclusion

This study presents a validation of a protocol to characterize muscle geometry and quantification of the fat infiltration with MRI. The combination of the Muscl'X software with the DPSO method and the three point Dixon method demonstrated good agreement, a reproducibility of less than 5% and led to a substantial gain in reconstruction time. The imaging protocol included in this work is broadly available for clinical scans and has the potential to assess muscular differences between patients and thus the ability to generate patient–specific musculoskeletal models.

In the following article, this protocol was then applied on a ASD population.

4.2 PRELIMINARY RESULTS ON QUANTITATIVE VOLUME AND FAT INFILTRATION OF SPINO-PELVIC MUSCULATURE IN ADULTS WITH SPINAL DEFORMITY

The protocol previously described with Dixon acquisition and DPSO method, has been applied in a prospective consecutive pilot series of 19 female ASD patients to offer an analysis of their spino-pelvic musculature.

At the difference of the protocol described in the section 4.1, the MRI acquisition which was performed for this study, was not the three point Dixon method, but the two point Dixon method. This can be explained by the fact between both studies, the center of acquisition changes the MRI machine. After multiple tests, it appears that the two point Dixon method was the one with best quality of image with the new MRI machine. However with this acquisition, the motion artifacts due to the breathing compromised of the accuracy of segmentation of the abdominal muscles (e.g. the rectus abdominus and obliquus). Those muscles were not included in the following analysis.

This article has been submitted to the Spine Journal in May 2014.

Authors: Bertrand Moal, Nicolas Bronsard, José G. Raya, Jean Marc Vital, Frank Schwab, Virginie Lafage, Wafa Skalli.

4.2.1 **INTRODUCTION**

The muscular system plays an essential role in the maintenance of postural balance; however, there has only been limited investigation into the relationship between the muscular system and structural alignment pathologies.

In adult spinal deformity (ASD), recent research has highlighted the critical role of sagittal spino-pelvic alignment in patient-reported pain and function[14,16,113,200]. Therefore, key muscles involved in pelvic-positioning and lumbar-stabilization are at the forefront of research needs.

Preliminary efforts have been directed towards understanding spine or thigh muscles using histological analyses[141–144], muscular strength[145–148] , electromyographical signals[149–151], muscle cross-sectional areas (via ultrasound, CT-scan or MRI) [147,151,153–155,157–164], measurement of muscular density with CT-scan[151,153–156], or muscular intensity with MRI[146,147,160,161,163–165]. However, difficulties arise in representing inter-muscle and inter-subject variability[167].

To overcome these limitations, Jolivet et al[170,171,176] developed a method of three-dimensional muscle reconstruction via segmentation of a few axial images (MRI or CT-scan). This method has been successfully implemented with CT scans for analysis of muscles involved in knee motion[172] and hip muscles[214]. Nevertheless, the radiation exposure from CT scans makes it unacceptable as a tool for studies involving ASD patients, frequently subjected to radiographic examination. Notably, the method has also been performed using MRI sequences[172]. However, contrary to CT scans, MRI cannot be interpreted in terms of tissue composition, so quantification of fat and muscle requires the use of dedicated MRI pulse sequences.

Dixon et al[166,178–181,215] developed a MRI method for fat quantification which exploits the slight difference in the Larmor frequency of fat and water protons (chemical shift). By acquiring the signal at different echo times, the modulation of the signal intensity can be fitted and the fat and water content can be separated.

Thus, by utilizing Dixon acquisitions and 3D muscular reconstructions, muscular volume and fat infiltration has been obtained and used to investigate the main functional groups of muscles associated with sagittal posture. The hypothesis is that volume loss and fat infiltration, previously demonstrated as factors of skeletal muscle degeneration due to aging[216,217], do not equally affect the different muscles.

4.2.2 MATERIALS & METHODS

Inclusion / Exclusion Criteria

This study is a prospective consecutive pilot series of ASD patients, recruited following IRB approval and written informed consent. Inclusion criteria were female patients over 35 years old and at least one of the following radiographic parameters: Thoraco-lumbar or lumbar coronal Cobb angle greater than 30°, Sagittal Vertical Axis (SVA) greater than 4 cm, or Pelvic Tilt (PT) greater than 20°. Patients with existing instrumentation, history of spine surgery, or presenting contraindication for MRI were excluded.

Radiographic Acquisition and Measurements

All patients underwent a full-length coronal and lateral x-ray in free standing position[218]. Radiographs were measured using a validated spine software[53,54] (SpineView, Laboratory of Biomechanics ENSAM ParisTech, France), which provided the following spino-pelvic parameters:

- Coronal plane: Cobb angle and apex location, coronal alignment.
- Sagittal plane: SVA, PT, Pelvic Incidence (PI), Pelvic incidence minus Lumbar Lordosis (PI-LL), Lumbar Lordosis (L1S1), Thoracic Kyphosis (T4T12).

Patients MRI Acquisition

MRI was performed on a 3T whole-body scanner (Magnetom Skyra, Siemens Healthcare, Erlangen, Germany) using a 24-channel spine matrix coil and three 16-channel flex coils from the same vendor. The imaging protocol included a T1-weighted TSE sequence for applying the two point Dixon method[166,179,181,215] (TR/TE = 820/11 ms, acquisition matrix = 448×308, phase oversampling= 100%, in plane resolution = 0.94×0.94 mm^2, 4 stages, 40 slices by stage, slice thickness = 5 mm, slice gap= 0 mm, flip angle = 157^o, turbo factor = 3, echo trains = 107, parallel imaging acceleration factor (iPat) =2, iPat references lines = 26, bandwidth = 319 Hz/pixel, echo spacing = 15.7, acquisition time per stage = 5:53 min, Total acquisition time= 25 min). Water and fat images were automatically generated by the scanner from in and out of phase images (Figure 2-32, page 64). Imaging volume covered the proximal tibia to the lumbar spine (T12 vertebra) and was acquired in four stages.

Phantom MRI Acquisition

In order to investigate the accuracy of the 2 points Dixon method for estimating fat versus water, the same MRI acquisition was performed on phantoms composed of four 10mL plastic vials. One vial was filled with soybean oil (100% fat) and another full of water (0% fat). The remaining two

vials contained an emulsion of 10% and 20% fat obtained from Intralipid 20% fat emulsion (Sigma-Aldrich, St. Louis, MO, USA). For the acquisition, the phantoms were submerged in a phosphate buffered saline solution.

3D Muscle Reconstruction

The 3D reconstruction of individual muscles, listed Table 4-7(page 134), was performed using Muscl'X software (ENSAM, Laboratory of Biomechanics, Paris, France)[164,170–172]. The reconstruction technique is based on the deformation of parametric specific objects (DPSO algorithm) as described in the section 2.5.1, page 61.

	Spine Extensor	Spine Flexor	Hip Extensor	Hip Flexor	Knee Extensor	Knee Flexor	Total Muscle
Quadratus lumborum	x						x
Erector spinae	x						x
Psoas		x		x			x
Iliacus		x		x			x
Biceps femoris short			x			x	x
Biceps femoris long			x			x	x
Semi-membranosus			x			x	x
Semi-tendinosus			x			x	x
Gluteus maximus			x				x
Rectus femoris				x	x		x
Gracilis				x		x	x
Sartorius				x		x	x
Adductor				x			x
Tensor fascia lata				x			x
Vastus lateralis intermedius					x		x
Vastus medialis					x		x

Table 4-7:Muscles analyzed in this study grouped by function and joint.

Some muscles were combined, since the low contrast made an accurate separation of the individual muscles difficult. The lumbar part of the psoas was reconstructed separately, but at a point where the distinction with the iliacus was not possible, it was then integrated into the iliacus. The external obturator, adductor longus, brevis and magnus and pectineus were reconstructed

into a single group named “Adductor”. The vastus lateralis and intermedius were reconstructed together. The muscle reconstructions were done on the fat images. Figure 4-4 presents the 3D reconstruction of the left muscles for one patient. The femurs were also reconstructed on the water images, the contrast between the cortical and cancellous bone was greater on water images.

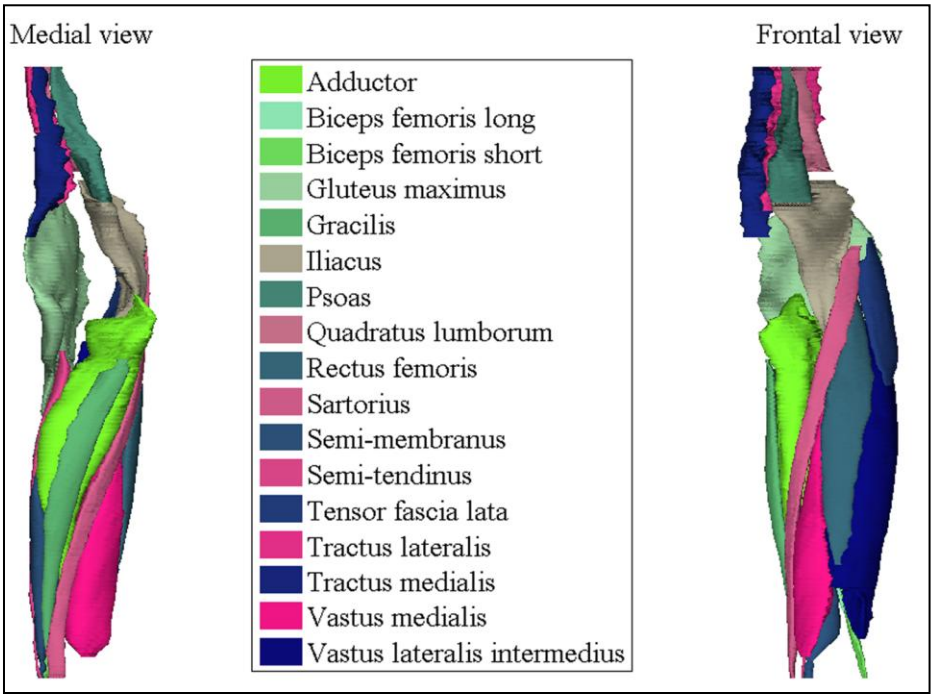

Figure 4-4: Medial and frontal view of all the left muscles reconstructed for one patient

Right and left muscles were grouped according to the joint (Spine, Hip, and Knee) and by mechanical action (Extensor/Flexor) (Table 4-7). The entire set of muscles were also grouped and named Total muscles.

Real fat water ratio: correction from fat_water ratio with Dixon method

From the fat and water images, the fat-water ratio by voxel was calculated using Equation 4.2.1 where SI_fat represents the signal intensity of the fat signal and SI_water the signal intensity of the water image,

$$Dixon\ fat\_water\ ratio\ = 100 * \frac{SI_{fat}}{SI_{fat}+SI_{water}}$$

[4.2.1]

From the Phantom acquisition, an 8-by-10 region of interest (ROI) was drawn in the center of each vial and the mean and the standard deviation of the Dixon fat_water ratio in each ROI were then calculated. Those results demonstrated a non linear relation between Dixon fat_water ratio and the real fat_water ratio. In order to correct the Dixon fat_water ratio, the non linear relation was approximated with a polynomial function of degree three (F) using the phantom acquisition. Then for each patients, the real fat_ water ratio was calculated for each voxel for with equation 4.2.2.

$$Real\ fat_{water}ratio = F\ (Dixon\ fat_{water}ratio)$$
$$= 0.0002 * (\text{Dixon fat}_{\text{water}}\text{ratio})^3 - 0.0071 * (\text{Dixon fat}_{\text{water}}\text{ratio})^2$$
$$+ 0.5607 * (\text{Dixon fat\_water ratio}) - 0.7714$$

[4.2.2]

If F(Dixon fat_water ratio) was less than 0%, real fat_water ratio was evaluated at 0 and if F(Dixon fat_water ratio) was greater than 100%, real fat_water ratio was evaluated at 100.

Quantification of fat components and muscle parameters

From the 3D reconstructions, muscular volumes were calculated (Vmuscle). The volume of infiltrated fat inside each muscles (Vfat) was calculated with the real fat-water ratio. The volumes were then normalized based upon the volume of the right femur, in an effort to limit the impact of the patient morphology. For each joint, the ratio of Vmuscle and Vfat between flexors and extensors were calculated. The percentage of fat infiltration (Pfat) was also expressed and was calculated as follow : Pfat= 100*Vfat/Vmuscle.

Statistical analysis

Muscular volumes and fat infiltration distribution were characterized as well as Pfat. Paired t-test were used to compare muscular volumes and fat infiltration distribution and Anova t-tests were used to compare muscular groups. Pearson's correlation coefficient was used to investigate the relationship between muscle parameters and demographic data. For each statistical analysis, the level of significance was set at 0.05.

4.2.3 RESULTS

Demographics

19 consecutive ASD patients with a mean age of 60 years old (range: 37-80) and a mean BMI of 22.3 kg/m^2 (range 17-31) were included (Table 4-8). There was no significant correlation between age and BMI.

	Min	Max	Mean	Standard deviation
Age (years)	37	80	60	13
Height (cm)	144	174	161	9
weight (kg)	38	92	59	11
BMI (kg/m^2)	17.00	31.00	22.32	3.48

Table 4-8: Demographic information

Radiographic analysis

In the coronal plane, the mean coronal alignment was 23 mm (range: 0-119 mm, 16% of the patients reached a threshold of 40 mm). The mean maximal Cobb angle was 40° (range: 0-60°, 79% of the patients reached the threshold of 30°). 47% of the patients had a double curve, 32% a single curve, and 21% did not exhibit any coronal curve.

Thoracic kyphosis ranged between -91° and -8° with average of -51±22°. The mean L1S1 was 54° (range: 15-75°) for a mean PI of 55° (range 30-77°). The analysis of PI-LL (mean=1°, range=-35°-55°) revealed that 21% of the patients were above the threshold defined by the SRS-Schwab classification [89,113]. SVA ranged from -66mm to +118mm. The analysis of the PT revealed that 38% of the patients reached a threshold of 20° [113].

Phantom analysis and correction of the Dixon fat_water ratio.

The Table 4-9 presented the mean and standard deviation of Dixon fat_water ratio for the phantom with the different concentrations of fat. As previously mentioned, the function F, presented in Equation 2, was used to approximated this non linear relation between the Dixon fat_water ratio and the real fat_water ratio (Figure 4-5).

Vails	Real fat concentration (%)	Dixon Fat_water ratio (%)
only soybean oil	100	85.4 ± 0.3
Intralipid 20% fat emulsion	20	38.7 ± 1.7
Intralipid 10% fat emulsion	10	22.2 ± 1.0
only water	0	1.4 ± 0.6

Table 4-9: mean and standard deviation of Dixon fat_water ratio for the phantom with the different concentrations of fat

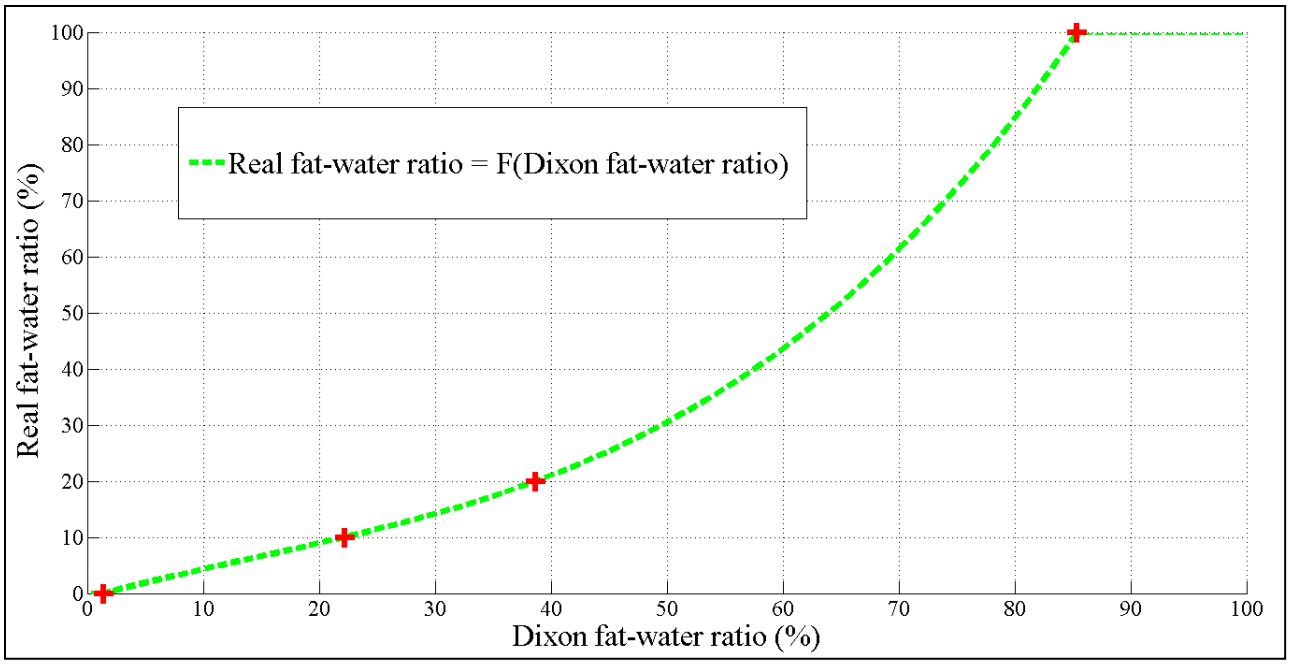

Figure 4-5: Average fat-water ratio for the phantom with different concentration of fat (0%, 10%, 20% and 100%) and the approximated function Real fat-water ratio = F(Dixon fat-water ratio)

Muscle Analysis

Femoral volume normalization

The average femoral volume was 414cm^3 ± 71. A larger femoral volume was associated with a larger muscular volume when considering the Total Muscle (Pearson r^2=0.837, p-value <0.001).

Muscle and fat infiltration repartition by functional groups

"Hip group" Vmuscle was significantly bigger than the "Knee group" Vmuscle which in turn was significantly bigger than those of the "Spine Group" (Table 4-10, Figure 4-6). The Spine extensor

group represented on average 9±2% of the total muscular volume but a greater proportion (21±7 %) of the total infiltrated fat volume ($p<0.001$) . The Hip extensor group represents 29±2% of the total muscular volume and 32±5 % of the total infiltrated fat volume ($p<0.001$). For the Spine extensor group and the Knee extensor group, the distribution of muscular volume and infiltrated fat was similar (respectively 7% and 17% with standard deviation less than 2%). For the Hip flexor and Knee extensor groups the distribution of infiltrated fat was significantly smaller than the distribution of muscular volume. ($p<0.001$).

	Muscular volume (Vmuscle)			
	Min	Max	Mean	STD
Spine Extensor	0.92	1.89	1.46	0.27
Spine Flexor	0.85	1.67	1.24	0.22
Hip Extensor	3.42	6.00	4.83	0.63
Hip Flexor	4.79	7.13	5.91	0.71
Knee Extensor	3.70	6.95	5.15	0.86
Knee Flexor	2.18	3.41	2.88	0.33
Total muscles	12.87	19.44	16.67	1.87

Table 4-10: Muscular Volumes of each muscle group. Reported values are normalized based upon the volume of the right femur of each patient (for example, the mean "Total Muscles" volume = 16.67 femurs volume)

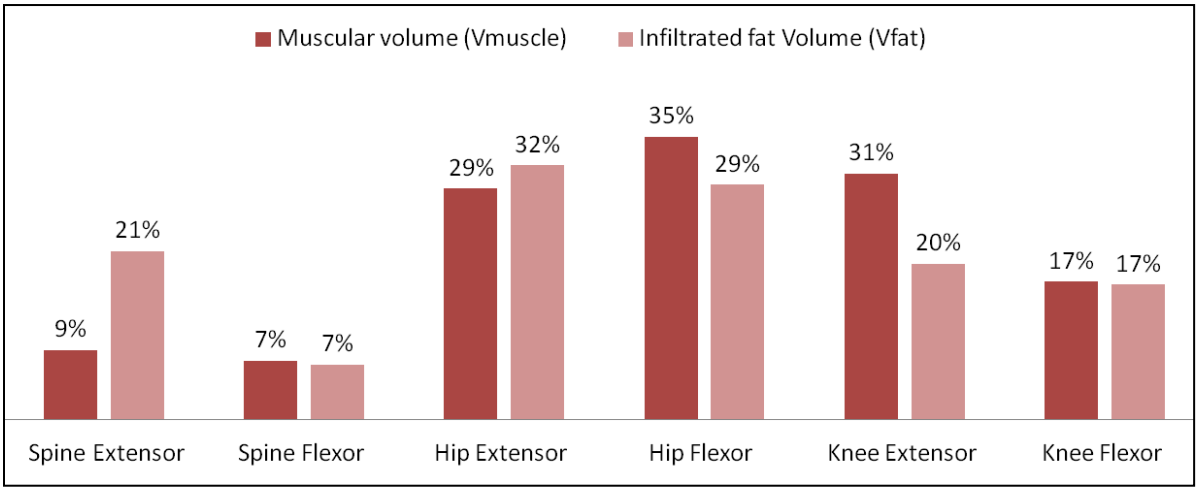

Figure 4-6: Distribution of Muscular (Vmuscle)and infiltrated fat volume expressed in percentage of the Total Muscle muscular volume and of the total infiltrated fat volume respectively

Percentage of fat infiltration : Pfat

The analysis of Pfat (Table 4-11) within each group of muscles revealed not only a large variability among patients (range: 6.1 - 28.8%, Figure 4-7 and Figure 4-8), but also highlighted the difference of Pfat between muscle groups. Muscles from the Spinal extensor group had a Pfat significantly greater than the other muscles groups, and the largest variability (Pfat = 31.9±13.8%, $p<0.001$). Muscles from the Hip extensor group ranked 2nd in terms of Pfat (14±8%), and were significantly greater than those of the Knee extensor ($p=0.030$). Muscles from the Knee extensor group demonstrated the least Pfat (12±8%). They were also the only group with a significant correlation between Vmuscle and Pfat ($r =-0.741$, $p<0.001$), however this correlation was lacking in the other groups.

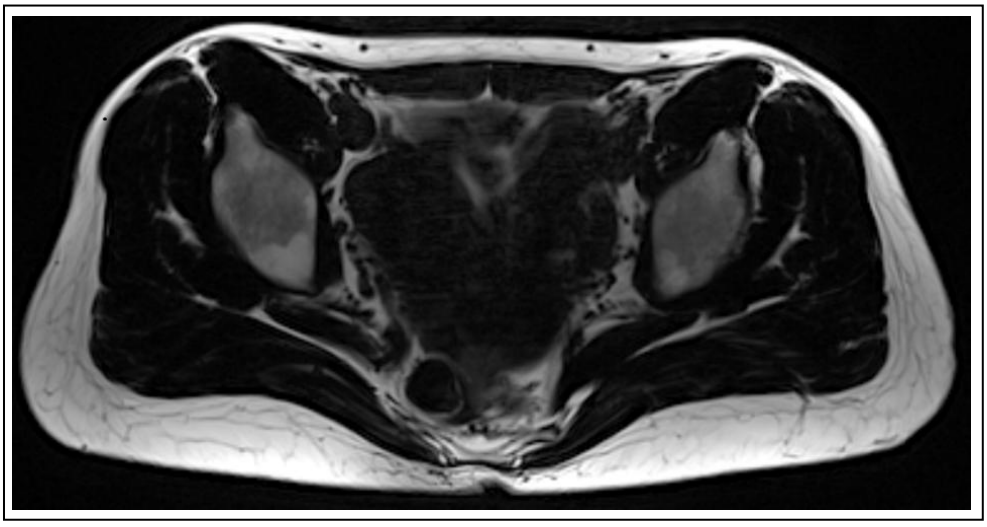

Figure 4-7: MRI sample of a 37-years-old female ASD patient with a BMI of 22kg/m2. This patient presents a sagittal deformity with hyperlordosis of the lumbar spine (PI-LL=-29°) and a thoraco-lumbar kyphosis of 45°. The analysis of the muscle quality revealed an 6.1% of fat infiltration on average.

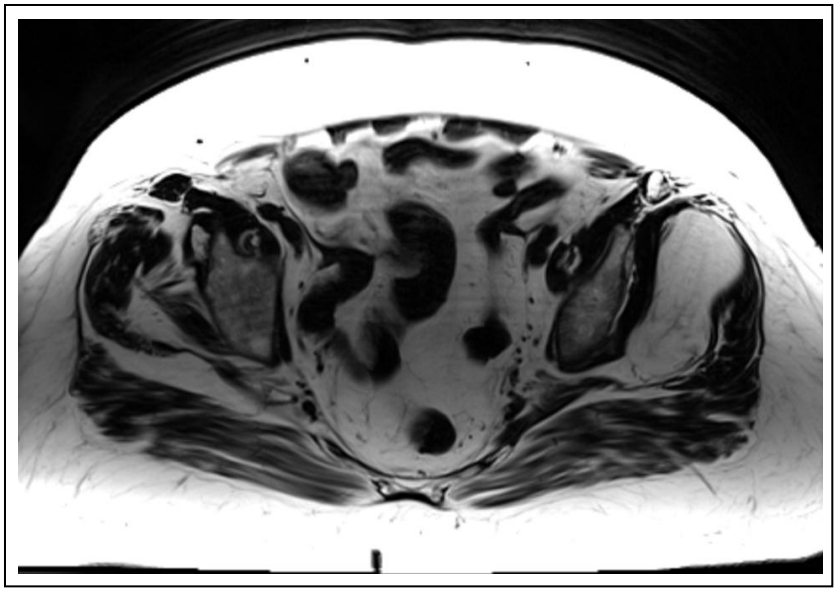

Figure 4-8: MRI sample of an 80-years-old female with a BMI of 31 kg/m2. This patient presents a degenerative scoliosis with a thoraco-lumbar Cobb angle of 32°, a hyperkyphosis of the thoracic spine (TK=63°) and a global sagittal misalignment (SVA=11 cm). The analysis of the muscle quality revealed an 28.8% of fat infiltration on average.

	Min	Max	Mean	STD
Spine Extensor	12.7	71.2	31.9	13.8
Spine Flexor	5.7	20.4	11.9	3.6
Hip Extensor	6.4	38.1	14.8	7.0
Hip Flexor	6.1	20.2	10.8	3.2
Knee Extensor	3.8	20.0	8.7	4.0
Knee Flexor	6.9	25.4	12.8	4.2
Total muscles	6.1	28.8	13.3	5.3

Table 4-11: Percentage of infiltrated fat (Pfat) expressed by functional groups

Flexors versus extensor

The comparison of flexor versus extensors revealed a larger flexor contribution with regards to Vmuscle for the hip. For the spine, the ratio Flex/Ext highlight the greater fat infiltration of the extensor(Table 6).

	Ratio Flex/Ext: Vmuscle				Ratio Flex/Ext: Vfat			
	Min	Max	Mean	STD	Min	Max	Mean	STD
Spine	0.61	1.21	0.87	0.17	0.10	0.68	0.36	0.14
Hip	1.02	1.43	1.23	0.13	0.54	1.31	0.95	0.19
Knee	0.42	0.72	0.57	0.08	0.66	1.10	0.87	0.12

Table 4-12: Ratio between flexors and extensors for each group of muscles (left= muscular volume, right=infiltrated fat volume)

Age versus muscle parameters (Table 4-13)

No correlation was found between Vmuscle and age except for the knee extensors (Pearson's r=-0.701, p=0.001). For Vfat, all groups were significantly and positively correlated with age (Pearson's r between 0.555 and 0.645) except the Spine groups. Except the spine extensor, Pfat was positively and significantly correlated with age.

BMI versus muscle parameters (Table 4-14)

For the Spine groups, no correlation was found between Vmuscle, Vfat or Pfat and BMI. Vmuscle of the hip extensors and the knee flexors was significantly and positively correlated with BMI (respectively, Pearson's r = 0.642, p=0.003 and Pearson's r = 0.470, p=0.042) . BMI was correlated with Vfat and Pfat in the hip and knee flexor and extensor.

		Vmuscle		Vfat		Pfat	
		r	p	r	p	r	p
Age	Spine Extensor	-0.208	0.393	0.420	0.073	0.480*	0.038
	Spine Flexor	-0.417	0.076	0.208	0.393	0.427	0.068
	Hip Extensor	0.018	0.943	0.564*	0.012	0.633**	0.004
	Hip Flexor	-0.309	0.198	0.555*	0.014	0.658**	0.002
	Knee Extensor	-0.701**	0.001	0.645**	0.003	0.680**	0.001
	Knee Flexor	-0.319	0.183	0.589**	0.008	0.679**	0.001
	All Muscles	-0.433	0.064	0.614**	0.005	0.676**	0.001

Table 4-13: Correlation between age and muscular volume (Vmuscle), infiltrated fat volume (Vfat) and percentage of fat component (Pfat).

		Vmuscle		Vfat		Pfat	
		r	p	r	p	r	p
BMI	Spine Extensor	0.127	0.606	0.017	0.944	-0.038	0.876
	Spine Flexor	-0.027	0.913	0.443	0.057	0.450	0.053
	Hip Extensor	0.642**	0.003	0.693**	0.001	0.587**	0.008
	Kip Flexor	0.159	0.515	0.657**	0.002	0.587**	0.008
	Knee Extensor	-0.236	0.330	0.596**	0.007	0.518*	0.023
	Knee Flexor	0.470*	0.042	0.761**	<0.001	0.570*	0.011
	All Muscles	0.207	0.394	0.592**	0.008	0.458*	0.049

Table 4-14: Correlation between age and muscular volume (Vmuscle), infiltrated fat volume (Vfat) and percentage of fat component (Pfat).

4.2.4 DISCUSSION

While the radiographic presentation of ASD patients commonly demonstrates coronal and sagittal components of misalignment, sagittal spino-pelvic parameters have been identified as the main radiographic drivers of disability[18,90,95,200]. The objective of the current study was to investigate the volume and fat infiltration of the main functional groups of muscles associated with sagittal posture

Relationship with posture

Fat infiltration within muscle groups ranged from 8.7 and 31.9% on average—the least affected being the knee extensors. This suggests that muscular degeneration, evaluated with fat infiltration, does not impact the groups of muscles to the same extent. The lumbar spine extensors had the greatest percentage of fat component (31.9%). This is particularly interesting in regard to the loss of lumbar lordosis present in most ASD patients[14] because lumbar spine extensors are highly involved in the maintain of lumbar lordosis. Furthermore, correlations between fat infiltration and age for the spine was smaller than for the other groups and no correlation was found with the BMI. These results suggest that the greater degeneration of those muscles is probably not solely attributed to age and BMI. However the study cannot conclude whether this observation is a cause or a consequence of the spinal deformity.

Moreover, in the ASD population, sagittal misalignment is highly associated with pelvic retroversion, described by PT[16] and the agonist of this retroversion, the hip extensor, has the second greatest percentage of fat infiltration.

Flexor and extensor fat infiltration ratios were found to be smaller for the spine groups. This finding in the ASD population studied may reflect the unfavorable balance of forces leading to sagittal plane deformity across the trunk. Coupled with the findings of hip extensors and loss of contractile component with ageing, components of sagittal spino-pelvic misalignment from a perspective of soft tissue imbalance are emerging.

Fat Infiltration, age and BMI

The difference between muscular volume and infiltrated fat volume demonstrated that muscle degeneration is not similar among the different functional groups. Those differences were highlighted by the difference of correlation between age and BMI. Only knee extensor muscular volume loss was correlated with age; however, infiltrated fat was correlated with age for each muscle group (except Spine Flexor p=0.068), reflecting that age-related muscular degeneration is

in general more associated with an increase of fat infiltration than an absolute muscular volume loss.

Greater BMI was associated with a greater percentage of infiltrated fat for Hip and Knee groups, but also associated for the Hip extensor and the Knee flexor groups with an increase of the muscular volume.

In light of the wide range of age and BMI values observed in this pilot study, the current findings will have to be confirmed in a larger population.

Fat and contractile component evaluation

The evaluation of the fat infiltration using the two points Dixon method has already been applied to investigate different organs (liver[178,179], bones[180] and muscles[181,182]). The decay in signal intensity between the in-phase and opposed phase images due to T2* was not taken into account[179]. The measurement of T2* would have required additional measurements or the use of sequences (e.g. multi echo gradient echo sequences) that were not available at our scanner. Even more, the limited ability of patients with spinal deformities to hold still in the magnet forced us to reduce the scan time, so we could not measure T2* on these patients. Recent studies have shown that the two point Dixon without T2* has excellent concordance with spectroscopy measured in the spine, bones[180], liver[178]. or spine muscles[182].

With the 3 points Dixon method applied onto phantoms filled with different proportions of fat and water, Kovanlikaya et al[219], demonstrated a linear correlation between the fat-water ratio and the proportion of fat. However in our phantom study, this relationship was not linear, explaining why we corrected the fat water ratio evaluated with the two Dixon method with a polynomial function.

This disagreement observed between the nominal and the measured fat fraction in phantoms can be caused partially because of the T1 weighting of the images. Fat have much shorter T1 values (300 ms) than water in muscle (900 ms) at 3T[220]. With a TR of 820 ms the magnetization from fat was almost completely relaxed ($TR/T1fat \approx 2.73$, $(1-e^{-TR/T1fat})=0.94$, i.e. 94% of the signal available for the next excitation), while the magnetization for water did not have enough time to recover ($TR/T1water \approx 0.91$, $(1-e^{-TR/T1water})=0.60$, i.e. 60% of the signal available for the next excitation). Therefore in our measurements the signal from water was underestimated and this resulted in overestimation of the fat fraction. Additional errors with the two-point Dixon included sensitivity to B0 inhomogeneity, which could explain why the differences between the in phase and out of phase in the 100% phantom lead to an underestimation of the fat fraction for large values of the fat fraction.

While investigations of the muscles of the thigh[181] or extensor of the spine[182] exist, they are based on a limited number of MRI slices and none of them report results on the entire muscular volume. To our knowledge, there is no study combining 3D reconstruction of muscles and fat component calculated with the two points Dixon method.

Limitations

Due to our experimental design, we cannot draw any definitive conclusions correlating ASD and muscular factors. The various deformities presented in this population limited the ability to associate changes in a specific muscle groups with deformation type. No males were included given the limited sample size and to avoid more confounding factors. Female subjects were considered due to the higher incidence of spinal deformity in the female population[142,158]. Data for a larger gender mixed population and an asymptomatic population are important next steps to evaluate more clearly the contractile component and correlation between muscle groups of the spino-pelvic complex and alignment.

Conclusion :

The applied MRI protocol permits a quantitative and qualitative characterization of the main muscles involved in the spino-pelvic complex. Regarding the differences between distribution of muscular and contractile components only, this study demonstrated the necessity of a complete characterization of the muscular system (including the quantification of the fat infiltration) and stress the limitations of considering only geometric parameters. Muscle degeneration seems more related to fat infiltration than volume loss but muscle degeneration does not affect all the muscles equally. In the studied ASD population, lumbar spine and hip extensor were the groups most affected by muscular degeneration, and muscle volume ratios between flexors and extensors were greatest in the spine group.

However the long time of manual segmentation necessary for the DPSO method, makes difficult its application in clinical practice. Therefore in the next article, a new method has been developed to characterize the muscular system of ASD population, with smaller time of manual segmentation compared to the DPSO method.

4.3 MUSCULAR VOLUME AND FAT-WATER DISTRIBUTION ESTIMATION FOR SPINO-PELVIC GROUPS OF MUSCLES: MRI AXIAL SECTIONS OF INTEREST

From the data collection of ASD patients described in the previous article, multi-linear models based on the manual segmentation of specific slices have been constructed to estimate the volume and the ratio between fat and water component of the main spino-pelvic muscular groups.

This article has been submitted in the journal : Computer Methods in Biomechanics and Biomedical Engineering: Imaging & Visualization in July 2014.

Authors : Bertrand Moal, Wafa Skalli, Jose G. Raya, Nicolas Bronsard, Jean-marc Vital, Themistocles Protopsaltis, Thomas J. Errico, Frank J. Schwab, Virginie Lafage.

4.3.1 **INTRODUCTION**

While the alignment of the skeletal system has been widely analyzed, little is known regarding the role of soft tissues in the context of adult spinal deformity (ASD). Recent research has highlighted the critical role of sagittal spino-pelvic alignment in patient-reported pain and function[13,16,113,134,200]. Therefore, assessing key muscles involved in pelvic-positioning and lumbar-stabilization is at the forefront of research needs.

In a recent study on adults with spinal deformity, analysis of the spino-pelvic musculature demonstrated that the lumbar spine extensor and hip extensor were the most affected by muscular degeneration[221]. In this referenced study, volume and distinction between fat and water component of the muscles were evaluated with the segmentation of MRI axial slices acquired using the Dixon method[166,178,180,181,215] from the patella to the thoracic spine. The segmentation of the muscles were obtained with the software Muscl'x (laboratory of biomechanics, Arts et Métiers ParisTech)[170,176,222]. The reconstruction technique was based on the deformation of parametric specific objects (DPSO algorithm)[170,222] and allowed, from the manual segmentation of a limited number of axial slices, a reconstruction of the complete 3D geometry of the muscle. The method's reproducibility has been demonstrated in several studies[170,172,214].

Utilizing a limited number of slices drastically reduces the time needed for 3D reconstruction as compared to the manual segmentation of each individual MRI slice[170,172,214]. However, the technique remains time consuming when considering routine clinical evaluation.

Our hypothesis is that volume and the ratio between fat and water component of the main spino-pelvic muscular groups can be estimated using a multi-linear regression model built on the cross-sectional area measured on a very limited number of segmented slices.

4.3.2 MATERIALS & METHODS

Study Design

This study is a retrospective analysis of the consecutive and prospective data collected on adults with spinal deformity detailed in the previous article 4.2 page 131. Inclusion criteria were female patients over 35 years of age with a radiographic diagnostic of ASD: Thoraco-lumbar or lumbar coronal Cobb angle greater than 30°, Sagittal Vertical Axis (SVA)[32] greater than 4 cm, or Pelvic Tilt (PT)[26] greater than 20°.

MRI acquisition, 3D reconstruction and fat-water distribution

Methods for the MRI acquisition, segmentations, and calculation of the volume and ratio of water component (RW) have already been described in the article 4.2 page 131 and are briefly summarized hereafter.

A total of 19 female ASD patients underwent an axial MRI acquisition from the knee to the thoraco-lumbar junction(T12) with a two point Dixon method [166,181,215]. 3D muscle reconstruction was performed with the DPSO method[170,222]. The Muscl'X uses a sub-set of manually segmented (MS) MRI axial slices to generate a 3D reconstruction of individual muscles. The optimal number of MS slices per muscle depends on the muscle morphology and has been reported to vary from 4 to 12 slices(Table 4-1 page 120).

Right and left muscles were grouped according to the joint (spine, hip, and knee) and by mechanical action (Extensor/Flexor) (Table 4-7, page 134). The entire set of muscles was also grouped and named Total muscle.

Volume and Fat and water distribution for the groups

Calculation of volume and RW within each of the defined muscle groups (Table 4-7, page 134) were obtained from individual muscle data and used as dependent parameters in the subsequent section of this study.

Prediction of muscular volume and ratio of water component for the muscular groups:

Segmentations of a limited number of MRI slices (1, 2, 3 or 4) were used to develop and validate a set of predictive models to obtain the volume and RW of the aforementioned muscle groups. Only segmentations of the right muscles were used.

Labeling of MRI slices relative to subject femur size

MRI slices were normalized with regard to longitudinal length of the subjects' right femurs, thus providing a common scale for the 19 patients independent of each subject height. Each MRI slice was then labeled based upon its location relative to the femur with S0 being the first MRI slice containing the two condyles, and S100 being the last MRI slice containing the femoral heads. The slices above the femoral head, covering the lumbar spine, had increasing indexes which finished between 143 and 163, depending on the patient.

Variable of the models

Data from 15 slices – equally distributed between the knee (S0) and T12 (S140) – were considered for each patient (S0, S10, S20, ... S140). For each of these 15 slices, data extracted from the original dataset stemmed from the segmentation of the muscles, thigh and femur. Variables considered for each model include:

- Muscle area (MA) in mm2 (including water and fat component)
- Fat component area (FA) in mm2 extracted from the segmentation
- Water component area (WA) in mm2 extracted from the segmentation
- Ratio between muscle and fat component area (RFA= FA /MA) component areas
- Ratio between muscle and water component area (RWA= WA/ MA) component areas
- Age of the patient
- Femoral length in mm

Of note MA=FA +WA and RFA+ RWA=1.

To summarize, the initial set of parameters considered to predict either the muscular volume or the RW of the different muscle groups were the Agei, FLi, MAi,j,k, FAi,j,k, WAi,j,k,, RFAi,j,k, RWAi,j,k where i= [1,2,...19] corresponds to the patients, j corresponds to the muscles (Table 1), the thigh and the femur and k=[0,10,20, ...,140] corresponds to the slices.

Statistics

A model was developed for the volume and the RW of each muscular groups defined previously.

Independent predictor of muscle volume and RW

For each model, after subtraction of the mean and division by the standard deviation for each variable, a principal component analysis was carried out and only components representing 99% of the variance were considered in the model construction. These components were then used as independent predictors in a set of multi-linear regressions with stepwise analysis[223], using the 'stepwisefit' matlab function. Only independent predictors with a p-value less than 0.10 were retained in the final models.

Model validation

Cross validation of the models was carried out with a leave-one-out method, meaning that each individual patient was used to validate models generated based on the remaining 18 patients. For each subject, models were built with the data of the 18 remaining subjects. The muscle volume and the RW of the subject leaved out was predicted based with the model build upon the remaining subjects. Errors of the models were computed as the root means square (RMS) of the difference between the predicted muscle volume and RW and the measured muscle volume and RW as equation 0.1 :

$$RMS_l = \sqrt{\frac{\sum_{i=1}^{n}(\frac{pred_{i,l} - y_{i,l}}{y_{i,l}})^2}{n}} \qquad [4.2.1]$$

i= [1,2,...19] corresponds to the patients, n corresponds to number total of patients(19), l corresponds to the muscular groups described Table 1, predi,l corresponds to the prediction of the RW or the volume of the muscular group l, for the patient i, with the model built with the data of the remained patients and yi,l correspond to the RW or the volume measured for the muscular group l, for the patient i.

Models selection based on slices permutations

Models were built based upon the combination of up to 4 slices. For each of these configurations (i.e. 1, 2, 3, or 4 slices) all the permutations of the 15 slices were considered. The RMS error in terms of volume reconstruction and RW of each muscle group was computed. Additionally the mean of the RMS errors among the muscular groups for the volume and the RW were calculated. Among all the permutations, the optimal model was the one with the smallest mean of the RMS error for the muscular volume. In addition, the solution with the smallest RMS error for the RW and the muscular volume for the spine extensor was identified for the models with 4 slices.

The RMS error for the models built with several slices (2, 3 or 4) was the minimal error of the models when considering all the partial permutations among the slices. For instance, in a model built with 2 slices (S and S'), RMS error of the model built with S, the model with S', and that of S and S', were each obtained individually. The smallest error of the three was named the RMS error for the overall model (Figure 4-9).

Comparison of the number of slices manually segmented between the DPSO methods and the multi-linear models

The number of segmentations by muscle needed to reconstruct all the muscles with the Muscl'x software (DPSO method) was evaluated as well as the number of segmentations used for the optimal models with 4 slices .

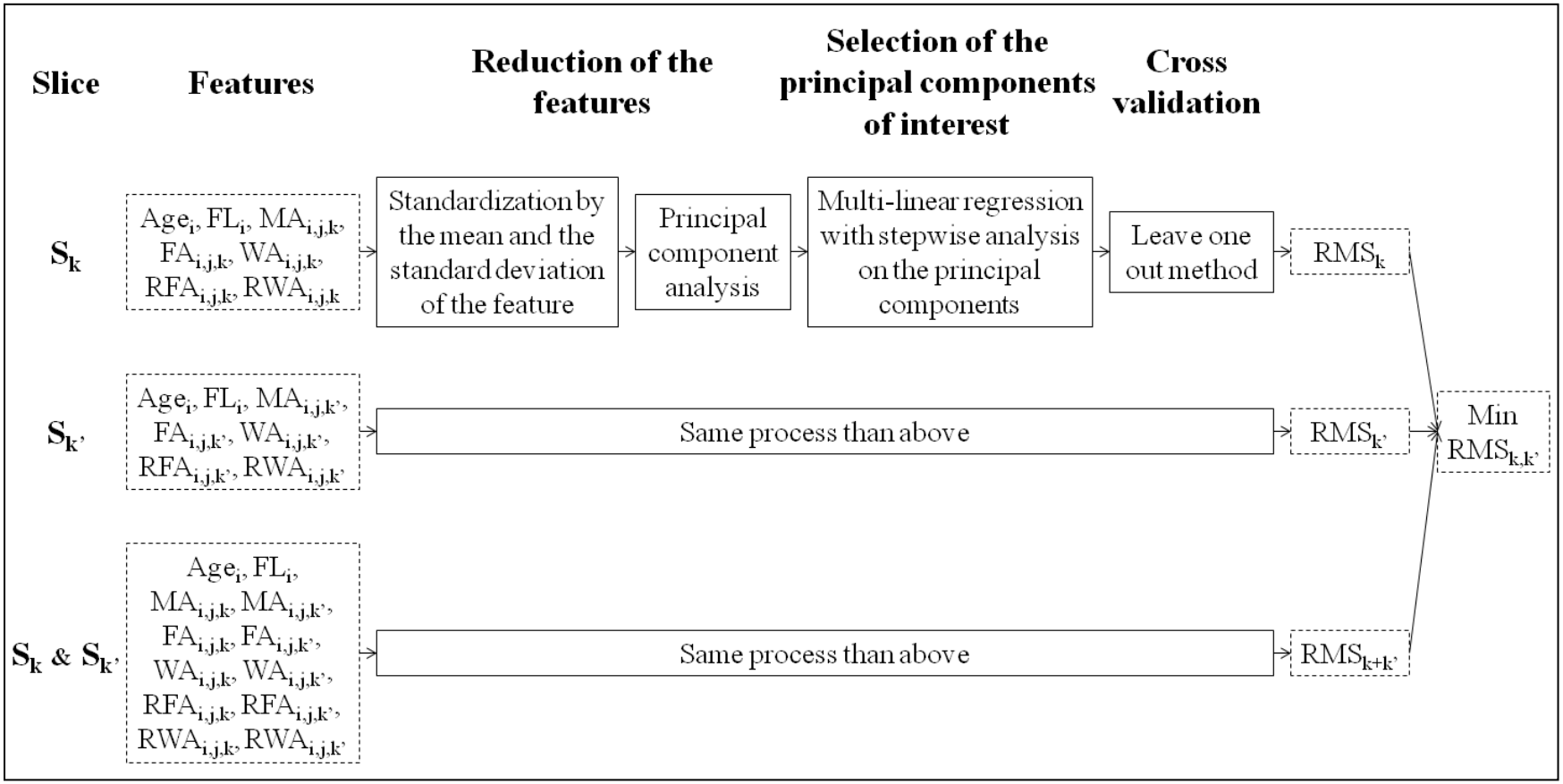

Figure 4-9: Evaluation of the root mean square (RMS) error for a model built with two slices Sk and Sk',Femur Length (FL)i, Muscle area (MA), Fat component area (FA), Water component area (WA), Ratio between muscle and fat component area (RFA), Ratio between muscle and water component area (RWA) and i= [1,2,...19] corresponds to the patients, j corresponds to the muscles, the thigh and the femur.

4.3.3 **RESULTS**

Demographics

19 consecutive ASD patients with a mean age of 60 years old (range: 37-80) and a mean BMI of 22.3 kg/m2 (range 17-31) were included (Table 4-8, page 137).

Multi-linear regression models:

Muscular volume:

The smallest volume was found for the erector and flexor of the spine, respectively 590.9±120.2 cm3 and 507.8±99.9 cm3. For the other groups the average volume was comprised between (1194.9 and 2438.7cm3) (Table 4-15).

The position of the slice used for the optimal model with 1 slice was 70%, i.e. in the proximal part of the femur. This slice was included in the models built with 2, 3, and 4 slices. The RMS error for the muscular volume based on one-slices models varied from 5.4% to 16.5% with an mean RMS error of 9.5% . The maximum RMS error was for the spine erector (Table 4-15).

In four-slices models the RMS error was less than 5.7% among all the groups except the spine erector (9.3%) (Table 4-15). For the solution specific to the spine erector with 4 slices, the RMS error for the volume was 6.4%(Table 4-16).

Ratio of water component (RW)

The spine erector had the smallest ratio of water component (i.e the greatest ratio of fat infiltration) with the greatest standard deviation (68.7 ±14.1) %. For the other groups, the ratio of water component was comprised between 85.2% ± 7.0 and 91.3%±4.0. (Table 4-15)

One-slice models resulted in a RMS error less than 3.5 % for all the groups except the spine extensor (35.5%). For the 4 slices-model the RMS error for the RW of the spine erector was 23.5% and less than 2.2% for the others muscular groups. The RMS error for the four-slice models with the smallest error for the ratio of water component was 13.1%.

The RMS error for the ratio of water component was in general smaller than the RMS error for the muscular volume.

Muscle segmentation:

In total for the 3D reconstructions of all the right and left muscles with the DPSO method, the operator had to segment ~240 muscular sections (~120 for the right muscles and ~120 for the left muscles). The number of the slices depends on the patient. For the models with 4 slices, 36 manual segmentations were performed, representing a 7 folds decreased when compared to the DPSO method.

Muscular Volume												
					Spine Extensor	Spine Flexor	Hip Extensor	Hip Flexor	Knee Extensor	Knee Flexor	Total muscles	
	Mean volume (cm^3)				590.9	507.8	1998.6	2438.7	2130.5	1194.9	6880.0	
	STD volume (cm^3)				120.2	99.9	413.4	465.3	488.5	239.5	1289.7	
number of slices	Position				RMS error							mean of RMS error
	Slice 1	Slice 2	Slice 3	Slice 4								
1	70	-	-	-	16.5	13.2	8.0	5.4	10.5	6.6	6.5	9.5
2	70	140	-	-	11.6	9.6	5.5	5.4	8.8	6.6	4.7	7.4
3	30	70	120	-	11.0	7.4	5.3	3.3	7.6	4.6	4.9	6.3
4	30	50	70	120	9.3	5.7	5.3	3.3	5.2	4.6	4.9	5.5

Ratio of water component (RW in %)												
					Spine Extensor	Spine Flexor	Hip Extensor	Hip Flexor	Knee Extensor	Knee Flexor	Total muscles	
	Mean of RW (%)				68.7	88.1	85.2	89.2	91.3	87.2	86.7	
	STD of RW (%)				14.1	3.6	7.0	3.2	4.0	4.2	5.3	
number of slices	Position				RMS error							mean of RMS error
	Slice 1	Slice 2	Slice 3	Slice 4								
1	70	-	-	-	35.5	3.2	3.5	1.0	1.4	1.8	2.5	7.0
2	70	140	-	-	14.0	2.5	3.3	1.0	1.4	1.5	1.1	3.5
3	30	70	120	-	23.5	2.2	2.4	0.8	1.4	1.0	2.0	4.8
4	30	50	70	120	23.5	2.0	2.2	0.5	1.4	0.6	1.3	4.5

Table 4-15: Muscular volume and ratio of water component RMS error for the optimal solution defined as the models with the smallest mean of RMS error for the muscular volume with 1, 2, 3 and 4 slices. The position of the slices are presented. The mean of RMS error among the groups are expressed. The mean and standard deviation for the volume and the ratio of water component among the population are expressed.

Combination with the smallest RMS error for the spine extensor respectively for the volume and the ratio of water component (RW)												
	Position				RMS error							mean of RMS error
	Slice 1	Slice 2	Slice 3	Slice 4	Spine Extensor	Spine Flexor	Hip Extensor	Hip Flexor	Knee Extensor	Knee Flexor	Total muscles	
Volume	20	30	50	100	6.4	9.1	6.6	5.8	8.3	4.6	6.4	6.7
RW	20	110	120	130	13.1	1.6	2.8	0.8	0.9	1.0	1.6	3.1

Table 4-16: Models with the combination of 4 slices with the smallest RMS error for the spine extensor for the volume and ratio of water component respectively. The position of the slices used for the models are also presented. The mean of RMS error among the groups are expressed

4.3.4 **DISCUSSION**

Depending on the level of accuracy required and the clinical or research purpose, the amount of time available to investigate muscular volume ant their fat-water distribution for spino-pelvic groups of muscles varies greatly. As such it is essential to develop clinical adapted tools that allow for accurate assessment of muscle volume and fat infiltration with minimal processing time.

This study shows that accurate estimation of the volume and distribution of fat and water component of the main muscular groups between the knee and the thoraco-lumbar junction is possible with the manual segmentation of only 4 MRI slices: one slice positioned in the lumbar area, and three others in the femur area (medial, proximal and distal parts)(Figure 4-10). When applying this method, it is first necessary to identify the distal slice containing the two condyles of the right femur and the top slice containing the right femoral head.

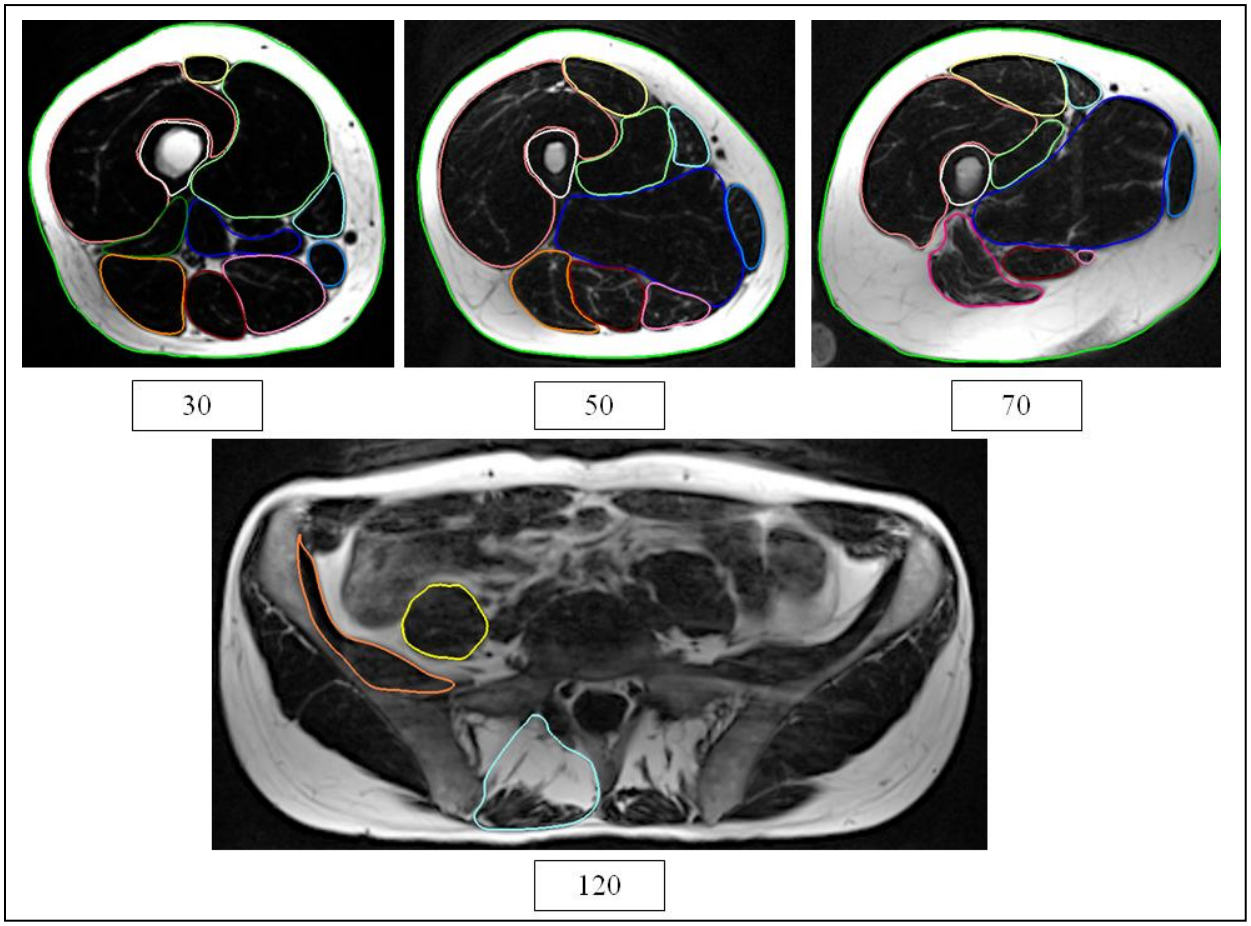

Figure 4-10: Example of manual segmentation of the four slices necessary to apply the optimal model with their relative position

Using these four slices seems an effective alternative to the previous DPSO method, for the volume and the distribution of fat and water component of main muscular groups assessment. The proposed approach requires seven times less manual segmentations as compared to the DPSO method implemented in the Muscle'X software. Moreover, fewer MRI axial slices used for the models can decrease MRI acquisition time.

Several studies have investigated the reproducibility of the DPSO method on the muscles but not on the muscular groups. Moreover the RMS error cannot be directly compared to the error of reproducibility, however the method proposed here show RMS errors with the same order of magnitude than muscle reproducibility. In a reproducibility analysis (3 operators) of the hip muscles of 30 subjects, Jolivet et al[222] reported error of 5-12% for the volume. On 13 muscles involved in the knee joint motion of 10 asymptomatic young men, Sudhoff et al[172] evaluate volume reproducibility error between 2 and 11% depending on the muscles. Similar error was found on another reproducibility study of two patients with three operators for the volume of the same muscles segmented in this study[214]. The reproducibility of the ratio of fat component was comprised between 1 and 11% depending on the muscles.

The four- slices model represent a compromise between processing time and accuracy in the prediction of muscular volume with the smallest error among all muscular groups.

For both the ratio of water component and the muscular volume the spine extensor had the greatest RMS error. The presented models are based on the link between the muscle in terms of volume and fat-water distribution. The muscular description of the current ASD population previously demonstrated that the spine erector had the greatest muscular degeneration. Yet, this degeneration seems less dependent of the global and regular degeneration associated with age. Herein may lay the greatest error of prediction. If there is particular interest in the spine erector, a detailed analysis of these muscles is necessary.

In addition, this study demonstrated that simple axial section of muscle taken independently is not representative of the muscular volume which highlight the limitation of study investigate muscles with only cross sectional area[147,151,153–155,157–164].

The present study has some limitations. The models are based on a specific population, including only females between 35 and 80 years old with a spinal deformity, and thus must be validated on a larger cohort with an asymptomatic population. However, despite the small sample size, the leave-one-out method allows validation of the models.

Conclusion

This study demonstrated that with the manual segmentations of only a few slices of interest, volume and fat-water distribution could be estimated with an error less than 6 % for the main spino-pelvic muscles groups, except the spine erector groups (error volume = 9.3% and error fat-water distribution: 23.5%). Findings from this study pave the way for routine muscle examination in a clinical setting, which should yield a better understanding of soft tissues' role in spine disorders.

4.4 SYNTHESIS: MUSCULAR EVALUATION AND ASD PATIENTS

Two methods for the characterization of the main muscles involved in the sagittal alignment have been validated in this section. The first one described in article 4.1 combines the DPSO method and the Dixon method and provides detailed 3D reconstruction of the muscles as well as a precise quantification of fat infiltration. This methods correspond more to research purpose than a clinical one due to the large time of operator processing but present the ability to generate patient–specific musculoskeletal models.

The second one, described in article 4.3, is based on multi-linear model and manual segmentation of specific slices obtained from Dixon acquisition. This methods estimates the volume and fat-water distribution of the main spino-pelvic muscles groups, with a considerable reduction of the operator processing compared to the DPSO method. This would be more adapted to clinical practice.

In addition to the development of both methods, the muscular volume and the fat infiltration of an ASD population has been described. Despite the lack of the data from an asymptomatic population and the limited number of the population, the results demonstrated clearly that the lumbar spine and hip extensor were the groups most affected by muscular degeneration which is particularly interesting in this population suffering from an anterior shift mainly due to a loss of lumbar lordosis.

5. CONCLUSION AND PERSPECTIVES

The work behind this thesis highlights the truly complex nature of ASD treatment and it draws particular attention to surgical restoration of the sagittal plane.

In an effort improve our methods of evaluating the efficacy of surgical treatment, both a clinical and radiological evaluation were carried out. The studies' methodologies outlined the approach for comparing patients' post-operative outcomes with their pre-operative states on an individual basis. Despite the complexity of this approach, it yielded a clear evaluation of the surgical treatment.

These studies brought to light the inherent difficulty of surgically restoring sagittal alignment and it led us to focus on the degree to which an individual's preoperative goals were realized at the conclusion of surgery. Three fundamental aspects of the surgical treatment emerged as areas in need of improvement, and they are discussed below.

First, patient-specific guidelines should be developed. While work on age-specific alignment objectives has begun[202], it fails to account for a patient's initial clinical state (i.e., metrics that include age, BMI, comorbities), potential pre-operative deformities, and possible surgical corrections. Further research is needed to address this issue.

Second, new intra-operative tools must be developed that collect real-time feedback on regional alignment. Without this technological progress, it seems inevitable that patients will experience inappropriate alignment corrections. To address this issue, new imaging systems should be explored, along with the development of surgical methods that allow for the use of pre-bent rods. Moreover, these intra-operative technologies should be incorporated into pre-operative surgical planning. Doing so would increase the degree to which a patient's pre-operative goals were achieved.

Finally, this analysis exposed limitations of pre-operative planning, including the fact that current predictions regarding post-operative positioning of the pelvis and the knee in the unfused area of the spine are not as accurate as they could be. This is an area ripe for development of new planning tools. This limitation could also be mitigated by incorporating muscular evaluation into pre-operative planning.

The inclusion of muscular analysis is critical for the improvement of ASD treatment efficiency, and this thesis has outlined and validated two novel protocols for the assessment of muscular volume and fat infiltration. It is important to note that while the current Muscl'X software based on the DPSO method with Dixon acquisition is mainly dedicated to research purposes, including the possible development of a 3D musculoskeletal model, multi-linear models based on the

segmentation of specific slices could help in progressing towards routine muscle examination in a clinical setting.

However, both protocols could be improved. In particular, more work could be done to improve the quality of MRI acquisition for instrumented patients. The long performed MRI acquisition creates artifact in the abdominal area, and excluded the analysis of the muscle of the lab belt. Efforts have been made to reduce the time required to acquire the image and they have yielded promising results in breath holding [224]. Moreover, shorter acquisitions more easily permit the inclusion of this exam in clinical practice, given the prohibitive cost of MRI exams and the limited availability of MRI machines.

Both methods tend to reduce the time required to obtain an MRI. This is especially true of the method that is based on multi-linear model. Nevertheless, the time required for manual segmentation could be reduced further using innovative image treatment. It is also important to note that even if MRI images take a long time to acquire, relevant information about other tissues can be collected. For example, Dixon methods have been used to characterize bone quality [180]. It might also be possible to collect information about the vertebral disc, as well as the vertebral canal. Improvements in MRI acquisition should be coupled with better post-processing. Taken as a whole, these suggestions lend credence to the idea that he MRI exam could more easily be incorporated into clinical practice.

In the process of analyzing ASD muscular systems, it was demonstrated that muscle degeneration mainly affects the erector of the spine and the hip—the two key muscle groups involved in the maintenance of sagittal alignment. However, due to the limited number of patients involved and the absence of data for an asymptomatic population, sagittal malalignment was not directly linked to a precise muscular deficiency and the muscle's role in the compensation mechanism was not properly understood.

The analysis has also highlighted the importance of characterizing fat infiltration, in addition to muscular volume, and preliminary projects have been dedicated to characterize muscular degeneration. But further work should be conducted in order to understand the development of fat infiltration inside the muscle.

In conclusion, the potential of the muscular evaluation in the fields of ASD treatment has been described, but it requires further development and increased data collection in order to gain relevance in clinical practice. In addition, several different ways in which surgical treatment could be improved for patients were discussed and consideration was given to how these improvements would give clinicians a better understanding of malalignment and associated compensatory mechanisms.

6. ARTICLES AND CONGRESS

6.1 PUBLISHED ARTICLES RELATED TO THE THESIS

1. Moal B., Schwab F., Ames C., Smith J., Ryan D, Mummaneni P., Mundis Jr. G, Terran J., Klineberg E., Hart R., Boachie-Adjei O., Shaffrey C., Skalli W., Lafage V., International Spine Study Group. Radiographic Outcomes of Adult Spinal Deformity Correction : A Critical Analysis of Variability and Failures Across Deformity Patterns. Spine Deformity. 2014 (Section 3.2, page 85)
2. Moal B., Raya J.G., Jolivet E., Schwab F., Blondel B., Lafage V., Skalli W.. (2014). Validation of 3D spino-pelvic muscle reconstructions based on dedicated MRI sequences for fat-water quantification. Irbm. 2013.12.011 (Section 4.1, page 115)

6.2 SUBMITTED ARTICLES RELATED TO THE THESIS

1. Moal B., Lafage V., Smith J., Ames C., Mundis G, Terran J., Klineberg E., Hart R., Boachie-Adjei B., Bess S., Skalli W., Schwab F., International Spine Study Group. Clinical Improvement Through Surgery for Adult Spinal Deformity: What Can Be Expected And Who Is Likely to Benefit Most?, Submitted to Spine Deformity (Section 3.1, page 69)
2. Moal B., Lafage V., Maier S., Liu S., Challier V., Skalli W., Protopsaltis T., Errico T., Schwab F.. Discrepancies in preoperative planning and operative execution in the correction of sagittal spinal deformities. Submitted to SPINE (Section 3.3, page 98)
3. Moal B., Bronsard N., Raya J.G, Vital J.M., Schwab F., Lafage V., Skalli W. Preliminary results on quantitative volume and fat infiltration of spino-pelvic musculature in adults with spinal deformity. submitted to the spine journal (Section 4.1, page 115)
4. Moal B., Skalli W., Raya J.G, Bronsard N., Vital J.M., Protopsaltis T., Errico T., Schwab F., Lafage V. Muscular volume and fat-water distribution estimation for spino-pelvic groups of muscles: MRI Axial sections of interest. Submitted to Computer Methods in Biomechanics and Biomedical Engineering: Imaging & Visualization Journal (Section 4.3, page 147)

6.3 ORAL PRESENTATION RELATED TO THE THESIS

1. Moal B.; Lafage V.; Maier S.; Shian L; Challier V.; Skalli W.; Protopsaltis T.; Errico T.; Schwab F. Discrepancies in Preoperative Planning and Operative Execution in the Correction of Sagittal Spinal Deformities. North american spine society, San Francisco, November 12-15 2014
2. Moal B., Bronsard N., Terran J., Raya J.G,Protopsaltis T.,Vital J.M., Skalli W., Frank J. Schwab,Lafage V., Muscular Volume and Fat Infiltration Parameters of the Spino-Pelvic Complex Correlate with HRQOL and Skeletal Malalignment in Adult Spinal Deformity. *International Meeting for Advanced Spine Technique IMAST, Vancouvert, July 10-13 (2013)*
3. Moal B, Lafage V, Smith J, Ames C, Mummaneni P, Mundis G, Terran J, Klineberg E, Hart R, Boachie-Adjei O, Shaffrey C, Schwab F, ISSG. Clinical Improvement Through Surgery for Adult Spinal Deformity (ASD): What can be Expected and Who is Likely to Benefit Most? *Spine Research Society (SRS), Chicago , 5-8 Sept (2012)*
4. Moal B, Schwab F, Ames C, Smith J, Terran J, Hart R, Shaffrey C, Lafage V. Clinical improvement through surgery for adult spinal deformity (ASD): Who is likely to benefit most? American Academy of Orthopaedic Surgeons (AAOS), Chicago, IL, March 19-23 (2013)

6.4 E-POSTER RELATED TO THE THESIS

1. Moal B; Lafage V; Maier S; Liu S; Challier V; Skalli W; S. Protopsaltis T; Errico T J.; Schwab F. Discrepancies in Preoperative Planning and Operative Execution in the Correction of Sagittal Spinal Deformities. International Meeting for Advanced Spine Technique IMAST, Valencia, July 16-29 (2014)
2. Moal B, Schwab F, Ames C, Smith J, Mummaneni P, Mundis G, Terran J, Klineberg E, Hart R, Boachie-Adjei O, Shaffrey C, Lafage V, ISSG. Radiographic Outcomes of Spinal Deformity Correction in Adult Patients: A Critical Analysis of Variability and Failures Across Deformity Patterns. *International Meeting for Advanced Spine Technique IMAST, Istanbul, July 18-21 (2012)*
3. Moal B., Schwab F., Raya J.G., Blondel B., Jolivet E., Lafage V., Skalli W. Quantitative analysis of key muscles of the thoraco-lumbar spino-pelvic complex: 3D geometry and homogeneity
    a. *Spineweek, Amsterdam, May 28 - June 1 (2012)*
    b. *European Society of Biomechanics, Lisbon, July1-4 (2012)*
    c. *International Meeting for Advanced Spine Technique IMAST, Istanbul, July 18-21 (2012)*

6.5 OTHERS PUBLISHED ARTICLES

1. Ames CP, Smith JS, Scheer JK, Shaffrey CI, Lafage V, Deviren V, Moal B, Protopsaltis T, Mummaneni PV, Mundis GM Jr, Hostin R, Klineberg E, Burton DC, Hart R, Bess S, Schwab FJ; the International Spine Study Group. A standardized nomenclature for cervical spine soft-tissue release and osteotomy for deformity correction. Journal of Neurosurgery Spine, July 2013
2. Smith JS, Klineberg E, Schwab F, Shaffrey CI, Moal B, Ames CP, Hostin R, Fu KM, Burton D, Akbarnia B, Gupta M, Hart R, Bess S, Lafage V; International Spine Study Group. Change in Classification Grade by the SRS-Schwab Adult Spinal Deformity Classification Predicts Impact on Health-Related Quality of Life Measures: Prospective Analysis of Operative and Non-operative Treatment. Spine June 2013
3. Blondel B., Pomero V., Moal B., Lafage V., Jouve JL., Tropiano P. , Bollini G., Dumas R., Viehweger E.. Sagittal spine posture assessment: Feasibility of a protocol based on intersegmental moments. Orthop Traumatol Surg Res.2012 Feb; 98(1): 109-13
4. Blondel B., Schwab F., Patel A., Demakakos J., Moal B., Farcy JP., Lafage V.. Sacro-Femoral-Pubic angle: A coronal parameter to estimate pelvic tilt. European Spine Journal 2011

6.6 OTHERS ORAL PRESENTATIONS

1. Zhang C, Moal B., Dubois G., Bronsard N., Raya JG., Schwab F., Lafage V., Skalli W. Comparison of two MRI sequences for subject-specific 3D thigh muscle reconstruction. *Comput Methods Biomech Biomed Engin* 2014;17 Suppl 1:136–7
2. Lafage V., Smith J., Schwab F., Moal B., Klineberg E., Ames C., Hostin R., Fu KM., Kebaish, Burton D., Akbarnia A., Gupta M., Deviren V., Mundis G., Boachie O., Hart R., Bess S., ISSG. Likelihood of Reaching Minimal Clinically Important Difference in Health Related Quality of Life Measures: Prospective Analysis of Operative and Non-operative Treatment of Adult Spinal Deformity. *North America Spine Society NASS, Dallas, October 24-27.(2012)*
3. Smith J., Klineberg E., Schwab F., Shaffrey C., Moal B., Ames C., Hostin R., Fu KM., Burton D., Akbarnia B., Gupta M., Hart R., Bess S., Lafage V., ISSG. Change in Classification Grade by the Schwab-SRS Adult Spinal Deformity (ASD) Classification Predicts Impact on Health Related Quality of Life (HRQOL) Measures: Prospective Analysis of Operative and Nonoperative Treatment. *Spine Research Society (SRS), Chicago , 5-8 Sept (2012)*
4. Schwab F., Lafage V., Shaffrey C., Smith J., Moal B., Ames C., Fu KM., Mummaneni P., Burton D., Gupta M., Deviren V., Mundis G., Hart R., Bess S., ISSG. The Schwab-SRS Adult Spinal

Deformity Classification: Assessment and Clinical Correlations Based On A Prospective Operative and Non-Operative Cohort. *Spine Research Society (SRS), Chicago , 5-8 Sept (2012)*

5. Lafage V., Schwab F., Ames C., Moal B., Hostin R., Mummaneni P., Kebaish K., Smith J., Deviren V., Shaffrey C., Klineberg E., Bess S., ISSG. Prevalence and Risk Factors for Proximal Junctional Kyphosis Following Realignment Surgery by Pedicle Subtraction Osteotomy: A Multicenter Review. *International Meeting for Advanced Spine Technique (IMAST) , Istanbul, 18-21 July (2012)*
6. Blondel B., Schwab F., Ames C., Le Huec JC., Smith J., Shaffrey C., Bess S., Demakakos J., Moal B., Tropiano P., Farcy JP., Lafage V. The Crucial Role of Cervical Alignment in Regulating Sagittal Spino-Pelvic Alignment in Human Standing Posture. *International Meeting for Advanced Spine Technique (IMAST), Istanbul, 18-21 July (2012)*
7. Blondel B., Pomero V., Moal B., Lafage V., Jouve JL., Tropiano P. , Bollini G., Dumas R., Viehweger E.. Postural spinal balance defined by moment in a segmental model. *European Society of Biomechanics,(Lisbon) July1-4 (2012)*
8. Blondel B., Schwab F., Chay E., Demakakos J., Moal B., Lenke L., Tropiano P., Ames C., Smith J., Shaffrey C., Glassman S., Gaines R., Farcy J.P., Lafage V. The comprehensive anatomical spinal osteotomy classification. *Spineweek, Amsterdam, May 28 - June 1 (2012)*
9. Moal B., Schwab F., Blondel B., Demakakos J., Smith J.,Bridwell K., Glassman S., Shaffrey C., Farcy J.P., Lafage V. Limited benefit of the coronal cobb angle correction in the setting of adult spinal deformity: A health related quality of life assessment on two year outcomes. *Spineweek, Amsterdam, May 28 - June 1 (2012)*
10. Blondel B., Schwab F., Moal B., Hostin R., Shaffrey C., Smith J., Akbarnia B., Mundis G., Christopher A., Kebaish, K., Hart R., Farcy J.P., Lafage V.. Combined assessment of pelvic tilt, pelvic incidence/ lumbar lordosis mismatch and sagittal vertical axis predicts disability in adult spinal deformity: A prospective analysis. *Spineweek, Amsterdam, May 28 - June 1 (2012)*
11. Blondel B., Schwab F., Ungar B., Moal B., Smith J.,Bridwell K.,Glassman S., Shaffrey C., Farcy J.P., Impact of the magnitude and percentage global sagittal plane correction on health related quality of life at 2 years follow-up. *Spineweek, Amsterdam, May 28 - June 1 (2012)*
12. Moal B., Schwab F., Smith J., Bridwell K., Blondel B., Glassman S., Demakakos J., Shaffrey C., Lafage V.. Coronal Cobb Angle Correction in the Setting of Adult Spinal Deformity: a Health Related Quality of Life Assessment on Two Year Outcomes. *International Society for the Advancement of Spine Surgery (ISASS), Barcelona, March20-24 (2012)*
13. Moal B., Blondel B., Schwab F., Bess S., Ames C., Hart R., Smith J., Shaffrey C., Boachie-Adjei O., Lafage V., International Spine Study Group. Posterior global malalignment after osteotomy for sagittal plane deformity. *International Society for the Advancement of Spine Surgery (ISASS), Barcelona, March20-24 (2012)*
14. Lafage V., Schwab F., Blondel B., Ames C., Moal B., Hart R., Deriven V., Akbarnia B., Demakakos J., Smith J., Shaffrey C., Kebaish K., Burton D., Bess S., Hostin R., Farcy J-P. Y-a-t-il une stratégie

unique permettant d'obtenir un équilibre sagittal postopératoire satisfaisant dans une population d'adultes porteurs de déformation rachidiennes ? *Société Francaise de Chirurgie du Rachis (SFCR), Marseille France, June 24-25 (2011)*

15. Blondel B., Schwab F., Moal B., Hostin R., Shaffrey C., Smith J., Akbarnia B., Mundis G., Christopher A., Kebaish, K., Hart R., Farcy J.P., Lafage V. Evaluation combinée de paramètres spino-pelviens dans la prédiction du handicap chez l'adulte atteint de déformation rachidienne : résultats d'une analyse prospective. *Société Francaise de Chirurgie du Rachis (SFCR), Marseille France, June 24-25 (2011)*
16. Blondel B., Pomero V., Moal B., Lafage V., Jouve JL., Tropiano P. , Bollini G., Dumas R., Viehweger E. Approche biomécanique de la posture dans la prise en charge des pathologies rachidiennes : résultats préliminaires d'un protocole caractérisant les moments articulaires. *Société Francaise de Chirurgie du Rachis (SFCR), Marseille France, June 24-25 (2011)*.

7. REFERENCES

[1] Pérennou D, Marcelli C, Hérisson C, et al. Adult lumbar scoliosis. Epidemiologic aspects in a low-back pain population. *Spine (Phila Pa 1976)* 1994;19:123–8.

[2] Kostuik JP, Bentivoglio J. The incidence of low-back pain in adult scoliosis. *Spine (Phila Pa 1976)* n.d.;6:268–73.

[3] Kebaish KM, Neubauer PR, Voros GD, et al. Scoliosis in adults aged forty years and older: prevalence and relationship to age, race, and gender. *Spine (Phila Pa 1976)* 2011;36:731–6.

[4] Schwab F, Dubey A, Pagala M, et al. Adult scoliosis: a health assessment analysis by SF-36. *Spine (Phila Pa 1976)* 2003;28:602–6.

[5] Bess S, Kai-Ming G. F, Lafage V, et al. Disease State Correlates for Pain and Disability in Adult Spinal Deformity (ASD); Assessment Guidelines for Health Care Providers. North Am. Spine Soc., 2013, p. New Orleans.

[6] Smith JS, Shaffrey CI, Glassman SD, et al. Risk-benefit assessment of surgery for adult scoliosis: an analysis based on patient age. *Spine (Phila Pa 1976)* 2011;36:817–24.

[7] Smith JS, Shaffrey CI, Berven S, et al. Operative versus nonoperative treatment of leg pain in adults with scoliosis: a retrospective review of a prospective multicenter database with two-year follow-up. *Spine (Phila Pa 1976)* 2009;34:1693–8.

[8] Smith JS, Shaffrey CI, Berven S, et al. Improvement of back pain with operative and nonoperative treatment in adults with scoliosis. *Neurosurgery* 2009;65:86–93; discussion 93–4.

[9] Bridwell KH, Glassman S, Horton W, et al. Does treatment (nonoperative and operative) improve the two-year quality of life in patients with adult symptomatic lumbar scoliosis: a prospective multicenter evidence-based medicine study. *Spine (Phila Pa 1976)* 2009;34:2171–8.

[10] Bridwell KH, Baldus C, Berven S, et al. Changes in radiographic and clinical outcomes with primary treatment adult spinal deformity surgeries from two years to three- to five-years follow-up. *Spine (Phila Pa 1976)* 2010;35:1849–54.

[11] Fu K-MG, Bess S, Shaffrey CI, et al. Adult Spinal Deformity Patients Treated Operatively Report Greater Baseline Pain and Disability than Patients Treated Nonoperatively: However, Deformities Differ Between Age Groups. *Spine (Phila Pa 1976)* 2014.

[12] Liu S, Schwab F, Smith JS, et al. Likelihood of reaching minimal clinically important difference in adult spinal deformity: a comparison of operative and nonoperative treatment. *Ochsner J* 2014;14:67–77.

[13] Glassman SD, Berven S, Bridwell K, et al. Correlation of radiographic parameters and clinical symptoms in adult scoliosis. *Spine (Phila Pa 1976)* 2005;30:682–8.

[14] Schwab FJ, Blondel B, Bess S, et al. Radiographical spinopelvic parameters and disability in the setting of adult spinal deformity: a prospective multicenter analysis. *Spine (Phila Pa 1976)* 2013;38:E803–12.

[15] Barrey C, Roussouly P, Perrin G, et al. Sagittal balance disorders in severe degenerative spine. Can we identify the compensatory mechanisms? *Eur Spine J* 2011;20 Suppl 5:626–33.

[16] Lafage V, Schwab F, Patel A, et al. Pelvic tilt and truncal inclination: two key radiographic parameters in the setting of adults with spinal deformity. *Spine (Phila Pa 1976)* 2009;34:E599–606.

[17] Obeid I, Hauger O, Aunoble S, et al. Global analysis of sagittal spinal alignment in major deformities: correlation between lack of lumbar lordosis and flexion of the knee. *Eur Spine J* 2011;20 Suppl 5:681–5.

[18] Blondel B, Schwab F, Ungar B, et al. Impact of magnitude and percentage of global sagittal plane correction on health-related quality of life at 2-years follow-up. *Neurosurgery* 2012;71:341–8; discussion 348.

[19] Diebo B, Liu S, Lafage V, et al. Osteotomies in the treatment of spinal deformities: indications, classification, and surgical planning. *Eur J Orthop Surg Traumatol* 2014;24 Suppl 1:11–20.

[20] Schwab F, Blondel B, Chay E, et al. The comprehensive anatomical spinal osteotomy classification. *Neurosurgery* 2014;74:112–20; discussion 120.

[21] Akbar M, Terran J, Ames CP, et al. Use of Surgimap Spine in sagittal plane analysis, osteotomy planning, and correction calculation. *Neurosurg Clin N Am* 2013;24:163–72.

[22] Le Huec J-CC, Leijssen P, Duarte M, et al. Thoracolumbar imbalance analysis for osteotomy planification using a new method: FBI technique. *Eur Spine J* 2011;20 Suppl 5:669–80.

[23] Lafage V, Bharucha NJ, Schwab F, et al. Multicenter validation of a formula predicting postoperative spinopelvic alignment. *J Neurosurg Spine* 2012;16:15–21.

[24] Aurouer N, Obeid I, Gille O, et al. Computerized preoperative planning for correction of sagittal deformity of the spine. *Surg Radiol Anat* 2009;31:781–92.

[25] Vital J-M. Anatomie descriptive et fonctionnelle de l'appareil locomoteur. Bergeret. 2014.

[26] Legaye J, Duval-Beaupère G, Hecquet J, et al. Pelvic incidence: a fundamental pelvic parameter for three-dimensional regulation of spinal sagittal curves. *Eur Spine J* 1998;7:99–103.

[27] Cobb J. Outline for the study of scoliosis. Am. Acad. Orthop. Surg. Instr. Course Lect., 1948, p. Vol. 5.

[28] Duval-Beaupère G, Schmidt C, Cosson P. A Barycentremetric study of the sagittal shape of spine and pelvis: the conditions required for an economic standing position. *Ann Biomed Eng* 1992;20:451–62.

[29] Roussouly P, Gollogly S, Noseda O, et al. The vertical projection of the sum of the ground reactive forces of a standing patient is not the same as the C7 plumb line: a radiographic study of the sagittal alignment of 153 asymptomatic volunteers. *Spine (Phila Pa 1976)* 2006;31:E320–5.

[30] Vialle R, Levassor N, Rillardon L, et al. Radiographic analysis of the sagittal alignment and balance of the spine in asymptomatic subjects. *J Bone Joint Surg Am* 2005;87:260–7.

[31] Gore D, Sepic S, Gardner G. Roentgenographic findings of the cervical spine in asymptomatic people. *Spine (Phila Pa 1976)* 1986;11.

[32] Stagnara P, De Mauroy J-C, Georges D, et al. Reciprocal angulation of vertebral bodies in a sagittal plane: approach to references for the evaluation of the kyphosis and lordosis. *Spine (Phila Pa 1976)* 1982;7:335.

[33] During J, Goudfrooij H, Keessen W, et al. Postural characteristics of the lower back system in normal and pathologic conditions. *Spine (Phila Pa 1976)* 1985;10.

[34] Gelb DE, Lenke LG, Bridwell KH, et al. An analysis of sagittal spinal alignment in 100 asymptomatic middle and older aged volunteers. *Spine (Phila Pa 1976)* 1995;20:1351–8.

[35] Jackson RP, Hales C. Congruent spinopelvic alignment on standing lateral radiographs of adult volunteers. *Spine (Phila Pa 1976)* 2000;25:2808–15.

[36] Vaz G, Roussouly P, Berthonnaud E, et al. Sagittal morphology and equilibrium of pelvis and spine. *Eur Spine J* 2002;11:80–7.

[37] Guigui P, Morvan G. [Evaluation of spinal alignment disorders in adults]. *J Radiol* 2002;83:1143–7.

[38] Duval-Beaupère G, Legaye J. Composante sagittale de la statique rachidienne. *Rev Rhum* 2004:105–19.

[39] Roussouly P, Gollogly S, Berthonnaud E, et al. Classification of the normal variation in the sagittal alignment of the human lumbar spine and pelvis in the standing position. *Spine (Phila Pa 1976)* 2005;30:346–53.

[40] Schwab F, Lafage V, Boyce R, et al. Gravity line analysis in adult volunteers: age-related correlation with spinal parameters, pelvic parameters, and foot position. *Spine (Phila Pa 1976)* 2006;31:E959–67.

[41] Gangnet N, Dumas R, Pomero V, et al. Three-dimensional spinal and pelvic alignment in an asymptomatic population. *Spine (Phila Pa 1976)* 2006;31:E507–12.

[42] Gangnet N, Pomero V, Dumas R, et al. Variability of the spine and pelvis location with respect to the gravity line: a three-dimensional stereoradiographic study using a force platform. *Surg Radiol Anat* 2003;25:424–33.

[43] Mac-Thiong J-M, Roussouly P, Berthonnaud E, et al. Sagittal parameters of global spinal balance: normative values from a prospective cohort of seven hundred nine Caucasian asymptomatic adults. *Spine (Phila Pa 1976)* 2010;35:E1193–8.

[44] Jackson RP, Peterson MD, Mcmanus AC, et al. Compensatory spinopelvic balance over the hip axis and better reliability in measuring lordosis to the pelvic radius on standing lateral radiographs of adult volonteers and patiens. *Spine (Phila Pa 1976)* 1998;23:1750–67.

[45] Duval-beaupere JHJMC, Raymond H. Relationship between pelvis and sagittal spinal curves in the standing position. *Rachis* 1993;5.

[46] Protopsaltis TS, Schwab F, Smith JS, et al. The T1 Pelvic Angle (TPA), a Novel Radiographic Measure of Sagittal Deformity, Accounts for Both Pelvic Retroversion and Truncal Inclination and Correlates Strongly with HRQOL. Scoliosis Res. Soc., Lyon: 2013.

[47] Steffen J-S, Obeid I, Aurouer N, et al. 3D postural balance with regard to gravity line: an evaluation in the transversal plane on 93 patients and 23 asymptomatic volunteers. *Eur Spine J* 2010;19:760–7.

[48] Steffen J. Modélisation tridimensionnelle globale du squelette pour l'aide au diagnostic et à la prise en charge thérapeutique des pathologies rachidiennes affectant l ' équilibre postural. Arts et metiers Paristech, 2010.

[49] Shea K, stevens P, Nelson M, et al. A comparison of manual versus computer assisted radiographic measurement. *SpineSpine* 1998;23:551–5.

[50] Segev E, Hemo Y, Wientroub S, et al. Intra- and interobserver reliability analysis of digital radiographic measurements for pediatric orthopedic parameters using a novel PACS integrated computer software program. *J Child Orthop* 2010;4:331–41.

[51] Srinivasalu S, Modi HN, Smehta S, et al. Cobb angle measurement of scoliosis using computer measurement of digitally acquired radiographs-intraobserver and interobserver variability. *Asian Spine J* 2008;2:90–3.

[52] Kim CH, Chung CK, Hong HS, et al. Validation of a simple computerized tool for measuring spinal and pelvic parameters. *J Neurosurg Spine* 2012;16:154–62.

[53] Champain S, Benchikh K, Nogier a, et al. Validation of new clinical quantitative analysis software applicable in spine orthopaedic studies. *Eur Spine J* 2006;15:982–91.

[54] Rillardon L, Levassor N, Guigui P, et al. Validation of a tool to measure pelvic and spinal parameters of sagittal balance. *Rev Chir Orthop Reparatrice Appar Mot* 2003;89:218–27.

[55] Dubousset J, Charpak G, Dorion I, et al. [A new 2D and 3D imaging approach to musculoskeletal physiology and pathology with low-dose radiation and the standing position: the EOS system]. *Bull Acad Natl Med* 2005;189:287–97; discussion 297–300.

[56] Deschênes S, Charron G, Beaudoin G, et al. Diagnostic imaging of spinal deformities: reducing patients radiation dose with a new slot-scanning X-ray imager. *Spine (Phila Pa 1976)* 2010;35:989–94.

[57] Rousseau M-A, Laporte S, Chavary-Bernier E, et al. Reproducibility of measuring the shape and three-dimensional position of cervical vertebrae in upright position using the EOS stereoradiography system. *Spine (Phila Pa 1976)* 2007;32:2569–72.

[58] Humbert L, De Guise J a, Aubert B, et al. 3D reconstruction of the spine from biplanar X-rays using parametric models based on transversal and longitudinal inferences. *Med Eng Phys* 2009;31:681–7.

[59] Baudoin a, Skalli W, de Guise J a, et al. Parametric subject-specific model for in vivo 3D reconstruction using bi-planar X-rays: application to the upper femoral extremity. *Med Biol Eng Comput* 2008;46:799–805.

[60] Chaibi Y. Adaptation des methodes de reconstruction 3D rapides par stereoradiographie: Modelisation du membres inferieur et calcul des indices en presence de deformation structurale. Arts et Metiers ParisTech, 2010.

[61] Berthonnaud E, Dimnet J, Roussouly P, et al. Analysis of the Sagittal Balance of the Spine and Pelvis Using 2005;18:40–7.

[62] Ascani E, Bartolozzi P, Logroscino A, et al. Natural history of untreated idiopathic scoliosis after skeletal maturity. *Spine (Phila Pa 1976)* 1986;11.

[63] Ploumis A, Transfledt EE, Denis F. Degenerative lumbar scoliosis associated with spinal stenosis. *Spine J* 2007;7:428–36.

[64] Basu PS, Elsebaie H, Noordeen MHH. Congenital spinal deformity: a comprehensive assessment at presentation. *Spine (Phila Pa 1976)* 2002;27:2255–9.

[65] Rajasekaran S. The problem of deformity in spinal tuberculosis. *Clin Orthop Relat Res* 2002:85–92.

[66] Moal B, Schwab F, Ames CP, et al. Radiographic Outcomes of Adult Spinal Deformity Correction : A Critical Analysis of Variability and Failures Across Deformity Patterns. *Spine Deform* n.d.

[67] Vital J-M, Gille O, Coquet M. Déformations rachidiennes : anatomopathologie et histoenzymologie. *Rev Rhum* 2004;71:262–4.

[68] Jagannathan J, Sansur CA, Shaffrey CI. Iatrogenic spinal deformity. *Neurosurgery* 2008;63:104–16.

[69] Jang J-S, Lee S-H, Min J, et al. Changes in sagittal alignment after restoration of lower lumbar lordosis in patients with degenerative flat back syndrome. *J Neurosurg Spine* 2007;7:387–92.

[70] Kim YJ, Bridwell KH, Lenke LG, et al. Proximal junctional kyphosis in adolescent idiopathic scoliosis following segmental posterior spinal instrumentation and fusion: minimum 5-year follow-up. *Spine (Phila Pa 1976)* 2005;30:2045–50.

[71] Follow-up MF, Kim YJ, Bridwell KH, et al. Proximal Junctional Kyphosis in Adult Spinal Deformity After Segmental Posterior Spinal Instrumentation and Fusion 2008;33:2179–84.

[72] MCHORNEY CA, JOHNE WJR, ANASTASIAE R. The MOS 36-Item Short-Form Health Survey (SF-36): II. Psychometric and Clinical Tests of Validity in Measuring Physical and Mental Health Constructs. *Med Care* 1993;31.

[73] McHorney CA, Ware JEJ, Rachel Lu JF, et al. The MOS 36-ltem Short-Form Health Survey (SF-36): III. Tests of Data Quality, Scaling Assumptions, and Reliability Across Diverse Patient Groups. *Med Care* 1994;32.

[74] Ware JEJ, Sherbourne CD. The MOS 36-ltem Short-Form Health Survey (SF-36): I. Conceptual Framework and Item Selection. *Med Care* 1992;30.

[75] WARE JEJR, KOSINSKI M, KELLER SD. A 12-Item Short-Form Health Survey: Construction of Scales and Preliminary Tests of Reliability and Validity. *Med Care* 1996;34.

[76] Fairbank JC, Pynsent PB. The Oswestry Disability Index. *Spine (Phila Pa 1976)* 2000;25:2940–52; discussion 2952.

[77] Fritz JM, Irrgang JJ. A comparison of a modified Oswestry Low Back Pain Disability Questionnaire and the Quebec Back Pain Disability Scale. *Phys Ther* 2001;81:776–88.

[78] Haher TR, Gorup JM, Shin TM, et al. Results of the Scoliosis Research Society instrument for evaluation of surgical outcome in adolescent idiopathic scoliosis. A multicenter study of 244 patients. *Spine (Phila Pa 1976)* 1999;24:1435–40.

[79] Asher M a, Min Lai S, Burton DC. Further development and validation of the Scoliosis Research Society (SRS) outcomes instrument. *Spine (Phila Pa 1976)* 2000;25:2381–6.

[80] Asher M a, Lai SM, Glattes RC, et al. Refinement of the SRS-22 Health-Related Quality of Life questionnaire Function domain. *Spine (Phila Pa 1976)* 2006;31:593–7.

[81] Glassman SD, Copay AG, Berven SH, et al. Defining substantial clinical benefit following lumbar spine arthrodesis. *J Bone Joint Surg Am* 2008;90:1839–47.

[82] Parker SL, Mendenhall SK, Shau D, et al. Determination of minimum clinically important difference in pain, disability, and quality of life after extension of fusion for adjacent-segment disease. *J Neurosurg Spine* 2012;16:61–7.

[83] Berven S, Deviren V, Demir-Deviren S. Minimal clinically important difference in adult spinal deformity: How much change is significant? Int. Meet. Adv. Spine Tech., Banff, Canada: 2005.

[84] Baldus C, Bridwell K, Harrast J, et al. The Scoliosis Research Society Health-Related Quality of Life (SRS-30) age-gender normative data: an analysis of 1346 adult subjects unaffected by scoliosis. *Spine (Phila Pa 1976)* 2011;36:1154–62.

[85] Smith JS, Fu K-M, Urban P, et al. Neurological symptoms and deficits in adults with scoliosis who present to a surgical clinic: incidence and association with the choice of operative versus nonoperative management. *J Neurosurg Spine* 2008;9:326–31.

[86] Bess S, Boachie-Adjei O, Burton D, et al. Pain and disability determine treatment modality for older patients with adult scoliosis, while deformity guides treatment for younger patients. *Spine (Phila Pa 1976)* 2009;34:2186–90.

[87] Dubousset J. Three-Dimensional analysis of the scoliotic deformity. Pediatr. Spine Princ. Pract., 1994, p. 479–95.

[88] Schwab FJ, Smith V a, Biserni M, et al. Adult scoliosis: a quantitative radiographic and clinical analysis. *Spine (Phila Pa 1976)* 2002;27:387–92.

[89] Terran J, Schwab F, Shaffrey CI, et al. The SRS-Schwab adult spinal deformity classification: assessment and clinical correlations based on a prospective operative and nonoperative cohort. *Neurosurgery* 2013;73:559–68.

[90] Glassman SD, Bridwell K, Dimar JR, et al. The impact of positive sagittal balance in adult spinal deformity. *Spine (Phila Pa 1976)* 2005;30:2024–9.

[91] Boissière L, Bourghli A, Vital J-M, et al. The lumbar lordosis index: a new ratio to detect spinal malalignment with a therapeutic impact for sagittal balance correction decisions in adult scoliosis surgery. *Eur Spine J* 2013;22:1339–45.

[92] Le Huec JC, Aunoble S, Philippe L, et al. Pelvic parameters: origin and significance. *Eur Spine J* 2011;20 Suppl 5:564–71.

[93] Ferrero E, Liabaud B, Challier V, et al. Global sagittal alignment analysis including lower extremities: role of pelvic translation and the lower extremities in compensation to spinal deformity. Groupe d'etude la scoliose, Nice: 2014.

[94] Champain S. CORRELATIONS ENTRE LES PARAMETRES BIOMECANIQUES DU RACHIS ET LES INDICES CLINIQUES POUR L'ANALYSE QUANTITATIVE DES PATHOLOGIES DU RACHIS LOMBAIRE ET DE LEUR TRAITEMENT CHIRURGICAL. École Nationale Supérieure d ' Arts et Métiers, 2008.

[95] Smith JS, Klineberg E, Schwab F, et al. Change in Classification Grade by the SRS-Schwab Adult Spinal Deformity Classification Predicts Impact on Health-Related Quality of Life Measures: Prospective Analysis of Operative and Non-operative Treatment. *Spine (Phila Pa 1976)* 2013.

[96] Scheer JK, Tang J a, Smith JS, et al. Cervical spine alignment, sagittal deformity, and clinical implications: a review. *J Neurosurg Spine* 2013;19:141–59.

[97] Barrey C, Jund J, Noseda O, et al. Sagittal balance of the pelvis-spine complex and lumbar degenerative diseases. A comparative study about 85 cases. *Eur Spine J* 2007;16:1459–67.

[98] Rajnics P, Templier A, Skalli W, et al. The importance of spinopelvic parameters in patients with lumbar disc lesions. *Int Orthop* 2002;26:104–8.

[99] Lafage V, Ferrero E, Lafage R, et al. Recruitment of Compensatory Mechanisms in Sagittal Spinal Malalignment is Age Dependent: An EOS analysis of Spino-pelvic Mismatch. SRS, Scoliosis Res. Soc., Anchorage: 2014.

[100] Korovessis P, Dimas A, Iliopoulos P, et al. Correlative analysis of lateral vertebral radiographic variables and medical outcomes study short-form health survey: a comparative study in asymptomatic volunteers versus patients with low back pain. *J Spinal Disord Tech* 2002;15:384–90.

[101] Lazennec JY, Riwan A, Gravez F, et al. Hip spine relationships: application to total hip arthroplasty. *Hip Int* 2007;17 Suppl 5:S91–104.

[102] ITOI, EIJI M. Roentgenographic Analysis of Posture in Spinal Osteoporotics. *Spine (Phila Pa 1976)* 1991;16.

[103] Kobayashi T, Atsuta Y, Matsuno T, et al. A longitudinal study of congruent sagittal spinal alignment in an adult cohort. *Spine (Phila Pa 1976)* 2004;29:671–6.

[104] Murata Y, Takahashi K, Yamagata M, et al. The knee-spine syndrome. *J Bone Jt Surg* 2003;85:95–9.

[105] Tsuji T, Matsuyama Y, Goto M, et al. Knee-spine syndrome: correlation between sacral inclination and patellofemoral joint pain. *J Orthop Sci* 2002;7:519–23.

[106] Lafage V, Schwab F, Skalli W, et al. Standing balance and sagittal plane spinal deformity: analysis of spinopelvic and gravity line parameters. *Spine (Phila Pa 1976)* 2008;33:1572–8.

[107] Ferrero E, Challier V, Ames CP, et al. Analysis of an Unexplored Group of Sagittal Deformity Patients: Low Pelvic Tilt Despite Sagittal Malalignment. Groupe d'etude la scoliose, Nice: 2014.

[108] Smith JS, Shaffrey CI, Kuntz C, et al. Classification systems for adolescent and adult scoliosis. *Neurosurgery* 2008;63:16–24.

[109] Bess S, Schwab F, Lafage V, et al. Classifications for adult spinal deformity and use of the Scoliosis Research Society-Schwab Adult Spinal Deformity Classification. *Neurosurg Clin N Am* 2013;24:185–93.

[110] Aebi M. The adult scoliosis. *Eur Spine J* 2005;14:925–48.

[111] Kuntz C, Shaffrey CI, Ondra SL, et al. Spinal deformity: a new classification derived from neutral upright spinal alignment measurements in asymptomatic juvenile, adolescent, adult, and geriatric individuals. *Neurosurgery* 2008;63:25–39.

[112] Lowe T, Berven SH, Schwab FJ, et al. The SRS classification for adult spinal deformity: building on the King/Moe and Lenke classification systems. *Spine (Phila Pa 1976)* 2006;31:S119–25.

[113] Schwab F, Ungar B, Blondel B, et al. Scoliosis Research Society-Schwab adult spinal deformity classification: a validation study. *Spine (Phila Pa 1976)* 2012;37:1077–82.

[114] King HA, Moe JH, Bradford DS, et al. The selection of fusion levels in thoracic idiopathic scoliosis. *J Bone Joint Surg Am* 1983;65:1302–13.

[115] LENKE N, BETZ RR, HARMS J, et al. Adolescent Idiopathic Scoliosis. *J Bone Jt Surg* 2001;26:42–7.

[116] Thaler M, Lechner R, Gstöttner M, et al. Interrater and intrarater reliability of the Kuntz et al new deformity classification system. *Neurosurgery* 2012;71:47–57.

[117] Liu Y, Liu Z, Zhu F, et al. Validation and reliability analysis of the new SRS-Schwab classification for adult spinal deformity. *Spine (Phila Pa 1976)* 2013;38:902–8.

[118] Schwab F, Farcy J-P, Bridwell K, et al. A clinical impact classification of scoliosis in the adult. *Spine (Phila Pa 1976)* 2006;31:2109–14.

[119] Schwab F, El-Fegoun AB, Gamez L, et al. A lumbar classification of scoliosis in the adult patient: preliminary approach. *Spine (Phila Pa 1976)* 2005;30:1670–3.

[120] Slobodyanyuk K, Poorman CE, Smith JS, et al. Clinical improvement through nonoperative treatment of adult spinal deformity: who is likely to benefit? *Neurosurg Focus* 2014;36:E2.

[121] Liu Z, Qiu Y, Liu Y, et al. Comparison of reliability of the SRS-Schwab classification between idiopathic and degenerative scoliosis in Adults. Int. Meet. Adv. Spine Tech. IMAST, Valencia: 2014.

[122] Nielsen DH, Hansen L V., Dragsted C, et al. Clinical correlation of SRS-Schwab classification with HRQL measures in a prospective non-US cohort of ASD patients. Int. Meet. Adv. spine Tech., Valencia: 2014.

[123] Bradford DS, Tay BK, Hu SS. Adult scoliosis: surgical indications, operative management, complications, and outcomes. *Spine (Phila Pa 1976)* 1999;24:2617–29.

[124] Marchesi DG, Aebi M. Pedicle fixation devices in the treatment of adult lumbar scoliosis. *Spine (Phila Pa 1976)* 1992;17:S304–9.

[125] Cho K-J, Kim Y-T, Shin S-H, et al. Surgical treatment of adult degenerative scoliosis. *Asian Spine J* 2014;8:371–81.

[126] Smith-Petersen MN, Larson CB, Aufranc OE. Osteotomy of the spine for correction of flexion deformity in rheumatoid arthritis. *Clin Orthop Relat Res* n.d.;66:6–9.

[127] Ponte A, Vero B, Siccardi G. Surgical treatment of scheuermann's hyperkyphosis. 19th Annu. Meet. Sco- liosis Res. Soc., 1984.

[128] Hassanzadeh H, Jain A, El Dafrawy MH, et al. Three-column osteotomies in the treatment of spinal deformity in adult patients 60 years old and older: outcome and complications. *Spine (Phila Pa 1976)* 2013;38:726–31.

[129] Voos K, Boachie-Adjei O, Rawlins B a. Multiple vertebral osteotomies in the treatment of rigid adult spine deformities. *Spine (Phila Pa 1976)* 2001;26:526–33.

[130] Wang MY, Berven SH. Lumbar pedicle subtraction osteotomy. *Neurosurgery* 2007;60:ONS140–6; discussion ONS146.

[131] Kim YJ, Bridwell KH, Lenke LG, et al. An analysis of sagittal spinal alignment following long adult lumbar instrumentation and fusion to L5 or S1: can we predict ideal lumbar lordosis? *Spine (Phila Pa 1976)* 2006;31:2343–52.

[132] Ondra SL, Marzouk S, Koski T, et al. Mathematical calculation of pedicle subtraction osteotomy size to allow precision correction of fixed sagittal deformity. *Spine (Phila Pa 1976)* 2006;31:E973–9.

[133] Van Royen BJ, Scheerder FJ, Jansen E, et al. ASKyphoplan: a program for deformity planning in ankylosing spondylitis. *Eur Spine J* 2007;16:1445–9.

[134] Lafage V, Schwab F, Vira S, et al. Spino-pelvic parameters after surgery can be predicted: a preliminary formula and validation of standing alignment. *Spine (Phila Pa 1976)* 2011;36:1037–45.

[135] Rose PS, Bridwell KH, Lenke LG, et al. Role of pelvic incidence, thoracic kyphosis, and patient factors on sagittal plane correction following pedicle subtraction osteotomy. *Spine (Phila Pa 1976)* 2009;34:785–91.

[136] Smith JS, Bess S, Shaffrey CI, et al. Dynamic changes of the pelvis and spine are key to predicting postoperative sagittal alignment after pedicle subtraction osteotomy: a critical analysis of preoperative planning techniques. *Spine (Phila Pa 1976)* 2012;37:845–53.

[137] Lafage V, Schwab F, Vira S, et al. Does vertebral level of pedicle subtraction osteotomy correlate with degree of spinopelvic parameter correction? *J Neurosurg Spine* 2011;14:184–91.

[138] Rousseau M-A, Lazennec J-Y, Tassin J-L, et al. Sagittal rebalancing of the pelvis and the thoracic spine after pedicle subtraction osteotomy at the lumbar level. *J Spinal Disord Tech* 2014;27:166–73.

[139] Thambiraj S, Boszczyk BM. Asymmetric osteotomy of the spine for coronal imbalance: a technical report. *Eur Spine J* 2012;21 Suppl 2:S225–9.

[140] Bakaloudis G, Lolli F, Di Silvestre M, et al. Thoracic pedicle subtraction osteotomy in the treatment of severe pediatric deformities. *Eur Spine J* 2011;20 Suppl 1:S95–104.

[141] Kawaguchi Y, Matsui H, Tsuji H. Back muscle injury after posterior lumbar spine surgery. Part 2: Histologic and histochemical analyses in humans. *Spine (Phila Pa 1976)* 1994;19:2598–602.

[142] Kawaguchi Y, Matsui H, Tsuji H. Back muscle injury after posterior lumbar spine surgery. A histologic and enzymatic analysis. *Spine (Phila Pa 1976)* 1996;21:941–4.

[143] Weber BR, Grob D, Dvorák J, et al. Posterior surgical approach to the lumbar spine and its effect on the multifidus muscle. *Spine (Phila Pa 1976)* 1997;22:1765–72.

[144] Taylor H, McGregor AH, Medhi-Zadeh S, et al. The impact of self-retaining retractors on the paraspinal muscles during posterior spinal surgery. *Spine (Phila Pa 1976)* 2002;27:2758–62.

[145] Flicker PL, Fleckenstein JL, Ferry K, et al. Lumbar muscle usage in chronic low back pain. Magnetic resonance image evaluation. *Spine (Phila Pa 1976)* 1993;18:582–6.

[146] Gejo R, Matsui H, Kawaguchi Y, et al. Serial changes in trunk muscle performance after posterior lumbar surgery. *Spine (Phila Pa 1976)* 1999;24:1023–8.

[147] Kim D-Y, Lee S-H, Chung SK, et al. Comparison of multifidus muscle atrophy and trunk extension muscle strength: percutaneous versus open pedicle screw fixation. *Spine (Phila Pa 1976)* 2005;30:123–9.

[148] Lee JC, Cha J-G, Kim Y, et al. Quantitative analysis of back muscle degeneration in the patients with the degenerative lumbar flat back using a digital image analysis: comparison with the normal controls. *Spine (Phila Pa 1976)* 2008;33:318–25.

[149] Humphrey AR, Nargol AVF, Jones APC, et al. The value of electromyography of the lumbar paraspinal muscles in discriminating between chronic-low-back-pain sufferers and normal subjects. *Eur Spine J* 2005;14:175–84.

[150] Mooney V, Gulick J, Perlman M, et al. Relationships between myoelectric activity, strength, and MRI of lumbar extensor muscles in back pain patients and normal subjects. *J Spinal Disord* 1997;10:348–56.

[151] Mayer TG, Vanharanta H, Gatchel RJ, et al. Comparison of CT scan muscle measurements and isokinetic trunk strength in postoperative patients. *Spine (Phila Pa 1976)* 1989;14:33–6.

[152] Hides JA, Richardson CA, Jull GA. Magnetic resonance imaging and ultrasonography of the lumbar multifidus muscle. Comparison of two different modalities. *Spine (Phila Pa 1976)* 1995;20:54–8.

[153] Danneels L a, Vanderstraeten GG, Cambier DC, et al. CT imaging of trunk muscles in chronic low back pain patients and healthy control subjects. *Eur Spine J* 2000;9:266–72.

[154] Hultman G, Nordin M, Saraste H, et al. Body composition, endurance, strength, cross-sectional area, and density of MM erector spinae in men with and without low back pain. *J Spinal Disord* 1993;6:114–23.

[155] Storheim K, Holm I, Gunderson R, et al. The effect of comprehensive group training on cross-sectional area, density, and strength of paraspinal muscles in patients sick-listed for subacute low back pain. *J Spinal Disord Tech* 2003;16:271–9.

[156] Airaksinen O, Herno A, Kaukanen E, et al. Density of lumbar muscles 4 years after decompressive spinal surgery. *Eur Spine J* 1996;5:193–7.

[157] Barker KL, Shamley DR, Jackson D. Changes in the cross-sectional area of multifidus and psoas in patients with unilateral back pain: the relationship to pain and disability. *Spine (Phila Pa 1976)* 2004;29:E515–9.

[158] Dangaria TR, Naesh O. Changes in cross-sectional area of psoas major muscle in unilateral sciatica caused by disc herniation. *Spine (Phila Pa 1976)* 1998;23:928–31.

[159] Parkkola R, Rytökoski U, Kormano M. Magnetic resonance imaging of the discs and trunk muscles in patients with chronic low back pain and healthy control subjects. *Spine (Phila Pa 1976)* 1993;18:830–6.

[160] Parkkola R, Kormano M. Lumbar disc and back muscle degeneration on MRI: Correlation to age and body mass. *J Spinal Disord* 1992;5:86–92.

[161] Valentin S, Licka T, Elliott J. Age and side-related morphometric MRI evaluation of trunk muscles in people without back pain. *Man Ther* 2014.

[162] Savage RA, Millerchip R, Whitehouse GH, et al. Lumbar muscularity and its relationship with age, occupation and low back pain. *Eur J Appl Physiol Occup Physiol* 1991;63:265–8.

[163] Peltonen JE, Taimela S, Erkintalo M, et al. Back extensor and psoas muscle cross-sectional area, prior physical training, and trunk muscle strength--a longitudinal study in adolescent girls. *Eur J Appl Physiol Occup Physiol* 1998;77:66–71.

[164] Gille O, Jolivet E, Dousset V, et al. Erector spinae muscle changes on magnetic resonance imaging following lumbar surgery through a posterior approach. *Spine (Phila Pa 1976)* 2007;32:1236–41.

[165] Elliott JM, Walton DM, Rademaker A, et al. Quantification of cervical spine muscle fat: a comparison between T1-weighted and multi-echo gradient echo imaging using a variable projection algorithm (VARPRO). *BMC Med Imaging* 2013;13:30.

[166] Dixon W. T. Simple proton spectroscopic imaging. *Radiology* 1984;153:189–94.

[167] Tracy BL, Ivey FM, Jeffrey Metter E, et al. A more efficient magnetic resonance imaging-based strategy for measuring quadriceps muscle volume. *Med Sci Sports Exerc* 2003;35:425–33.

[168] Barnouin Y, Butler-Browne G, Voit T, et al. Manual segmentation of individual muscles of the quadriceps femoris using MRI: a reappraisal. *J Magn Reson Imaging* 2014;40:239–47.

[169] Frédéric Cordier NMT, Cordier F, Thalmann NM. Comparison of Two Techniques for Organ Reconstruction Using Visible Human Dataset. VISIBLE Hum. Proj. CONF. PROC, 1998, p. 1–11.

[170] Jolivet E, Daguet E, Pomero V, et al. Volumic patient-specific reconstruction of muscular system based on a reduced dataset of medical images. *Comput Methods Biomech Biomed Engin* 2008;11:281–90.

[171] JOLIVET E. MODÉLISATION BIOMÉCANIQUE DE LA HANCHE DANS LE RISQUE DE FRACTURE DU FÉMUR PROXIMAL. 2007.

[172] Südhoff I, de Guise J a, Nordez a, et al. 3D-patient-specific geometry of the muscles involved in knee motion from selected MRI images. *Med Biol Eng Comput* 2009;47:579–87.

[173] Gilles B, Magnenat-Thalmann N. Musculoskeletal MRI segmentation using multi-resolution simplex meshes with medial representations. *Med Image Anal* 2010;14:291–302.

[174] Baudin P, Azzabou N, Carlier PG, et al. GRAPH-BASED SEED PLACEMENT 2012.

[175] Li F, Laville A, Bonneau D, et al. Study on cervical muscle volume by means of three-dimensional reconstruction. *J Magn Reson Imaging* 2014;39:1411–6.

[176] Jolivet E, Dion E, Rouch P, et al. Skeletal muscle segmentation from MRI dataset using a model-based approach. *Comput Methods Biomech Biomed Eng Imaging Vis* 2014;2:138–45.

[177] Trochu F. A contouring program based on dual kriging interpolation. *Eng Comput* 1993;9:160–77.

[178] Kim H, Taksali SE, Dufour S, et al. Comparative MR study of hepatic fat quantification using single-voxel proton spectroscopy, two-point dixon and three-point IDEAL. *Magn Reson Med* 2008;59:521–7.

[179] Hamilton G, Chavez AD, B BSJ. Fatty Liver Disease : MR Imaging Techniques for the Detection and Quantification of Liver Steatosis 1 2009:231–61.

[180] Shen W, Gong X, Weiss J, et al. Comparison among T1-weighted magnetic resonance imaging, modified dixon method, and magnetic resonance spectroscopy in measuring bone marrow fat. *J Obes* 2013;2013:298675.

[181] Gaeta M, Messina S, Mileto A, et al. Muscle fat-fraction and mapping in Duchenne muscular dystrophy: evaluation of disease distribution and correlation with clinical assessments. Preliminary experience. *Skeletal Radiol* 2012;41:955–61.

[182] Fischer MA, Nanz D, Shimakawa A, et al. Quantification of muscle fat in patients with low back pain: comparison of multi-echo MR imaging with single-voxel MR spectroscopy. *Radiology* 2013;266:555–63.

[183] Glover GH, Schneider E. Three-point dixon technique for true water/fat decomposition withB0 inhomogeneity correction. *Magn Reson Med* 1991;18:371–83.

[184] Baldus C, Bridwell KH, Harrast J, et al. Age-gender matched comparison of SRS instrument scores between adult deformity and normal adults: are all SRS domains disease specific? *Spine (Phila Pa 1976)* 2008;33:2214–8.

[185] Berven S, Deviren V, Demir-Deviren S, et al. Studies in the modified Scoliosis Research Society Outcomes Instrument in adults: validation, reliability, and discriminatory capacity. *Spine (Phila Pa 1976)* 2003;28:2164–9; discussion 2169.

[186] Smith JS, Singh M, Klineberg E, et al. Surgical treatment of pathological loss of lumbar lordosis (flatback) in patients with normal sagittal vertical axis achieves similar clinical improvement as surgical treatment of elevated sagittal vertical axis. *J Neurosurg Spine* 2014:1–11.

[187] Charlson ME, Pompei P, Ales KL, et al. A new method of classifying prognostic in longitudinal studies : Developpement and Validation. *J Chronic Dis* 1987;40:373–83.

[188] Soroceanu A, Ching A, Abdu W, et al. Relationship between preoperative expectations, satisfaction, and functional outcomes in patients undergoing lumbar and cervical spine surgery: a multicenter study. *Spine (Phila Pa 1976)* 2012;37:E103–8.

[189] Gum JL, Glassman SD, Carreon LY. Clinically important deterioration in patients undergoing lumbar spine surgery: a choice of evaluation methods using the Oswestry Disability Index, 36-Item Short Form Health Survey, and pain scales: clinical article. *J Neurosurg Spine* 2013;19:564–8.

[190] Daubs MD, Lenke LG, Cheh G, et al. Adult spinal deformity surgery: complications and outcomes in patients over age 60. *Spine (Phila Pa 1976)* 2007;32:2238–44.

[191] Smith JS, Shaffrey CI, Glassman SD, et al. Clinical and radiographic parameters that distinguish between the best and worst outcomes of scoliosis surgery for adults. *Eur Spine J* 2013;22:402–10.

[192] Slover J, Abdu W a, Hanscom B, et al. The impact of comorbidities on the change in short-form 36 and oswestry scores following lumbar spine surgery. *Spine (Phila Pa 1976)* 2006;31:1974–80.

[193] Djurasovic M, Glassman SD, Howard JM, et al. Health-related quality of life improvements in patients undergoing lumbar spinal fusion as a revision surgery. *Spine (Phila Pa 1976)* 2011;36:269–76.

[194] Schwab FJ, Patel A, Shaffrey CI, et al. Sagittal realignment failures following pedicle subtraction osteotomy surgery: are we doing enough?: Clinical article. *J Neurosurg Spine* 2012;16:539–46.

[195] Blondel B, Lafage V, Schwab F, et al. Reciprocal sagittal alignment changes after posterior fusion in the setting of adolescent idiopathic scoliosis. *Eur Spine J* 2012;21:1964–71.

[196] Mac-Thiong J-M, Transfeldt EE, Mehbod A a, et al. Can c7 plumbline and gravity line predict health related quality of life in adult scoliosis? *Spine (Phila Pa 1976)* 2009;34:E519–27.

[197] Ploumis A, Liu H, Mehbod A a, et al. A correlation of radiographic and functional measurements in adult degenerative scoliosis. *Spine (Phila Pa 1976)* 2009;34:1581–4.

[198] Sánchez-Mariscal F, Gomez-Rice A, Izquierdo E, et al. Correlation of radiographic and functional measurements in patients who underwent primary scoliosis surgery in adult age. *Spine (Phila Pa 1976)* 2012;37:592–8.

[199] Schwab F, Patel A, Ungar B, et al. Adult Spinal Deformity — Postoperative Standing Imbalance Assessing Alignment and Planning Corrective Surgery 2010;35:2224–31.

[200] Schwab F, Lafage V, Patel A, et al. Sagittal plane considerations and the pelvis in the adult patient. *Spine (Phila Pa 1976)* 2009;34:1828–33.

[201] Lazennec J-Y, Even J, Skalli W, et al. Clinical outcomes, radiologic kinematics, and effects on sagittal balance of the 6 df LP-ESP lumbar disc prosthesis. *Spine J* 2013:1–7.

[202] Schwab FJ, Lafage R, Lafage V, et al. Does One Size Fit All? Defining spino-pelvic alignment thresholds based on age. *Nass Commun* 2014.

[203] Raizman NM, O'Brien JR, Poehling-Monaghan KL, et al. Pseudarthrosis of the spine. *J Am Acad Orthop Surg* 2009;17:494–503.

[204] Cho K-J, Bridwell KH, Lenke LG, et al. Comparison of Smith-Petersen versus pedicle subtraction osteotomy for the correction of fixed sagittal imbalance. *Spine (Phila Pa 1976)* 2005;30:2030–7; discussion 2038.

[205] Cho K-J, Suk S-I, Park S-R, et al. Risk factors of sagittal decompensation after long posterior instrumentation and fusion for degenerative lumbar scoliosis. *Spine (Phila Pa 1976)* 2010;35:1595–601.

[206] Keller A, Gunderson R, Reikerås O, et al. Reliability of computed tomography measurements of paraspinal muscle cross-sectional area and density in patients with chronic low back pain. *Spine (Phila Pa 1976)* 2003;28:1455–60.

[207] Salminen JJ, Erkintalo-Tertti MO, Paajanen HE. Magnetic resonance imaging findings of lumbar spine in the young: correlation with leisure time physical activity, spinal mobility, and trunk muscle strength in 15-year-old pupils with or without low-back pain. *J Spinal Disord* 1993;6:386–91.

[208] Jolivet E, Daguet E, Bousson V, et al. Variability of hip muscle volume determined by computed tomography. *Irbm* 2009;30:14–9.

[209] Glover GH. Multipoint Dixon technique for water and fat proton and susceptibility imaging. *J Magn Reson Imaging* n.d.;1:521–30.

[210] Yeung HN, Kormos DW. Separation of true fat and water images by correcting magnetic field inhomogeneity in situ. *Radiology* 1986;159:783–6.

[211] Bland JM, Altman DG. Statistical methods for assessing agreement between two methods of clinical measurement. *Lancet* 1986;1:307–10.

[212] Mitton D, Landry C, Véron S, et al. 3D reconstruction method from biplanar radiography using non-stereocorresponding points and elastic deformable meshes. *Med Biol Eng Comput* 2000;38:133–9.

[213] Bley T a, Wieben O, François CJ, et al. Fat and water magnetic resonance imaging. *J Magn Reson Imaging* 2010;31:4–18.

[214] Moal B, Raya JG, Jolivet E, et al. Validation of 3D spino-pelvic muscle reconstructions based on dedicated MRI sequences for fat-water quantification. *Irbm* 2014.

[215] Ragan DK, Bankson J a. Two-point Dixon technique provides robust fat suppression for multi-mouse imaging. *J Magn Reson Imaging* 2010;31:510–4.

[216] Cruz-Jentoft AJ, Baeyens JP, Bauer JM, et al. Sarcopenia: European consensus on definition and diagnosis: Report of the European Working Group on Sarcopenia in Older People. *Age Ageing* 2010;39:412–23.

[217] Song M-Y, Ruts E, Kim J, et al. Sarcopenia and increased adipose tissue infiltration of muscle in elderly African American women. *Am J Clin Nutr* 2004;79:874–80.

[218] Horton WC, Brown CW, Bridwell KH, et al. Is there an optimal patient stance for obtaining a lateral 36" radiograph? A critical comparison of three techniques. *Spine (Phila Pa 1976)* 2005;30:427–33.

[219] Kovanlikaya A, Guclu C, Desai C, et al. Fat quantification using three-point dixon technique: in vitro validation. *Acad Radiol* 2005;12:636–9.

[220] De Bazelaire CMJ, Duhamel GD, Rofsky NM, et al. MR imaging relaxation times of abdominal and pelvic tissues measured in vivo at 3.0 T: preliminary results. *Radiology* 2004;230:652–9.

[221] Moal B, Bronsard N, Terran JS, et al. Volume and Fat Infiltration Parameters of the Spino-Pelvic Complex Correlate with HRQOL and Skeletal Malalignment in Adult Spinal Deformity. Int. Meet. Adv. Spine Tech. IMAST, Vancouvert: 2013.

[222] Jolivet E. Biomechanical modelisation of hip and its soft tissue for hip fracture risk. Laboratory of Biomecanics, Arts et Metiers ParisTech, 2007.

[223] Draper N, Smith H. Applied Regression Analysis. Wiley-Inte. 1998.

[224] Zhang C, Moal B, Dubois G, et al. Comparison of two MRI sequences for subject-specific 3D thigh muscle reconstruction. *Comput Methods Biomech Biomed Engin* 2014;17 Suppl 1:136–7.

ADULTES AVEC DEFORMATION RACHIDIENNE : TRAITMENT CHIRURGICAL ET EVALUATION MUSCULAIRE

RESUME : Les déformations rachidiennes se réfèrent aux patients avec une courbure anormal de la colonne vertébrale qui ont terminé leur croissance. Par leur prévalence, leur impact clinique, et le taux relativement élevé d'échecs chirurgicaux, elles représentent un défi thérapeutique. La recherche a permis de démontrer que la préservation ou la restauration de l'alignement, sont des éléments clé du traitement chirurgical. L'objectif de cette thèse était d'analyser le traitement des patients avec DR, avec un intérêt particulier pour la restauration de l'alignement sagittal et l'évaluation musculaire. Fondé sur une analyse rétrospective d'une base de données multicentriques, les deux premiers articles présentent une évaluation du traitement chirurgical en termes d'efficacité clinique et de réalignement radiographique. Les écarts entre la planification préopératoire et l'exécution opérationnelle ont aussi été étudiés avec une collecte de données prospectives, et ont mis en évidence la nécessité de mieux comprendre le rôle des muscles dans le maintien de la posture. Par conséquent, deux protocoles pour la caractérisation des principaux muscles impliqués dans l'alignement sagittal ont été validés. Les deux méthodes sont basées sur la segmentation manuelle d'acquisition IRM spécifique (méthode de Dixon) afin d'obtenir l'infiltration graisseuse en plus du volume musculaire. Une des méthodes permet d'obtenir la reconstruction 3D des muscles et donc de générer des modèles musculo-squelettiques personnalisés. L'autre ouvre la voie à une pratique clinique car nécessite seulement la segmentation de quatre coupes pour obtenir une évaluation des principaux groupes musculaires. Enfin, à partir de la première méthode, le système musculaire de patients avec DR a été décrit.

Mots clés : adulte avec déformation rachidienne, posture, alignement sagittal, traitement, réalignement chirurgical, système musculaire.

ADULTS WITH SPINAL DEFORMITY: SURGICAL TREATMENT AND MUSCULAR EVALUATION

ABSTRACT : Adult spinal deformity(ASD) refers to abnormal curvatures of the spine in patients who have completed their growth. Due to its prevalence, clinical impact, and the relatively high rate of surgical failures, they represent a therapeutic challenge. Research has been able to demonstrate that the preservation or the restoration of the sagittal alignment, are key objectives of surgical treatment. The objective of this thesis is to analyze the treatment of ASD patients, with particular interest in restoration of sagittal alignment and to develop tools to assess the spino-pelvic musculature of ASD patients. Based on an analysis of a multicenter database, the first two articles present an evaluation of the surgical treatment in term of clinical effectiveness and radiographic realignment. In addition, the discrepancies between surgical preoperative planning and operative execution have been studied with a prospective data collection, and have highlighted the necessity to understand better the role of the muscles in the maintaining of the posture. Therefore two methods for the characterization of the muscles involved in the sagittal alignment have been validated. Both methods are based on manual segmentation of specific MRI acquisition (Dixon methods) in order to obtain precise fat infiltration quantification in addition to muscular volume. One method permits to obtain 3D reconstruction able to generate patient–specific musculoskeletal model. The other one open the path to a clinical purpose, because necessitate only segmentation of four slices to obtain an relevant evaluation of the muscular system. Finally, thanks to the first protocol the muscular system of ASD patients have been described.

Keywords : adult with spinal deformity, posture, sagittal alignment, treatment, surgical realignment, muscular system.